MEETING POST AERATION REQUIREMENTS USING STEPPED STRUCTURES

By
Ghada Nassri Kassab

Supervisor
Dr. Adnan Al-Salihi

Submitted in Partial Fulfillment of the Requirements for the
Degree of Master of Science in
Civil Engineering/Environmental Engineering and Water Resources.

Faculty of Graduate Studies
University of Jordan

٩٩/٨/١٣

August 1999

This thesis was defended successfully on: 14/8/1999

Signature

1. Dr. Adnan AL-Salihi (Chairman of committee)
   Civil Engineering Department

2. Dr. Nabil AL Kuhrey (Member of committee)
   Civil Engineering Department

3. Dr. Tawfiq Sama'neh (Member of committee)
   Civil Engineering Department

4. Dr. Fawzi AL-Ryan (Member of committee)

Dedication

To ...

Every Member

of My Family

Acknowledgement

I wish to Acknowledge Dr. Adnan Al-Salihi for his precious advises and his endless efforts in accomplishing this research and especially for his patience with me.

Also I would like to thank the laboratory technicians for their great help and the discussion committee for their constructive advises.

CONTENTS

List of Tables

List of Figures

Symbols and Abreviations

a	Specific surface area.
a_{mean}	Mean specific interface area.
A	Air-water surface area.
A′	Channel cross-section area.
B	Channel width.
c	Local air concentration.
C	Concentration of dissolved chemical in the water.
Cd	Discharge coefficient.
C_{ds}	Downstream concentration.
C_{us}	Upstream concentration.
C_e	Average air concentration.
C_g	Concentration in the gas phase.
C_{mean}	The depth average mean concentration.
C_s	Saturation concentration.
C*	Equilibrium concentration in the liquid phase.
d_b	Flow depth at the brink of the step.
d_b'	The air bubble diameter.
d_c	Critical flow depth.
d_{char}	Characteristic water flow depth.
d_e	Water flow depth for uniform aerated flow.
d_i	Nappe thickness at the impact with receiving pool.
d_p	Height of water in the pool behind the overlaying jet.
d_o	Water flow depth for uniform non-aerated flow
d_t	Tail water depth.
d_t'	Optimum tail water depth.
d*	Depth at the point of inception measured normal to the free surface.
d_1	Flow depth at section 1. (Figure 2.4).
d_2	Flow depth at section 2. (Figure 2.4).
D	Drop height.
D_{gas}	Molecular diffusivity.
D_H	Hydraulic diameter.
DO	Dissolved oxygen.
E	Aeration efficiency.
E′	Kinetic energy, correction coefficient.
E_{HJ}	Efficiency of the hydraulic jump.
E_{jet}	Aeration efficiency of plunging jet.
E_{SA}	Self aeration efficiency.
f	Friction factor.
f_e	Friction factor for uniform aerated flow.
F_g	Gravity force.
F_I	Inertia force.
F_J	Jet Froude number.
F_P	Pressure force.

Fr	Froude number.
F_v	Viscosity force.
F*	Froude number in terms of roughness height.
g	Gravity constant.
h	Step height.
h_m	Model step height.
h_p	Prototype step height.
H	Henry's law constant.
H'	Depth of water above the V-notch.
H_1	Total head at section 1. (Figure 2.4).
H_2	Total head at section 2. (figure 2.4).
H_{dam}	Dam height.
H_{max}	Max head available.
H_{res}	Residual head.
ΔH	Head loss.
K	Bulk transfer coefficient.
K_1, K_o	Coefficient, equations (2.52), & (2.50)
K_g	Gas film coefficient.
K_L	Liquid film coefficient.
K_s	Roughness height.
L	Step Length.
L_d	Distance from the vertical face of the step to position of the depth d_1. Figure (2.4)
L_m	Model length.
L_o	Length of the bubble zone.
L_p	Prototype length.
L_r	Length ratio.
L_{ro}	Length of the hydraulic jump roller.
$L_{spillway}$	Spillway length.
L*	Distance from the start of boundary layer to the point of inception.
M	Parameter of water quality.
n	Number of steps
N	Parameter of weir geometry.
N_A	Flux per unit surface area.
p_w	Wetted perimeter.
p*	Equilibrium gas pressure in the gas phase.
Δp	Pressure difference.
q_c	Critical discharge.
q_m	Model discharge per unit width.
q_p	Prototype discharge per unit width.
q_J	Jet discharge per unit jet perimeter.
q_w	Discharge per unit width of the channel or of the weir.
$(q_w)_c$	Characteristic discharge.
Q_{act}	Actual flowrate.
Q_m	Model flowrate.
Q_p	Prototype flowrate.

Q_{th}	Theoretical flowrate.
r	Deficit ratio.
r_T	Deficit ratio at temperature T.
R	Hydraulic radius.
Re	Reynolds number.
Re_m	Model Reynolds number.
Re_p	Prototype Reynolds number.
R_G	Gas film resistance.
R_I	Interface resistance.
R_L	Liquid film resistance.
R_T	Total resistance.
t	Time.
T	Temperature.
T_o	Reference temperature.
u_r	Bubble rise velocity.
U_w	Mean flow velocity.
v	Flow velocity
v'	Turbulent velocity normal to free surface.
V	Control volume.
V_c	Critical velocity.
V_i	Velocity of the nappe at the intersection of the falling nappe with the receiving pool.
V_o	Uniform non-aerated flow velocity.
x	Factor, [equation (2.41)].
y	Distance measured perpendicular to the invert
y_{90}	The depth where the air concentration is 90%.
σ	Surface tension between air and water.
μ_w	Dynamic viscosity of water.
ρ_w	Water density.
α	Spillway slope.
ϕ	Angle of the falling nappe with the horizontal.
τ_o	Average shear stress between the skimming flow and the recirculating fluid underneath.
ν	Kinematic viscosity
$\wp$	Fluid unit weight.
θ	Angle of the pooled step.
φ	Angle of the inclined step.
β	V-notch angle.
λ	Exponent, [equation (2.84)]

ABSTRACT

Meeting Post Aeration Requirements Using Stepped Structures

By
Ghada Nassri Kassab

Supervisor
Dr. Adnan Al-Salihi

The present study aims to obtain the most efficient use of stepped structure regarding aeration efficiency, through alternating it's hydraulic characteristics (i.e type of cascade, step height, height to length ratio and operating discharge)

The experimental part of this research was carried out in the Hydraulics Laboratory of Civil Engineering Department of University of Jordan. The tests were conducted over stepped structure, through:

- Three types of cascade;

1- Horizontal.

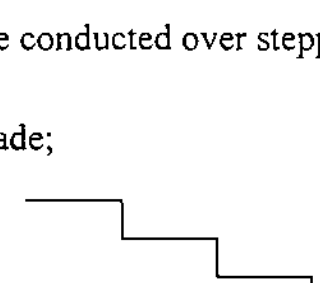

2- Pooled.

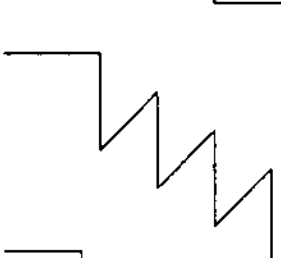

3- Inclined.

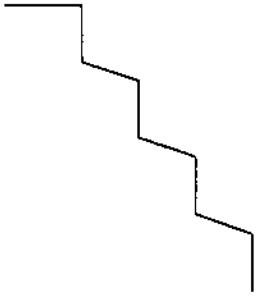

- Four prototype step heights (h_p)
  - 15cm.
  - 30cm.
  - 45cm.
  - 60cm.

- Two height to length ratios ($h/_L$)
  - 1/2.
  - 1/4.

- Two types of flow
  - Nappe flow
  - Skimming flow

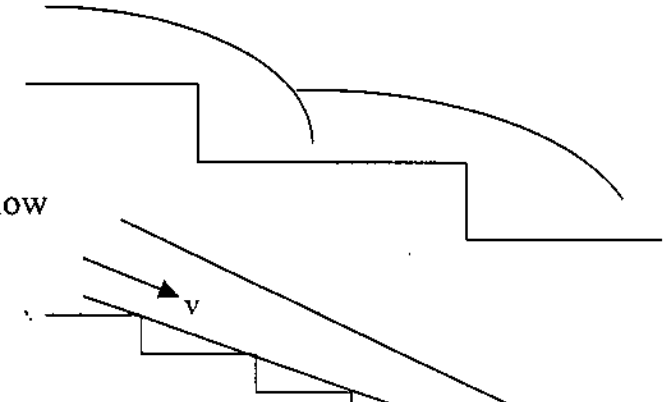

It was concluded from this research, that horizontal cascade achieved highest aeration efficiency ranging between 30% and 64% for different step heights followed by pooled type with little difference than the horizontal cascade with efficiencies ranges between 18% to 60% for different step heights and finally comes the inclined type cascade with the least ranges between 10% to 28%. Step height h_p = 45 cm was the best regarding aeration efficiency for horizontal type cascade. For pooled and inclined, step height of h_p = 60cm was the best. In nappe flow, the ratio (h/L) = 1/2 was better than the ratio (h/L) = 1/4 with respect to aeration efficiency, while in skimming flow the opposite is true, for horizontal cascade type.

Chapter One

Introduction

Chapter One

Introduction

One thing is becoming clear with every passing day, that water problem is not only the quantity, but the quality is the most critical.

One of the important water quality parameters in surface water is dissolved oxygen (DO) concentration. Dissolved oxygen level is a critical parameter for treated sewage effluent, if it's to be reused or disposed into river and streams, especially when the expected quantity of treated wastewater in Jordan for the year 2000 will be around 60 MCM.

Stepped cascade has become a popular method to enhance the air-water transfer of atmospheric gases, free of charge. It can be used in the wastewater treatment plants, and along rivers and streams to re-oxygenate effluent or water which are low in dissolved oxygen content, or to meet post aeration requirements. Cascade aeration is the least costly method, the easiest from construction point of view and need limited maintenance works (Chanson, 1994b).

Stepped spillways increase significantly the rate of energy dissipation of water flowing over spillway face and reduce the size of the required downstream energy dissipation basin (Chanson, 1993a).

Stepped structures were developed independently by several ancient civilizations. The world's oldest stepped spilling are probably those of Khosr River dams, in Iraq (Chanson, 1995b). The Knosr River dams were built around B.C. 694 by the Assyrian King Sennacherib. They were designed to supply water to the Assyrian capital city Nineveh (near the actual Mosul). Remains of these dams are still in existence. Both dams

featured a stepped downstream face and were intended to discharge the river over their crests.

Much later, the Romans built stepped overflow dams in their empire; remains can still be found in Syria, Libya, and Tunisia. After the fall of the Roman empire. Moslem civil engineers gained experience from the Nabataens, the Romans and the Sabaens. Stepped spillways built by Moslems can be found in Iraq and Spain (e.g. Adheim dam, Mestella weir). Following the reconquest of Spain, Spanish engineers benefited from the Roman and Moslem precedents and design dams with overflow stepped spillway. After the conquest of America, the Spanish dam-building was exported to the new Indies. In central Mexico, several stepped overflow dams were built by the Spanish during the 18^{th} and 19^{th} centuries.

French engineers built canals included several stepped channels and cascades to dissipate flow energy and to prevent scouring. English engineers built dams that included stepped weirs near furnaces and water mills. In the northest part of America timber dams with stepped overflow weirs were reported as early as AD 1600 (Chanson, 1995b).

Drop structures and stepped profiles were used also in some early irrigation systems. In Saba, the Sabaens used stepped channel profiles in the early Antiquity. In Peru, the Indians civilizations used stepped channels and drop structures prior to Spanish conquest.

Since Antiquity, the design of stepped spillways and channels was recognized to reduce flow velocities and to prevent scouring. Some ancient engineers might have known the concepts of nappe and skimming flow. But there is evidence that, even at the beginning of 20^{th} century, hydraulic engineers had no quantitative information on the main flow properties, i.e. flow resistance and head loss.

Despite recent advances in technology, the characteristics (geometry and discharge) of stepped spillway show a continuity since the Antiquity up to now. The new spillway design has a similar range of step height as the older constructions, and designed for maximum discharge capacity no greater than ancient designs.

The design of stepped chutes involves many factors; e.g. economic, environmental, geology, hydraulics, hydrology. First step in designing stepped channels is to determine the purpose of the structure ; e.g. energy dissipation, water treatment, flood releases or emergency spillway. Second step in the design is to specify the constraints; e.g. geometry, hydrology, material availability, topogrophy and geology. While, the design procedure includes (1) assessment of the design flood; (2) assissment of the spillway geometry; slope, height and width. (3) selection of optimum step height and length. (4) calculation of the hydraulic flow characteristics for selected step geometry; e.g. the flow depth, velocity, the amount of air entrainment and energy dissipation. (5) calculation of the downstream dissolved gas content, and aeration efficiency of the structure for the climatic conditions of the site, and the chemical properties of the water. In this study, the purpose of the cascade structure is water treatment.

The main objective of this research is to achieve maximum aeration efficiency of a cascade structure, through alternating its hydraulic characteristics. To achieve this objective, the research will be based on a review of previous works in one hand, and on laboratory experimental research on the other. The review part in this research will concentrate on previous studies concerning air-clean water aeration along cascade structure, to specify the model slope and discharge ranges that give nappe flow or skimming flow regime, as shown in Chapter Two.

Concerning the laboratory experimental research, models are designed with different scales according to Froude number to suit the large flume and the equipments available in the Hydraulics Laboratory in the Civil Engineering Department of University of Jordan, as developed in Chapter Three.

Three types of cascade are tested; horizontal, pooled and inclined. Each type is studied for four step heights; 15cm, 30cm, 45cm and 60cm. For height to length ratio of the step equal 1/2 and limited 1/4 for comparison, except for the horizontal type which is tested comprehensively for height to length ratio 1/4. All the results are analyzed and discussed in Chapter Four. Conclusions and recommendations are listed in Chapter Five.

Chapter Two
Literature Review

Chapter Two
Literature Review

2.1 Introduction

In recent decades, stepped spillway have become a popular method for handling flood releases through dams and in particular the roller compacted concrete (RCC) dams. For a stepped chute, the steps increase significantly the rate of energy dissipation taking place along the spillway face, and eliminate or reduce greatly the need for large energy dissipater at the toe of the spillway, which leads to a great saving in the construction cost beside water quality enhancement, stepped cascades are used also in water treatment plants to enhance air-water transfer of atmospheric gases (oxygen, nitrogen) and of volatile organic components (Chanson, 1994b). Stepped channels can also be used along or beside rivers and streams to re-oxygenate water with low dissolved oxygen content.

Aeration over chute spillway and cascades, theory of oxygen transfer, flow regimes over stepped structures and energy dissipation are reviewed through this chapter. The previous works are discussed to introduce the concepts, to tackle the research problem which can start with the theory of oxygen transfer in the next section.

2.2 Theory of Oxygen Transfer:

The transfer of oxygen into a fluid is usualy considered as a transfer process from a bubble of gas into water. The process needs also to be considered in terms of the equilibrium conditions which determines the

solubility of the gas and therefore its ultimate concentration at the prevailing temperature and pressure. Thus, for a given gas pressure and temperature, there will be equilibrium concentration (C^*) in the liquid and, conversely, for a given concentration (C^*) in the liquid there will be an equilibrium gas pressure (P^*) in the gas phase, as shown in (Figure 2.1).

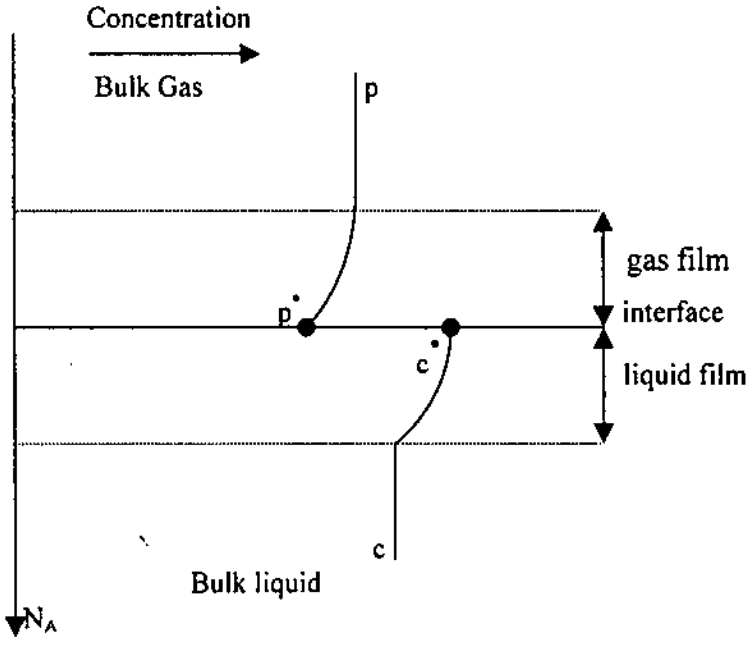

Figure (2.1) Schematic representation of a bubble water interface showing the oxygen pressure and concentration variation.

The transfer of oxygen from the bulk gas to the bulk liquid phase takes place in a series of stages:

(a) Diffusion from the bulk gas to the gas/liquid interface. This process is quick and establishes a saturation concentration at the interface

(b) Passage across the interface.

(c) Diffusion from the liquid side of the interface into the bulk liquid phase.

The interface of a bubble is composed of three regions: the interface itself, a static gas film and a static liquid film (Figure 2.1). The resistance to the transfer of oxygen resides in these films. Since the molecules in the films

have; high velocity, short mean free path and therefore, large number of collisions. The net passage of gas molecules through the film is therefore slow. The total resistance (R) to the transfer of oxygen can be considered as the summation of the individual resistances; i.e.

$$R_T = R_G + R_L + R_I \quad \text{..... (2.1)}$$

Where;

R_T = total resistance.

R_G = gas film resistance.

R_L = liquid film resistance.

R_I = interface resistance.

However, due to the difficulty in quantifying the magnitude of the individual resistances, it is more common to consider the mass transfer coefficients, K_L and K_G, where $K_L = 1/R_L$ and $K_G = 1/R_G$. So the total resistance to mass transfer of oxygen is

$$\frac{1}{K} = \frac{1}{K_L} + \frac{1}{H K_g} \quad \text{..... (2.2)}$$

Where; K = bulk transfer coefficient.

K_L = liquid-film coefficient;

K_g = gas-film coefficient;

H = Henry's law constant (an equilibrium partitioning coefficient).

In order to determine whether the liquid or the gas film resistance is dominant in equation (2.2) or both must be considered, an H value for the component of interest and a ratio of K_g/K_L are required. Munz and Roberts(1989) found the ratio of ($K_g/K_L = 40$), is the most applicable to mechanical surface aeration. A similar K_g/K_L ratio would be expected for most plunging jets (Gulliver et al., 1997). For such ratio, Munz and Roberts, found at least 95% of the gas

transfer resistance forms in the liquid-phase for $H \geq 0.55$. Since oxygen and nitrogen have a Henry's law constant significantly larger than 0.55, the liquid-film resistance will be assumed dominant for these gases in plunging liquid jets, in a sense of $K \approx K_L$.

The transfer interfacial area will also affect the rate of oxygen transfer where greater area leads to higher transfer rate. Assuming lateral fluxes and reaction rates are relatively small, the flux of any chemical in a moving control volume across an air-water interface may be defined by the following equation:

$$N_A = V \frac{dC}{dt} = KA\left(\frac{C_g}{H} - C\right) \quad \text{.....(2.3)}$$

Where;

N_A = flux per unit surface area;
V = control volume over which C and A are measured;
C = concentration of the dissolved chemical in the water;
t = time;
A = air-water surface area;
C_g = concentration in the gas phase (usually the atmosphere);
C_g/H = Saturation concentration, C_s.

Since oxygen has a dimensionless H greater than 0.55, and consequently $K \approx K_L$ as mentioned before, equation (2.3) may be written as

$$\frac{dC}{dt} = K_L \frac{A}{V}\left(\frac{C_g}{H} - C\right) \quad \text{..... (2.4)}$$

If C_s is assumed to be constant, the integration of equation (2.4) between upstream and downstream a hydraulic structure results in an equation for **Transfer efficiency**. (Gulliver and Rindels, 1993).

$$E = \frac{C_{ds} - C_{us}}{C_s - C_{us}} = 1 - \exp\left(- \int_{id}^{tu} K_L \frac{A}{V} dt \right) \quad \text{..... (2.5)}$$

Where subscripts *us* and *ds* refer to locations upstream and downstream of the hydraulic structure, respectively. A transfer efficiency of E = 1 means gas transfer up to the saturation level has occurred, i.e. the downstream water has become saturated, and a value of E = 0 means no gas transfer has occurred.

2.3 Flow Regimes over Stepped Structures:

A stepped channel consists of an open channel with a series of drops along the invert where the total fall is divided into a number of smaller falls. Various step geometry's are used: horizontal step, inclined step, and pooled step. Many researches handled horizontal steps and established correlation's for flow regimes, energy dissipation and aeration efficiency above horizontal steps, while only few handled inclined and pooled steps.

The geometry of a horizontal step is defined by its height, h, and horizontal length, L, as shown in (Figure 2.2) The step height and length are related to the spillway slope, α, by

$$\tan \alpha = \frac{h}{L} \quad \text{..... (2.6)}$$

The geometry of inclined step is defined by its height, h, inclined length, L and downgrade percentage (i%), as shown in (Figure 2.3b), while the geometry of pooled type step is defined by it's drop height, h, horizontal length of the pool, L and upgrade percentage (i%), as shown in (Figure 2.3a).

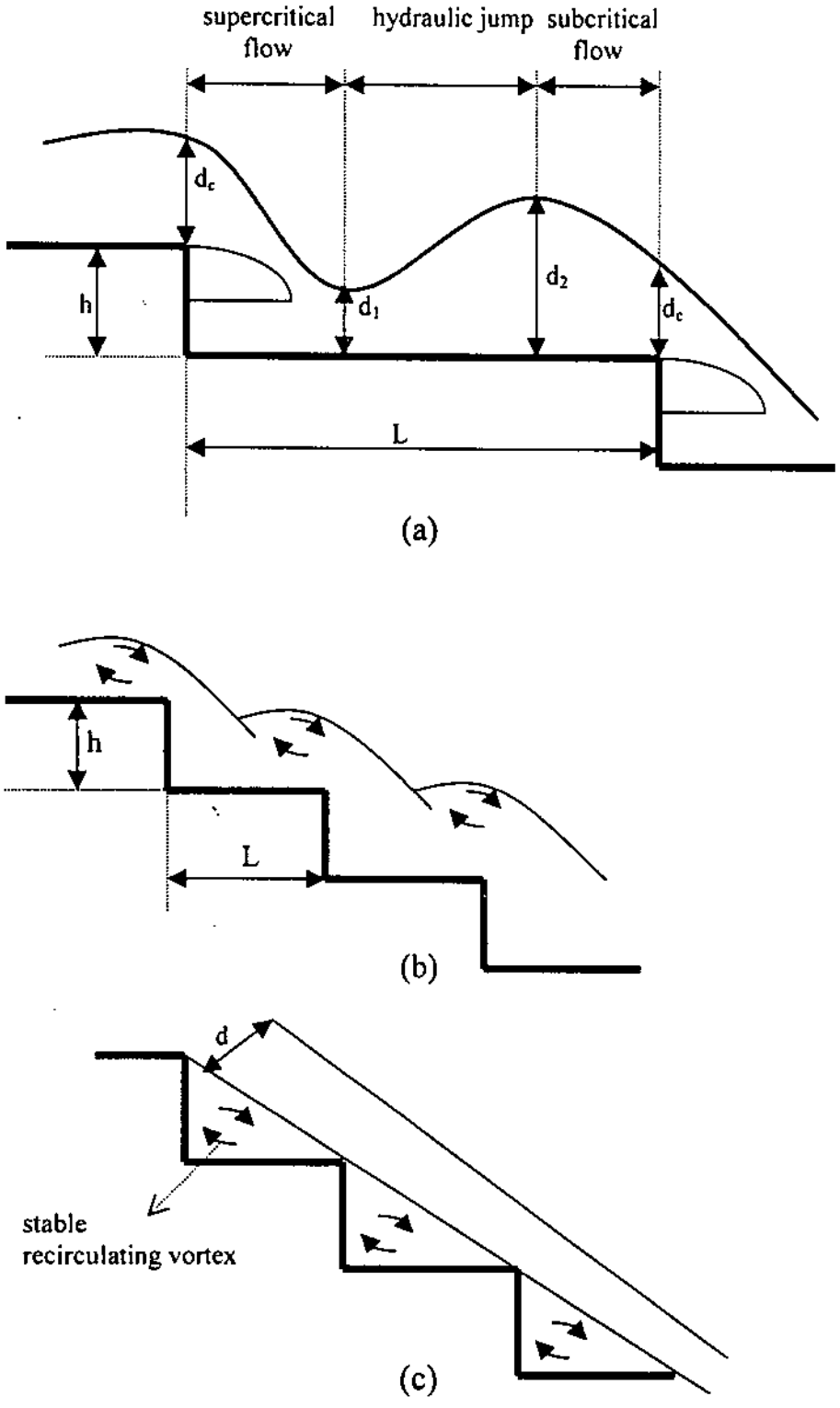

Figure (2.2) (a) Nappe flow with fully developed hydraulic jump; (b) Nape flow with partially developed hydraulic jump; (c) skimming flow above a stepped spillway.

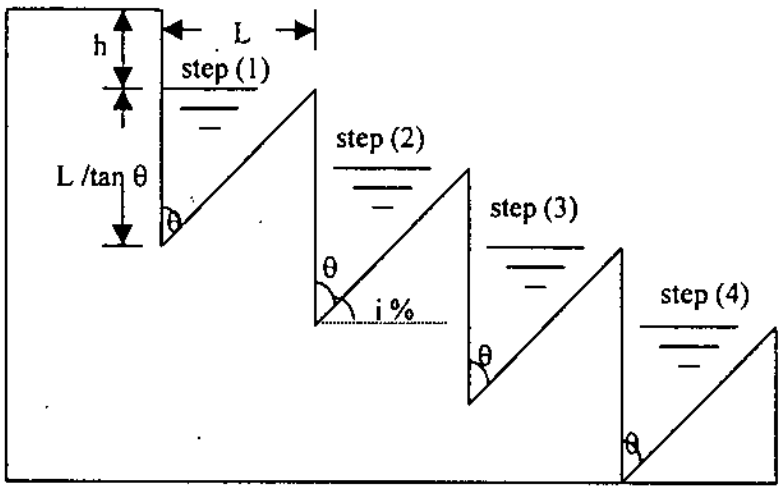

(a)

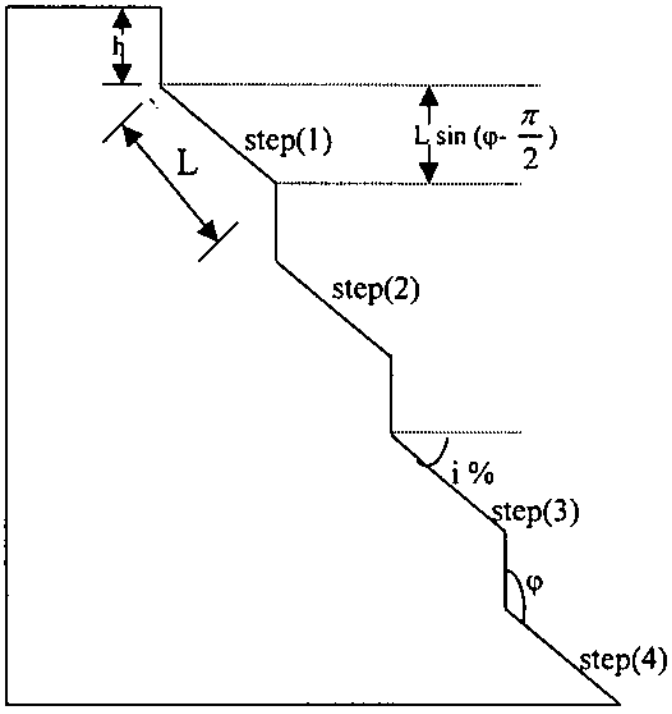

(b)

Figure (2.3). (a) Section of pooled type cascade ; (b) Section of inclined type cascade.

Regardless of step geometry two types of flow regime occur above the stepped spillway: nappe flow and skimming flow (Rajaratnam,1990) (Figure 2.2).

In nappe flow regime, the water proceeds in a series of plunges from one step to another. The flow from each step hits the step below as a falling jet.

Peyras, Royet and DeGoutte (1992) described two types of nappe flow: (i) nappe flow with fully developed hydraulic jump for low discharge and small flow depth (isolated nappe flow) (Figure 2.2a); and, (ii) nappe flow with partially developed hydraulic jump (partial nappe flow), (Figure 2.2b).

Air entrainment in nappe flow occurs near the impact of the falling jet with the horizontal step and at the hydraulic jump. Energy dissipation occurs by jet break up in air, jet mixing on the step, and with the formation of a fully developed or partial hydraulic jump on the step.

Moore (1943) and Rand (1955) analyzed a single-step drop structure (Figure 2.4). For horizontal step, the flow conditions near the end of the step change from subcritical to critical at some section a short distance back from the edge. The flow depth at the brink of the step d_b is:

$$d_b = 0.715 * d_c \quad \text{.....(2.7)}$$

Where; d_c is the critical flow depth.

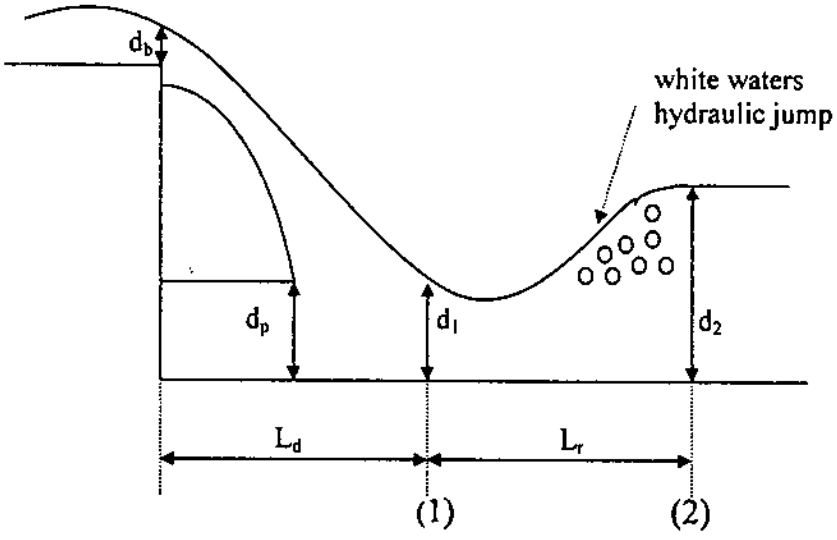

Figure (2.4) Flow at drop structure

Application of the momentum equation to the base of the overfall leads to (White, 1943):

$$\frac{d_1}{d_c} = \frac{2^{1.2}}{2^{\frac{3}{3.2}} + \sqrt{\frac{3}{2} + \frac{h}{d_c}}} \quad \text{.....(2.8)}$$

Where;

d_1 = the flow depth at section 1 (Figure 2.4);

h = the step height.

The total head H_1 at section 1 can be expressed non-dimensionally as:

$$\frac{H_1}{d_c} = \frac{d_1}{d_c} + \frac{1}{2} * \left(\frac{d_c}{d_1}\right)^2 \quad \text{.....(2.9)}$$

The flow depth and total head at section 2 (Figure 2.4) are given by the classical hydraulic jump equations:

$$\frac{d_2}{d_1} = \frac{1}{2} * \left(\sqrt{1 + 8 * Fr_1^2} - 1\right) \quad \text{..... (2.10)}$$

$$\frac{H_1 - H_2}{d_c} = \frac{(d_2 - d_1)^3}{4 * d_1 * d_2 * d_c} \quad \text{..... (2.11)}$$

Where;

Fr_1 is the Froude number defined at section 1, $Fr_1 = q_w / \sqrt{g * d_1^3}$

q_w is the flow rate per unit width of channel;

g is gravity constant.

Rand (1955) assembled several sets of experimental data and developed the following correlations:

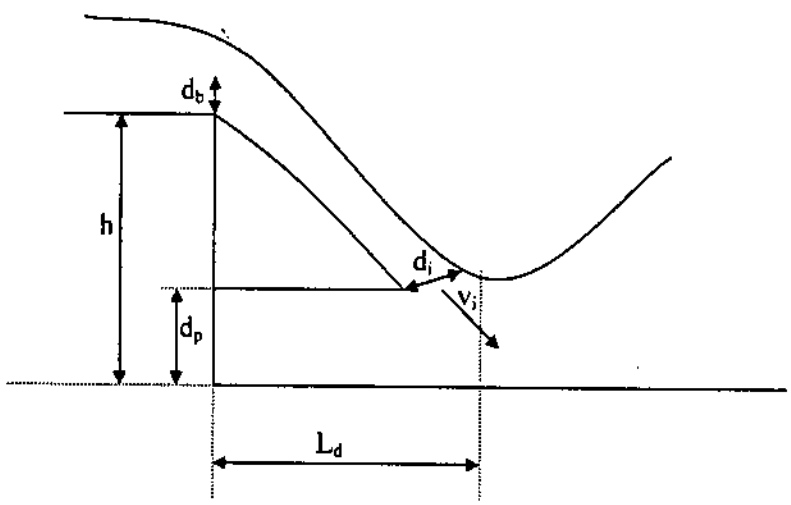

Figure (2.5) Nappe geometry

$$\frac{d_1}{h} = 0.54 * \left(\frac{d_c}{h}\right)^{1.275} \quad \text{..... (2.12)}$$

$$\frac{d_2}{h} = 1.66 * \left(\frac{d_c}{h}\right)^{0.81} \quad \text{..... (2.13)}$$

$$\frac{d_p}{h} = \left(\frac{d_c}{h}\right)^{0.66} \quad \text{..... (2.14)}$$

$$\frac{L_d}{h} = 4.30 * \left(\frac{d_c}{h}\right)^{0.81} \quad \text{..... (2.15)}$$

Where; d_p is the height of the water in the pool behind the overlaying jet and L_d is the distance from the vertical face of the step to the position of the depth d_1 (Figure 2.4). Equation (2.12) is an empirical correlation that fits well equation (2.8). Equations (2.12) to (2.15) were obtained for an aerated nappe.

Using the momentum equation, the flow conditions at the impact of the nappe with the receiving pool can be deduced. Assuming that the velocity of the aerated flow nappe at the brink of the step is horizontal, and when the fluid leaves the step, with a vertical acceleration only and equals minus the gravity constant. The time t, taken to reach the pool free-surface is given by:

$$d_p = \frac{-1}{2} * g * t^2 + \left(h + \frac{d_b}{2}\right) \quad \text{..... (2.16)}$$

Where; d_b is the flow depth at the brink of the step.

The nappe thickness d_i and the flow velocity V_i at the intersection of the falling nappe with the receiving pool are :

$$\frac{d_i}{d_c} = \left(\left(\frac{d_c}{d_b}\right)^2 + 2 * \frac{h + \frac{d_b}{2} - d_p}{d_c}\right)^{-1/2} \quad \text{..... (2.17)}$$

$$\frac{V_i}{V_c} = \sqrt{\left(\frac{d_c}{d_b}\right)^2 + 2 * \frac{h + \frac{d_b}{2} - d_p}{d_c}} \quad \text{..... (2.18)}$$

The angle of the falling nappe with the horizontal (Figure 2.5) is given by:

$$\tan\phi=\sqrt{2}*\sqrt{\frac{d_b}{d_c}}*\sqrt{\frac{h+\frac{d_b}{2}-d_p}{d_c}} \quad \text{.......... (2.19)}$$

Using equations (2.7) and (2.14) the nappe thickness d_i, the nappe velocity V_i and the angle of the nappe, ϕ with the horizontal, at the impact, can be correlated in term of d_c/h ratio by:

$$\frac{d_i}{d_c}=0.687*\left(\frac{d_c}{h}\right)^{0.483} \quad \text{.......... (2.20)}$$

$$\frac{V_i}{V_c}=1.455*\left(\frac{d_c}{h}\right)^{-0.483} \quad \text{.......... (2.21)}$$

$$\tan\phi=0.838*\left(\frac{d_c}{h}\right)^{-0.586} \quad \text{.......... (2.22)}$$

where; V_c is the critical velocity.

Downstream of the impact of the nappe (Figure 2.4), the roller length of a fully-developed hydraulic jump is estimated as (Hager et al. 1990):

$$\frac{L_{ro}}{d_1}=8*(Fr_1-1.5) \quad \text{.......... (2.23)}$$

where; L_{ro} is the length of roller and d_1 and Fr_1 are the depth of the flow and the Froude number immediately upstream of the jump.

If the length of the drop L_d plus the length of the roller L_{ro} is smaller than the length of a step L, a fully developed hydraulic jump can take place (Figure 2.4). Combining equations (2.15) and (2.23), a condition for nappe flow regime with fully developed hydraulic jump is deduced. A nappe flow

with fully-developed hydraulic jump occurs for discharge smaller than a critical value and it can be defined by:

$$\left(\frac{d_c}{h}\right)_{char} = 0.0916\left(\frac{h}{L}\right)^{-1.276} \quad \text{..... (2.24)}$$

Nappe flow conditions with fully developed-hydraulic jump occur for $dc/h < (d_c/h)_{char}$. Note that the correlation (2.24) was obtained for:

$0.2 \leq h/L \leq 6.$

Along a stepped spillway, critical flow conditions occur near the end of each step, and equation (2.8) to (2.23) provide the main flow parameters for a nappe flow regime with fully-developed hydraulic jump. Peyras, Royet and DeGoutte (1992) indicated that these equations can be applied also with reasonable accuracy to nappe flows with partially developed hydraulic jump.

An increase in discharge or of slope of stepped channel, might induce the transition from a nappe flow regime to a skimming flow regime. In the skimming flow regime, the water flows down the stepped face as a steady stream, skimming over the steps, and is cushioned by the recalculating fluid trapped between them (Figure 2.2c). The external edges of the steps form a pseudo-bottom, over which the flow passes. Beneath this, recalculating vortices develop and are maintained through the transmission of shear stress from the water flowing past the edge of the steps. In addition, small-scale vorticity will be generated continuously at the corner of the steps. For horizontal steps, the onset of skimming flow is a function of the discharge (i.e. critical depth) and the step height and length. Experimental data obtained by Essery and Horner (1978) and Peyras, Royet and DeGoutte (1992) showed that the onset flow conditions may be estimated as:

$$\left(\frac{d_c}{h}\right)_{onset} = 1.01 - 0.37\frac{h}{L} \quad \text{..... (2.25)}$$

and skimming flows occur for $d_c/h > (d_c/h)_{onset}$.

Assuming a long stepped spillway and that the uniform flow conditions are reached before the end of the spillway, the uniform flow depth can be deduced from the momentum equation:

$$\tau_o P_w = \rho_w g A' \sin\alpha \quad \text{..... (2.26)}$$

Where;

τ_o = the average shear stress between the skimming flow ;and the recirculating fluid underneath.

P_w = the wetted perimeter;

ρ_w = the water density;

A' = the channel cross section area.

The average bottom shear stress, τ_o for open channel flow, is defined as (Henderson, 1966, Streeter et al, 1981):

$$\tau_o = \frac{f}{8} \rho_w V_o^2 \quad \text{..... (2.27)}$$

Where; f = friction factor.

V_o = the uniform non-aerated flow velocity.

For a wide channel, the uniform flow parameters, V_o and d_o, are deducted from the continuity and momentum equations, and can be written in dimensionless form as:

$$\frac{V_o}{V_c} = 3\sqrt{\frac{8\sin\alpha}{f}} \quad \text{..... (2.28)}$$

$$\frac{d_o}{d_c} = 3\sqrt{\frac{f}{8\sin\alpha}} \quad \text{.....(2.29)}$$

Where; α = spillway slope;

d_o = water flow depth for uniform non-aerated flow.

It must be emphasized that these results were obtained for non-aerated flow. The effects of air entrainment on the flow properties, will be discussed later.

Morris (1955) and Knight and Mac-Donald (1979) analyzed skimming flows over large roughness elements of rectangular cross section. Their results indicated that the classical flow resistance calculation must be modified to take into account the shape of the roughness element. The shear stress, τ_o, used in equation (2.26), represents the turbulent shear stress between the main stream and the recirculating fluid trapped between the steps of spillway. For stepped spillway, the steps form the dominant surface roughness (Sorensen, 1985). If the roughness height, K_s, is estimated as the depth of a step normal to the flow (i.e. $K_s = h \cos\alpha$), the dimensions of the step are defined completely by K_s and the spillway slope. Dimensional analysis suggests that the friction factor is a function of a Reynolds number, the roughness height (K_s), and the spillway slope:

$$f = f\left(\mathrm{Re};\ \frac{K_s}{D_H};\ \alpha\right) \quad \text{.....(2.30)}$$

If the uniform flow conditions are known, the friction factor can be deduced from the momentum equation (2.26):

$$f = \frac{8\,g\,(Sin\,\alpha)\,d_o^2}{q_w^2}\left(\frac{D_H}{4}\right) \qquad \text{.....(2.31)}$$

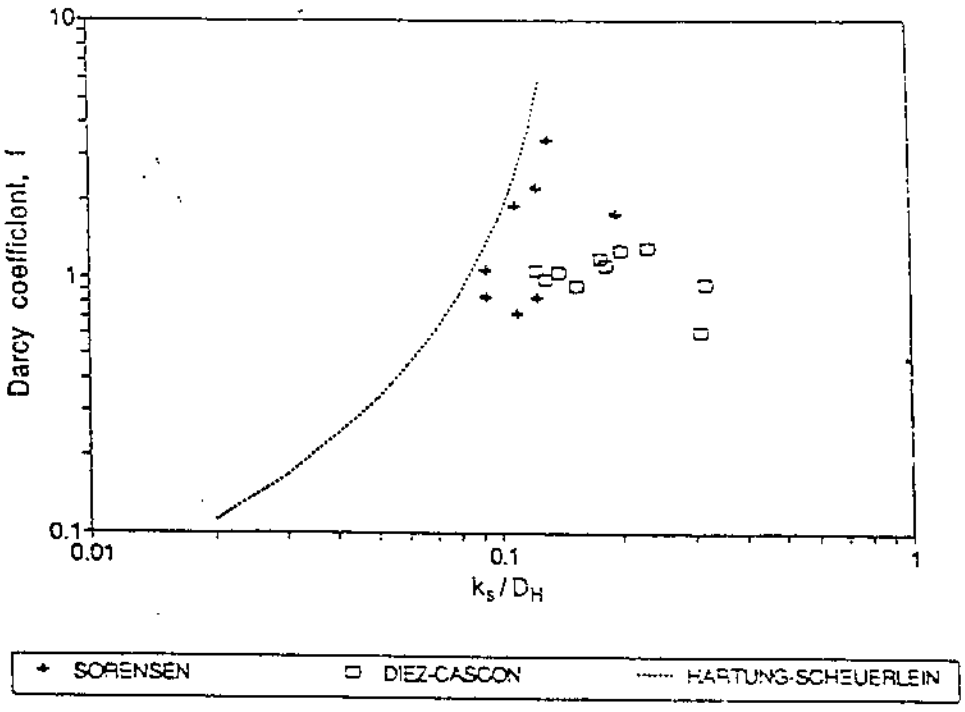

Figure (2.6) Non-aerated friction factor on stepped spillways: Sorenson (1980), Diez-Cascon et al. (1991), Hartung and Scheuerlein (1970) for a slope, α, of 30°.

Sorensen (1985) and Diez-Cascon, Blanco, Revilla and Garcia (1991) measured flow depths at the bottom of long stepped spillway models. Their data were reanalyzed using equation (2.31) and neglecting the aeration of the flow. The results are presented in Figure (2.6), with the friction factor plotted as a function of the relative roughness. Figure (2.6) indicates friction factors in the range of 0.6-3.5, with an average value of 1.30. Such large values of the friction factor imply smaller flow velocity and greater flow depth than on a smooth spillway, and enhance aeration and energy dissipation.

Hartung and Scheuerlein (1970) studied open channel flows on rockfill dams, with great natural roughness and steep slopes. For slopes in the range of 6-34°, and in the absence of air entrainment, their results are presented as:

$$\frac{1}{\sqrt{f}} = -3.2\ \log_{10}\left[(1.7+8.1\sin\alpha)\frac{K_s}{D_H}\right] \qquad (2.32)$$

For a slope of 30° and $K_s/D_H = 0.1$, equation (2.32) provides a value of the friction factor $f = 1.7$ of similar order of magnitude as the results obtained on stepped spillways (Figure 2.6).

Skimming flows are characterized by large friction losses and a strong air entrainment process. In the case of large dams, it has been shown that they dissipate more energy than nappe flows (Chanson, 1994b).

2.4 Energy Dissipation:

2.4.1 Energy Dissipation in Nappe Flow Regime:

In a nappe flow condition with fully developed hydraulic jump, the head loss at any intermediary step equals the step height. The total head loss along the spillway, ΔH, equals the difference between the maximum head available, H_{max}, and the residual head at the bottom of the spillway, H_1, (equation 2.9) and can be written in dimensionless form:

$$\frac{\Delta H}{H_{max}} = 1 - \left[\frac{d_1}{d_c} + \frac{1}{2}\left(\frac{d_c}{d_1}\right)^2\right] / \left[\frac{3}{2} + \frac{H_{dam}}{d_c}\right] \qquad (2.33)$$

where; H_{dam} is the dam height and d_1 is given by equation (2.8) and equation (2.12), The maximum head available and the dam height are related by:

$$H_{max} = H_{dam} + 1.5\ d_c \qquad (2.34)$$

The residual energy is dissipated at the toe of the spillway by hydraulic jump in the dissipation basin. Combining equations (2.12) and (2.33), the total energy loss becomes:

$$\frac{\Delta H}{H_{max}} = 1 - \frac{0.54\left(\frac{d_c}{h}\right)^{0.275} + \frac{3.43}{2}\left(\frac{d_c}{h}\right)^{-0.55}}{\frac{3}{2} + \frac{H_{dam}}{d_c}} \quad \text{..... (2.35)}$$

Equations (2.33) and (2.35) were obtained for nappe flows with fully developed hydraulic jump. Peyras, Royet and DeGoutte (1992) performed experiments for nappe flows with fully and partially developed hydraulic jumps. The rate of energy dissipation of nappe flows with partially developed hydraulic jump was within 10% of the values obtained for nappe flows with fully developed hydraulic jumps for similar flow conditions. Therefore, it is believed that equation (2.25) may be applied to most of the nappe flow situations with reasonable accurcy.

2.4.2 Energy Dissipation in Skimming Flow Regime:

In skimming flow, most of the energy is dissipated in the maintenance of stable depression vortices. If uniform flow conditions are reached at the downstream end of the spillway, the total head loss is:

$$\frac{\Delta H}{H_{max}} = 1 - \frac{\frac{d_o}{d_c}\cos\alpha + \frac{E'}{2}\left(\frac{d_c}{d_o}\right)^2}{\frac{H_{dam}}{d_c} + \frac{3}{2}} \quad \text{..... (2.36)}$$

where; E′ is the kinetic energy correction coefficient. Using equation (2.29), the head loss may be rewritten in terms of the friction factor, the spillway slope, the critical depth, and the dam height:

$$\frac{\Delta H}{H_{max}} = 1 - \left[\left(\frac{f}{8\sin\alpha}\right)^{1/3}\cos\alpha + \frac{E'}{2}\left(\frac{f}{8\sin\alpha}\right)^{-2/3}\right] \Big/ \left[\frac{H_{dam}}{d_c} + \frac{3}{2}\right] \quad \text{..... (2.37)}$$

For a high dam, the residual energy term is small and equation (2.37) is similar to the expression obtained by Stephensen (1991):

$$\frac{\Delta H}{H_{max}} = 1 - \left[\left(\frac{f}{8\sin\alpha}\right)^{1/3}\cos\alpha + \frac{E'}{2}\left(\frac{f}{8\sin\alpha}\right)^{-2/3}\right]\frac{d_c}{H_{dam}} \quad \text{..... (2.38)}$$

Equation (2.38) shows that the energy loss ratio increase with the height of the dam. For high dams, it becomes more appropriate to talk of residual head, H_{res}, than total head loss:

$$\frac{H_{res}}{d_c} = \left(\frac{f}{8\sin\alpha}\right)^{1/3}\mathrm{Cos}\,\alpha + \frac{E'}{2}\left(\frac{f}{8\sin\alpha}\right)^{-2/3} \quad \text{.....(2.39)}$$

Equations (2.37) and (2.39) suggest that the total energy dissipation above the spillway and the residual energy at the bottom of the spillway are functions of the friction factor, spillway slope, discharge (i.e. critical depth), and dam height. These calculations, equations (2.37) and (2.39) depend critically upon the estimation of the friction factor, and as friction factor is affected significantly by the rate of aeration, equations (2.37) and (3.38) must be used with caution. On steep spillways, the flow aeration reduces the flow resistance and hence the rate of energy dissipation, (Chanson,1993a).

2.5 Air- water Gas Transfer

One of the most important water quality parameters in rivers and streams is dissolved oxygen (DO). The oxygen concentration is a prime indicator of the quality of the water. Dams and weirs across a stream affect the air-water gas transfer dynamics. Deep and slow pools of water upstream of a dam reduce the gas transfer process and the natural re-aeration as compared with an open river; but some hydraulic structures (e.g. spillway and stilling basin) can enhance the oxygen transfer during water releases.

The flow conditions above a stepped spillway are characterized by a high level of turbulence, and large quantities of air are entrained. Turbulent mixing and air-entrainment contribute to an enhancement of the air-water gas transfer along stepped spillway, as compared with smooth spillway. The gas transfer must be taken into account for the re-oxygenation of polluted streams and rivers, but also to explain the high fish mortality downstream of large hydraulic structures caused by nitrogen supersaturation. In this section the air-water gas transfer theory for glacis spillway is discussed first and then followed by this research main subject, the aeration through cascade structure.

2.5.1 Predicting Oxygen Content Downstream Spillway and Waterways:

During storm and flood events, large water bodies are released in storm waterways and spillways, and induce supercritical flows with air entrainment at the free surface. This self-aeration contributes to the air-water transfer of oxygen and nitrogen since air bubbles within the flow increase substantially the air-water interface area. Figure (2.7) shows a typical weir structure includes a spillway followed by a dissipation basin with a hydraulic jump. Aeration occurs along the spillway and at the hydraulic jump in the stilling basin.

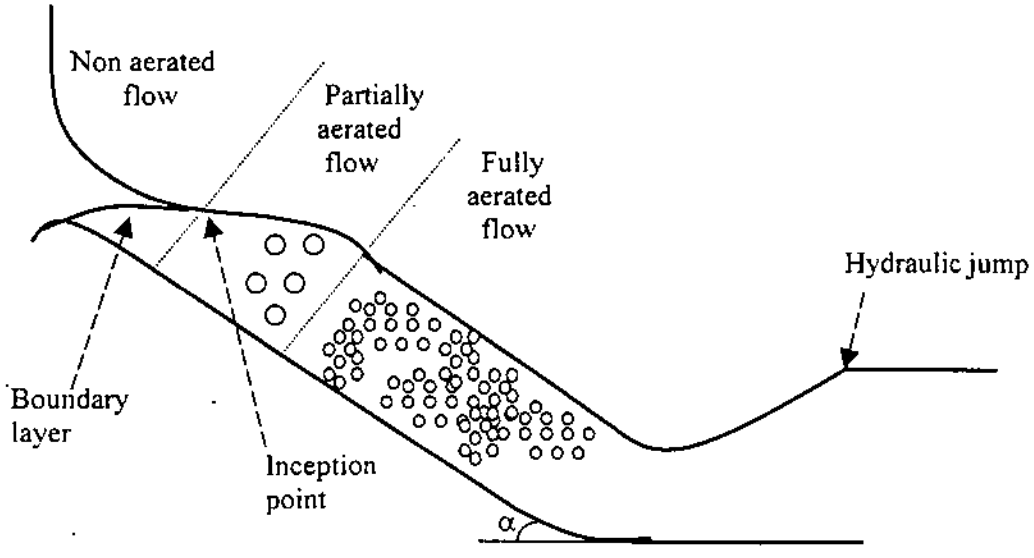

Figure (2.7) Self-aerated flow over a channel.

Air-water gas transfer

As mentioned before Fick's law states that the mass transfer rate of a chemical across an interface and in a quiescent fluid varies directly as the coefficient of molecular diffusion and the negative gradient of gas concentration. The gas transfer of a dissolved gas (e.g. Oxygen) across an air water interface is controlled by the liquid. Using Henry's law, it is usual to write Fick's law by equation (2.4).

$$\frac{dC}{dt} = K_L\, a\,(C_s - C)$$

Where; C_s = The saturation concentration.

A recent review of the transfer coefficient calculation in turbulent flows showed that K_L is almost constant regardless of the bubble size and flow situations (Kawase and Moo-Young, 1992). Using Higbie's (1935) penetration theory, the transfer coefficient of large bubbles (i.e. $d_b > 0.25$ mm) affected by surface active impurities can be estimated as:

$$K_L = 0.47\ \sqrt{D_{gas}}\left(\frac{\mu_w}{\rho_w}\right)^{-1/6} \sqrt[3]{g} \qquad \text{..... (2.40)}$$

Where; D_{gas} is the molecular diffusivity.

In free-surface flows along a spillway, the pressure variations are small, and the liquid density and viscosity can be assumed functions of the temperature only. In most practical applications, the temperature and salinity are constant along a chute, and the coefficient of transfer K_L and the saturation concentration C_s become two constants in equation (2.4). Along a channel and at each location, equation (2.4) can be averaged over the cross-section, and it yields (Chanson, 1995 a):

$$\frac{dC}{dx} = \frac{K_L a_{mean}}{U_w}(C_s - x\,C) \quad \text{.....(2.41)}$$

where; U_w is the mean flow velocity, a_{mean} is the mean specific interface area, and x is a factor (close to unity) varying with the distributions of air-water interface area and dissolved gas concentration. If the equation (2.41) is integrated along a channel, flow aeration at weirs and spillway can be measured by the deficit ratio r defined as

$$r = \frac{C_s - C_{us}}{C_s - C_{ds}} \quad \text{.....(2.42)}$$

Where; C_{us} is the upstream dissolved gas concentration, and C_{dS} is the dissolved gas concentration at the downstream end of the channel. Another measure of aeration is the aeration efficiency E as

$$E = \frac{C_{ds} - C_{us}}{C_s - C_{us}} = 1 - \frac{1}{r} \quad \text{.....(2.43)}$$

The temperature effect on the flow aeration was examined by several researchers (Table 2.1). Standard methods for the examination of water and wastewater (APAHA, AWWA and WPCF, 1989) suggests the use of an exponential relation to describe the temperature dependence on oxygen transfer

$$\frac{In(r)}{In(r_{T_o})} = 1.0241^{(T-T_o)} \quad \text{.....(2.44)}$$

where r is the deficit ratio at temperature T, T_o is the reference temperature, and the constant 1.0241 was obtained by Elmore and West (1961).

Table (2.1): Temperature dependence of flow aeration.

References	Temperature dependence	Comments
Gameson et al (1958)	$\frac{Ln(r_T)}{Ln(r_{15})} = 1 + 0.027(T - 288.15)$	273.15 < T< 313.15K
Elmore and West (1961)	$\frac{Ln(r_T)}{Ln(r_{20})} = 1.00241^{(T-293.15)}$	278.15 < T < 303.15K
Holler (1971)	$\frac{Ln(r_T)}{Ln(r_{To})} = \theta^{(T-T_o)}$	θ in the range 1.014 - 1.047
Danil and Gulliver (1988)	$\frac{Ln(r_T)}{Ln(r_{20})} = \sqrt{\left[\left(\frac{T}{293}\right)\right]\left(\frac{\nu_{20}}{\nu}\right)\sqrt{\frac{\rho_{20}}{\rho}}}$	273.15 < T < 313.15K
Gulliver et al. (1990)	$\frac{Ln(r_T)}{Ln(r_v)} = \sqrt{\left[\left(\frac{T}{T_o}\right)\right]\left(\frac{\mu_{To}}{\mu_T}\right)^{3/4}\left(\frac{\rho_{To}}{\rho_T}\right)^{17/20}\left(\frac{\sigma_{To}}{\sigma_T}\right)^{3/5}}$	273.15 < T < 313.15K
Danil et al. (1991)	$\frac{Ln(r_T)}{Ln(r_{20})} = 1 + 0.02103(T - 273.15) + 8.261*10^{-5}(T - 273.15)^2$	

Self aeration efficiency

Chanson (1995a) performed a series of oxygen transfer calculations in self aerated flows, assuming zero salinity, constant channel slopes ranging from 15° up to 60°, channel length between 20m and 250m, discharges from 0.5 m^2/s to 50 m^2/s, roughness heights between 0.1mm and 10mm, and temperature between 5° and 30°. The analysis of the oxygen transfer computations indicates that the free-surface aeration efficiency is independent of the initial gas content. For discharges larger than 0.5 m^2/s, the numerical results suggest that the self aeration efficiency can be correlated by

$$E_{SA} = \left(1 - \frac{q_w}{(q_w)_c}\right)^{(15.38 - 0.03517)(\sin\alpha)^{-1/3.13}} \quad \text{.....(2.45)}$$

Where $(q_w)_c$ is the discharge for which the growing boundary layer reaches the free surface at the spillway end, and no self-aeration occurs. The characteristic discharge $(q_w)_c$ can be assumed by Wood's (1985) formula:

$$(q_w)_c = 0.0805\,(L_{spillway})^{1.403}\,(\mathrm{Sin}\alpha)^{0.382}\,K_s^{0.0975} \quad \ldots\ldots\ldots\ldots\ldots\ldots\ldots\ldots (2.46)$$

where; $L_{spillway}$ is the spillway length, and K_s is the roughness height.

Self-aeration measurements and calculations indicate that aeration efficiency increases with temperature and decreases when the discharge increase. It must be emphasized that the calculations become inaccurate for flat slopes (i.e. $\alpha < 15^{\circ}$). For flat channels, little self-aeration occurs.

At the downstream end of a spillway, most flows are supercritical and the total head is larger than that of the downstream river. Most river and stream flow regimes are subcritical: a transition from supercritical to subcritical (i.e. hydraulic jump) occurs near the end of the spillway (Figure2.7). The hydraulic jump is characterized by the development of large-scale turbulence, energy dissipation, and air entrainment. Gas transfer results from the large number of entrained air bubbles and turbulent mixing in the jump. Several researchers have proposed correlations to predict the oxygen transfer at the hydraulic jump (Table 2.2).

The overall aeration efficiency, at a weir (Figure 2.7) is

$$E = E_{SA} \times E_{HJ}\,(1-E_{SA}) \quad \ldots\ldots\ldots\ldots\ldots\ldots\ldots\ldots\ldots\ldots\ldots\ldots\ldots\ldots (2.47)$$

Where E_{SA} is the self-aeration efficiency, and E_{HJ} is the efficiency of the hydraulic jump. It should be emphasized that E_{SA} and E_{HJ} must be taken at the same temperature of reference.

Table (2.2): Oxygen transfer at hydraulic jump.

References	Formula	Comments
Holler (1971)	$r_{20} - 1 = 0.0463\ \Delta V^2$	Model experiments $0.61 < \Delta V < 2.44$ m/s $277.15 < T < 299.15$K
Apted and Novak (1973)	$r_{15} = 10^{(0.24\ \Delta H)}$	Model experiments $2 < Fr < 8$ $q_w = 0.04\ m^2/s$
Avery and Novak (1975)	$r_{15} - 1 = 0.023 \left(\frac{q_w}{0.0345}\right)^{3/4} \left(\frac{\Delta H}{d}\right)^{4/5}$	Model experiments $2 < Fr < 9$ $1.45E+4 < Re < 7.1E+4$ $287.15 < T < 291.35$K B = 0.1 m
Avery and Novak (1978)	$r_{15} - 1 = k' Fr^{2.1} Re^{0.75}$ $k' = 1.0043E-6$: tap water with 0% $NaNO_2$ $k' = 1.244E-6$: tap water with 0.3%$NaNo_2$ $k' = 1.5502E-6$: tap water with 0.6% $NaNO_2$	Model experiments $1.45E+4 < Re < 7.1E+4$ $v = 1.143E-6\ m^2/s$ B= 0.381 m
Wilhelms et al. (1981)	$r_{15} - 1 = 4.924E-8\ Fr^{2.106} Re^{1.034}$	Model experiments $1.89 < Fr < 9.5$ $2.4E+4 < Re < 4.3E+4$ B= 0.381 m

2.5.2 Aeration at weirs of single drop:

A substantial number of researchers have studied aeration of weirs with single drop and cascades. Three factors are evidently of main importance, namely: (1) fall height; (2) discharge; and (3) tail water depth.

Various empirical equations for aeration efficiency at weirs are tabulated in Table (2.3).

Avery and Novak, contributed substantially to the theory of weir-aeration as they performed a series of tests and proposed prediction equation for aeration efficiency at base of free overfall.

Table (2.3): Prediction equations for aeration efficiency at weirs.

Reference	prediction equation	Units	Source
Gameson et al (1958)	$r = 1+0.11\ M\ N\ (1+0.046T)h$	h, in ft	model
Javis (1970)	$r_{15} = 1.05\ h^{0.4344}$	h, in m	model
Holler (1971)	$r_{20} = 1+0.91\ h$	h, in m	model
Holler (1971)	$r_{20} = 1+0.21\ h$	h, in m	prototype
dept. of env. (1973)	$r = 1+0.38ah\ (1-0.11h)(1+0.046T)$*	h, in m	model
dept. of env. (1973)	$r = 1+0.69h\ (1-0.11h)(1+0.0464T)$*	h, in m	model
Avery&Novak (1978)	$r_{15}=K_t(g/2)^{0.445}(\nu)^{-0.53}\ h^{1.335}\ q_j^{-0.36}$	h in m, q_j in m^2/s	model
Nakasone (1987)	$\text{Ln}\ r_{20}=A(D+1.5d_c)^a\ q_w^b\ d_t^c$	D,d_c in m, q_w in $m^3/h.m$, d_t in m	model
Princince (1991)	$\text{Ln}\ r_{20}=0.042\ h^{0.872} q_w^{0.504}$** $\text{Ln}\ r_{20}=0.077\ h^{0.623}\ q_w^{0.66}$***	h in m q_w in $m^3/m.h$	model
Labocha et. al. (1996)	$\text{Ln}\ r_{20}=A\ h^a\ Q^b$	h in m, Q in m^3/s	model

* Optimum depth conditions.
** Primary clarifier
*** Secondary clarifier

Avery and Novak (1978) conducted experiments with jets discharged by a 100mm circular and rectangular notch, and 220mm and 300mm wide rectangular notches also.

These jets fell freely to a pool of width 1m, length 1.5m and of various depths and bed elevations. They studied the effect of pool geometry, effect of jet shape and proposed correlation equation for aeration efficiency of falling jets.

Effect of pool geometry: For a particular weir and pool bed elevation, the oxygen transfer will increase as the pool depth increases until an optimum depth is reached. This depth corresponds to the depth to which the bubbles penetrate if unimpeded, and therefore maximum contact time of bubbles is attained. Further increase in depth lead to a drop in the oxygen transfer, since

there is no further gain in contact time while there has been a reduction in the height of fall of the jet. Also Avery and Novak (1978) performed some tests as shown in Figure (2.8) on the effect of reducing the pool width. The sides of the channel will influence the hydraulic conditions within the pool, but should not alter the quantities of air entrained. A significant reduction in the pool width will restrict the sideways spread of the bubbles, thus possibly adversely affecting the contact time although the increased velocity along the length of the channel will lengthen the path traveled by the bubbles to the interface. From Figure (2.8) it is apparent that effects of the pool width on the oxygen transfer are noticeable at the larger heights of fall when a decrease of the deficit ratio with narrowing of the pool occurred; this decrease occurs in the vicinity of the optimum depth.

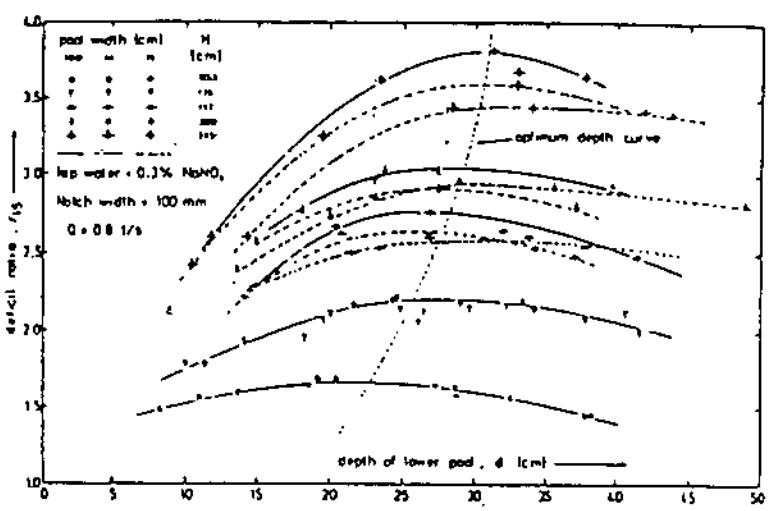

Figure (2.8) Effect on oxygen transfer of lower pool geometry for fixed discharge and various elevations of pool (Avery and Novak, 1978).

Effect of jet shape: The effect of jet shape is complicated, with a constant discharge and at each height of fall, alternating the jet shape from circular (100mm notch) to broadly rectangular (220 mm, 300 mm notches) reduced the hydraulic radius and resulted in a reduction in the optimum depth (i.e. depth of bubble penetration). Despite the resultant reduced contact time, there was a noticeable increase in the recorded oxygen uptake which is indicative of the greater relative quantities of air entrained which offset the accompanying reduced contact time. Because of this conflict between effects of bubble contact time and quantities of air entrained, a concept of jet Froud number has been established. Jet Froude number has been defined (Avery and Novak, 1978) as:

$$F_J = \left(\frac{\pi\sqrt{2gh^5}}{Q}\right) = \left(\frac{gh^3}{2q_J^2}\right)^{0.25} \quad \text{..... (2.48)}$$

Where;

q_J = the jet discharge per unit jet perimeter at the point of impact, $q_J = R\sqrt{2gh}$;

R = The hydraulic radius of the jet at the impact.

Avery and Novak (1978) reported their experiments as a relationship between d'_1 (the optimum tail water depth) divided by h (the fall height) and Froude number for the full range of circular and rectangular jets:

$$\frac{d'_1}{h} = \frac{7.5}{F_J^{0.53}\, h^{0.42}} \quad \text{..... (2.49)}$$

The relationship between the Froude number and deficit ratio is shown in Figure (2.9) for depths equal to or exceeding the optimum. For constant Froude number, there is a significant variation in the quantities of oxygen transferred. This is in part, due to differing depths of jet penetration associated

with the different jet shapes, but also to different heights and thus energy losses or turbulence in the downstream pool.

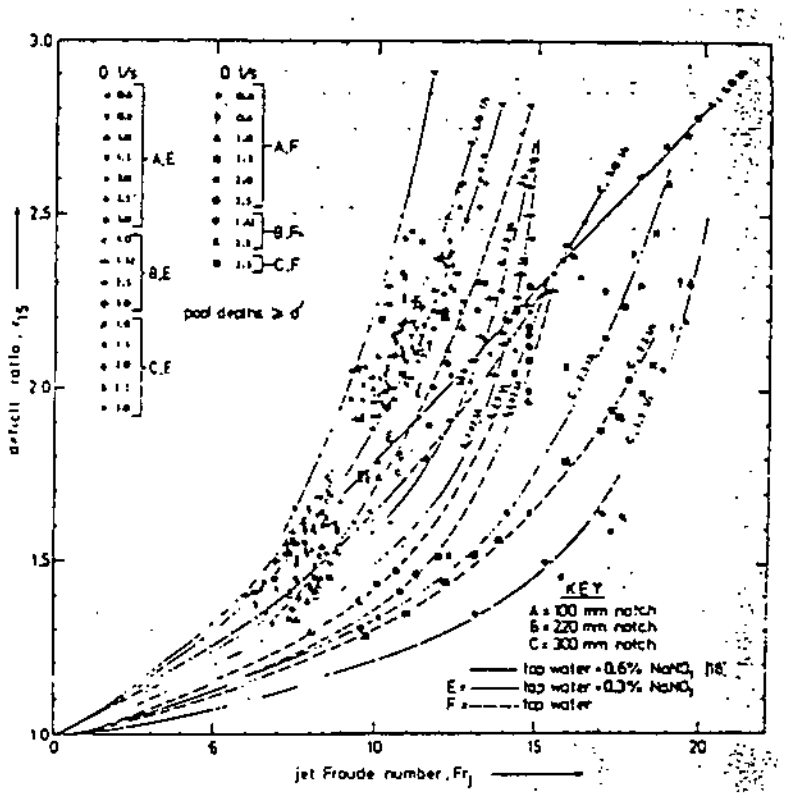

Figure (2.9) Deficit ratio vs. jet Froude number for various free overfall jets (Avery and Novak, 1978).

The results for pool depths equal to or exceeding the optimum, are described by the following equation:

$$r_{15} - 1 = K_o F_j^{0.72} h^{0.8} \text{ .....(h in cm)} \quad \text{.....} \quad (2.50)$$

Where K_o is the function of the dissolved sodium nitrite concentration .

Equations (2.49) and (2.50) can be re-expressed for $\nu = 1.143 \times 10^{-6}$ m^2/s as:

$$d'_i = 7.5 \left(\frac{2\nu^2}{g}\right)^{0.19} \mathrm{Re}^{0.39} F_j^{0.24} = 0.0306\, \mathrm{Re}^{0.39} F_j^{0.24} \quad \text{.....} \quad (2.51)$$

and

$$r_{15} - 1 = K_1 \, \mathrm{Re}^{0.53} \, F_J^{1.78} \quad \ldots\ldots (2.52)$$

where; r_{15} is the deficit ratio at 15°C; K_1 is a function of the concentration of dissolved sodium nitrite Na_2SO_3 and equal to 0.627×10^{-4} for tap water; and Re is the Reynolds number.

Equation (2.52) can also be written as:

$$r_{15} - 1 = K_1 \left(\frac{g}{2}\right)^{0.445} (\nu)^{-0.53} \, h^{1.335} \, q_J^{-0.360} \quad \ldots\ldots (2.53)$$

Equation (2.53) includes fall height and discharge and it is applicable to multiple jet weirs and cascades. If one circular jet of Froude number F_J is split into N jets of equal diameter, the resultant Froude number can be attained for the same discharge and height of fall by splitting the jet; therefore greater aeration is achieved (Avery and Novak, 1978). This has been experimentally confirmed (Van Der Kroon and Schram, 1969).

Since a cascade weir consist of a series of free overfalls with pools strung together, use can be made of equation (2.53) to be applied to each step and thus trace the dissolved oxygen profile through the cascade. If the cascade consisted of a series of n equal steps, the deficit ratio for this type of cascade will be r^n in which r deficit ratio for one step. Figure (2.10) shows a comparison of aeration efficiency at hydraulic jump, free overfall weir and cascade weir.

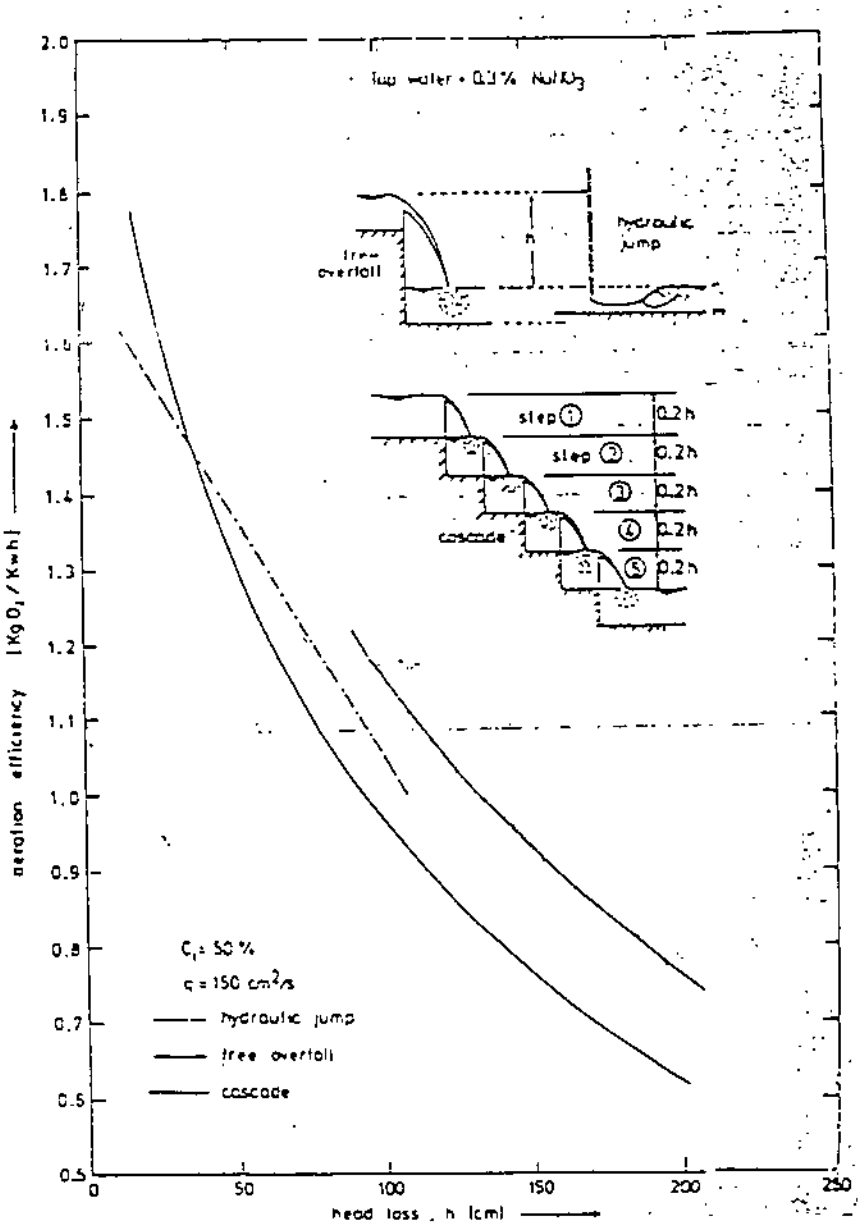

Figure (2.10) Comparison of aeration efficiency for hydraulic jump, free overfall weir, and cascade weir (Avery and Novak, 1978).

Nakasone (1987) conducted similar studies on aeration at weirs, he proposed an efficiency equation which is actually a set of four sub-equations (see Figure 2.11 for symbols):

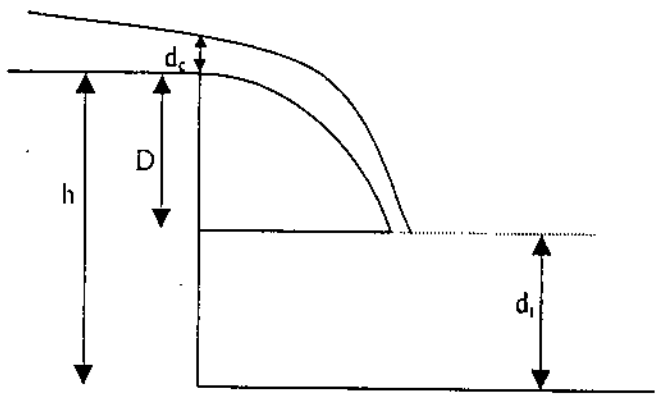

Figure (2.11) Velocity of nappe.

For $(D + 1.5\ d_c) \leq 1.2m$ and $q_w \leq 235\ m^3/h.m$

$$Ln\ r_{20} = 0.0785\ (D + 1.5\ d_c)^{1.31}\ q_w^{0.428}\ d_t^{0.310} \quad \ldots\ldots\ldots\ldots\ldots\ldots \quad (2.54a)$$

For $(D + 1.5\ d_c) > 1.2m$ and $q_w \leq 235\ m^3/h.m.$

$$Ln\ r_{20} = 0.0861\ (D + 1.5\ d_c)^{0.816}\ q_w^{0.428}\ d_t^{0.310} \quad \ldots\ldots\ldots\ldots\ldots\ldots \quad (2.54b)$$

For $(D + 1.5\ d_c) \leq 1.2m$ and $q_w > 235\ m^3/h.m$

$$Ln\ r_{20} = 5.39\ (D + 1.5\ d_c)^{1.31}\ q_w^{-0.363}\ d_t^{0.310} \quad \ldots\ldots\ldots\ldots\ldots\ldots \quad (2.54c)$$

For $(D + 1.5\ d_c) > 1.2m$ and $q_w > 235\ m^3/h.m.$

$$Ln\ r_{20} = 5.92\ (D + 1.5\ d_c)^{0.816}\ q_w^{-0.363}\ d_t^{0.310} \quad \ldots\ldots\ldots\ldots\ldots\ldots \quad (2.45d)$$

Where; D = the drop height in m;

d_t = the tailwater depth in m, for downstream channels having horizontal beds;

r_{20} = the deficit ratio at 20°C.

For deficit ratios at other water temperatures the following equation may be used (Gameson et al., 1958) as recommended by Nakasone:

$$\text{Ln } r_T = \text{Ln } r_{20} (1+0.0168 (T-20)) \quad \ldots\ldots (2.55)$$

Nakasone (1987) found that, for weir aeration, oxygen transfer from air occurs at: (1) the surface of the falling nappe, (2) the air-bubbles entrained in the water body of the receiving basin; and (3) the surface of the cushion. Nakasone observed that the mechanism of the entrained air bubbles is responsible for more than 95% of oxygen transfer. Three types of penetration might occur (Figure 2.12); type (1) bubbles leave the cushion almost immediately after entrainment, type (2) bubbles turn around at half depth, and type (3) bubbles reach the bottom of the basin before they return to the surface.

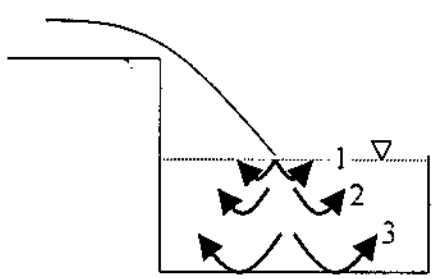

Figure (2.12) Movement of entrained bubbles.

Based on Nakasone (1987) experimental work aeration correlation, there is a distinct coherent relation between the deficit ratio and the discharge, fall height and tail water depth. The mathematical relation between the deficit ratio and the tailwater depth is an ascending continuos function. The continuos function show fractional transition at $q_w = 235$ $m^3/h.m$ for discharge and at $(D + d_c) = 1.2$ m for fall height.

Regarding the discharge, equation (2.54) shows that aeration efficiency increases with discharge up to a certain point and then decreases with a further increase of discharge, which is applicable to the results of

Grindrod (1962), Albrecht (1969), and disagree with the results of Avery and Novak (1978), and Van Der Kroon (1969) which state that aeration efficiency decreases with an increase of discharge. The results of this research coincide with the results of Nakasone(1987).

Concerning the tailwater depth, Nakasone states that aeration efficiency increase with increasing tailwater depth up to a certain limit, because the penetrating air bubbles will not go to infinite depths, and for each combination of discharge and fall height, there would be an approximate maximum depth to which the bubbles would penetrate, thus limiting the aeration efficiency and defining its maximum value. Albrecht (1969) and Popel (1974) found that the aeration efficiency remained stable for tailwater depths greater than 2/3 h.

Avery and Novak (1978) proposed an empirical formula equation (2.51) for optimal tailwater depth, as mentioned earlier:

$$d_t' = 0.0306\ Re^{0.39}\ F_J^{0.24} \text{ in cm}$$

Differentiating equation (2.54) to d_t and setting $dr/dd_t = 0$, the optimal tailwater depth d_t' can be computed by:

$$d_t' = 0.236\ (D + 1.5\ d_c) \text{ for } (D + 1.5\ d_c) \leq 1.2 \text{ m} \quad \ldots\ldots\ldots\ldots\ldots \quad (2.56a)$$

$$d_t' = 0.378\ (D + 1.5\ d_c) \text{ for } (D + 1.5\ d_c) > 1.2\text{m} \quad \ldots\ldots\ldots\ldots\ldots \quad (2.56b)$$

For practical application equations (2.56a) and (2.56b) may be simplified to

$$d_t' = 0.3\ (D + 1.5\ d_c) = 0.3h \quad \ldots\ldots\ldots\ldots\ldots\ldots\ldots\ldots\ldots\ldots \quad (2.57)$$

Nakasone and Van Der kroon stated that aeration efficiency may be increased by splitting the nappe into narrow individual nappes. The width

of each of the resulting individual nappes should be less than 1m. Also the downstream waterbody, or "cushion" should be long enough to fully effectuate the transfer of oxygen from the entrained air-bubbles into the water. For shallow tailwater depths where the entrained air- bubbles hit the bed of the downstream section, the necessary length L_o can be calculated from:

$$L_o = 0.0629\,(D + 1.5\,d_c)^{0.134}\; q_w^{0.666} \qquad (2.58)$$

In which ;L_o, D, d_c are in m and q_w is in $m^3/h.m$

Shorter lengths are acceptable for design purposes but not less than (0.7 L_o) since the air bubbles will not reach the bed of the channel especially at large depths of tail water.

Princince (1991) developed two equations for predicting oxygen deficit ratio at clarifier troughs, one for primary and another for secondary clarifiers.

Primary clarifiers:

$$\text{Ln}\; r_{20}^{\bullet} = 0.042\; h^{0.872}\; q_w^{0.504} \qquad (2.59)$$

Secondary clarifiers:

$$\text{Ln}\; r_{20}^{\bullet} = 0.077\; h^{0.623}\; q_w^{0.66} \qquad (2.60)$$

Princince (1991) concluded that tailwater depth did not influence oxygen uptake during his experiments. This contradicts the earlier findings of Grindrod (1962), Avery and Novak (1978) and Nakasone (1987), who all reported that tailwater depth is an important weir operating parameter that influence mass transfer.

Equations (2.59) and (2.60) suggests that the oxygen deficit ratio increase with an increase of hydraulic weir loading.

Labocha, Corsi and Zytne, (1996) conducted experiments on a piolt-scale weir model, with straight edge sharp-crested weir, thin plate 90-deg V-notch weir, and modified 60-deg V-notch weir, using tap water and wastewater taken from the effluent of a primary clarifier. Experiments with all three weir types indicated that the drop height is the most important factor influencing reareation and aeration increase almost linearly with an increase in drop height.

The manner in which hydraulic loading influences oxygen uptake seems to be closely related to the cross-sectional weir geometry and to the flow regime occurring for given weir discharge. In particular, the transition from attached-film to a free-falling water jet is associated with a significant jump in the values of r. The influence of tailwater depth was investigated; results indicate that tailwater depth had little influence on oxygen transfer. This observation is in agreement with observations made by Princince (1991), but disagree with the results of Grindrod (1962), Avery and Novak (1978) and Nakasone (1987) as mentioned earlier.

Labocha, Corsi and Zytne, (1996) developed correlation's for oxygen uptake at clarifier weirs. Separate correlation's were developed for cleanwater (cw) and primary wastewater (ww).

Thin plate V-notch weir

$$\text{Ln } r_{20} = 0.0045\, h^{1.26}\, Q^{-0.09} \quad \text{(cw)} \qquad (2.61)$$

$$\text{Ln } r_{20}^{*} = 0.0020\, h^{0.36}\, Q^{-0.15} \quad \text{(ww)} \qquad (2.62)$$

Modified V-notch weir

$$\text{Ln } r_{20} = 0.0016\, h^{1.10}\, Q^{0.39} \text{ (cw)} \quad \ldots\ldots (2.63)$$

$$\text{Ln } r_{20}^{*} = 0.0014\, h^{0.97}\, Q^{0.36} \text{ (ww)} \quad \ldots\ldots (2.64)$$

As it's obvious for the thin plate V-notch weir, r_{20} was inversely proportion to discharge. The opposite was true for modified V-notch weirs. Also the sensitivity of r_{20} to Q was greater for modified V-notch weirs.

2.5.3 Air - Water Gas Transfer at Stepped Cascade:

Flow conditions above stepped spillway are characterized by a high level of turbulence, and large quantities of air are entrained (Figure 2.13). Turbulent mixing and air entrainment contribute to an enhancement of the air-water gas transfer along stepped chutes. In rivers, artificial stepped cascades and weirs can be introduced to enhance the dissolved oxygen content of low oxygen content streams. For large dams, the downstream nitrogen content is another important parameter. In the treatment of drinking water, cascade aeration is used to remove gases (volatile organic compounds) and to eliminate or reduce offensive taste or odour. Inclined corrugated channels or drop structures are effective means for water treatment, and the operation requires little maintenance and no running cost. In previous sections the aeration over smooth spillway and aeration of falling jet at single drop were discussed. In this section aeration over stepped channel, in nappe and skimming flow regime, will be discussed according to flow regime.

Nappe flow regime

In a nappe flow regime, the air-water gas transfer at each step results from the gas transfer at the plunge point and at the downstream hydraulic

jump (Figure 2.13a). The aeration efficiency at one individual step is (Chanson,1994b):

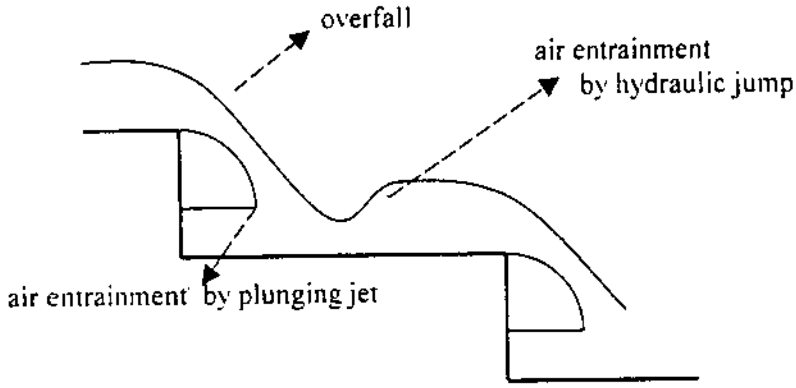

(a)

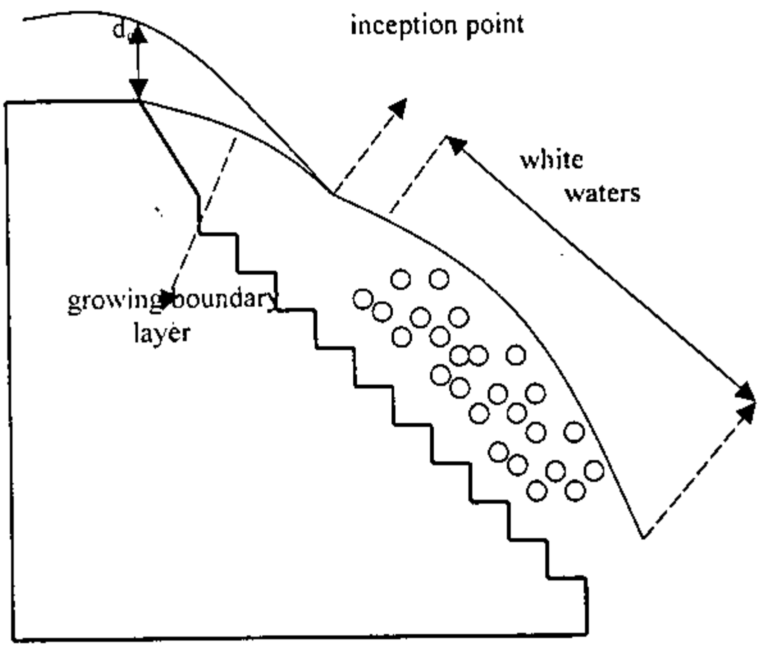

(b)

Figure (2.13) Air entrainment on stepped spillways (a) Nappe flow regime. (b) skimming flow regime.

$$E_i = E_{jet} + E_{HJ}\,(1 - E_{jet}) \quad \ldots\ldots (2.65)$$

Where;

E_{jet} = the aeration efficiency of plunging jet flow;

E_{HJ} = the aeration of the hydraulic jump.

The aeration efficiency is defined as:

$$E = \frac{C_{ds} - C_{us}}{C_s - C_{us}} \quad \text{.....(2.66)}$$

For a series of n_{step} steps, the aeration efficiency of the complete cascade can be expressed in terms of the aeration efficiency of each step:

$$E = 1 - \Pi_{i=1}^{n_{step}} (1 - E_i) \quad \text{.....(2.67)}$$

Where;

E_i = the aeration efficiency of the i-th step, estimated using equation (2.65).

For a stepped chute with n_{step} steps equal characteristics, the aeration efficiency of the chute becomes:

$$E = 1 - (1 - E_i)^{n_{step}} \quad \text{.....(2.68)}$$

The total air-water gas transfer results from the successive aeration of the flow at each step. At each individual step, the flow is aerated by a combination of air bubble entrainment at the intersection of the falling nappe with the receiving pool of water on the step, and air entrainment at the following hydraulic jump(Chanson,1994b).

For design purpose, a crude estimate of the dissolved oxygen transfer can be obtained by feeding empirical correlations into equations (2.67) and (2.68). Table (2.2) summarize the previously computed correlations for oxygen transfer at hydraulic jump.

Equations (2.53) and (2.54) can be used as an empirieal correlations for the aeration efficiency of the plunging jet. Such approximatians for computing the dissolved oxygen transfer might provide a first estimate if the flow conditions are within the range of validity of the empirical correlations, but they will become very inaccurate outside the range of validity of the correlations.

Skimming flow regime

The mechanisms of air entrainments in skimming flow over stepped spillway are similar to the mechanisms of air entrainment over smooth spillway. Once the flow becomes fully developed, the stepped spillway behave in the same way as a smooth one (Chanson, 1994b).

Air entrainment is caused by turbulent velocities acting at the air-water free surface. Through this interface, air is continuously trapped and released. Air entrainment occurs when the turbulent kinetic energy is large enough to overcome both surface tension and gravity effects. The turbulent velocity normal to the free surface, v', must overcome the surface tension pressure (Ervine and Falvey, 1987) and be greater than the bubble rise velocity component for the bubbles to be carried away. These conditions are (Chanson,1993a).

$$v' > \sqrt{\frac{8\sigma}{\rho_w d_b'}} \quad \text{.....} \quad (2.69)$$

$$v' > u_r \cos \alpha \quad \text{.....} \quad (2.70)$$

where; σ is the surface tension, d_b' the air bubble diameter, u_r the bubble rise velocity.

Calculations using equations (2.69) and (2.70) suggest that air entrainment occurs for turbulent velocities, v′, greater than 0.1-0.3m/s (Chanson, 1992b). The flow conditions above a stepped spillway are characterized by a high degree of turbulence, and both velocity conditions are satisfied. As a consequence, large quantities of air are entrained along a stepped spillway.

For stepped spillway flows (Figure 2.13), the entraining region follows a region where the flow over the spillway is smooth and glassy. Next to the boundary, turbulence is generated and the boundary layer, reaches the free surface. When the outer edge of the boundary layer reaches the free surface, the turbulence may initiate natural free surface aeration. The location of the start of air entrainment is called the point of inception. Downstream of the point of inception, a layer containing a mixture of both air and water extends gradually through the fluid. For downstream, the flow becomes uniform, and for a given discharge, the flow depth and the air concentration and velocity distribution do not vary along the chute. This region is defined as the uniform equilibrium flow region.

The local air concentration, c, is defined as the volume of air per unit volume. The characteristic water flow depth, d_{char}, is defined as(Chanson,1995a)

$$d_{char} = \int_0^{y_{90}} (1-c)\, dy \quad \text{..... (2.71)}$$

Where; y is measured perpendicular to the spillway surface and y_{90} is the depth where the local air concentration is 90%. The depth averaged mean air concentration, C_{mean}, is defined as

$$(1 - C_{mean})\, y_{90} = d_{char} \quad \text{..... (2.72)}$$

The average water velocity, U_w, is defined as

$$U_w = \frac{q_w}{d_{char}} \quad \text{..... (2.73)}$$

On smooth spillway, the position of the point of inception is primarily a function of the discharge and the spillway roughness. Keller and Rastogi (1977) suggested the following:

$$\frac{L^*}{K_s} = f_1(F^*, \sin\alpha) \quad \text{..... (2.74 a)}$$

$$\frac{d^*}{K_s} = f_2(F^*, \sin\alpha) \quad \text{..... (2.74b)}$$

where; L^* is the distance from the start of the growth of the boundary layer to the point of inception; d^* is the depth at the point of inception measured normal to the free surface; and F* is a Froude number defined in terms of the roughness height $F^* = q_w / \sqrt{g(\sin\alpha)K_s^3}$. For smooth concrete spillways, Wood (1985) estimated equation (2.74) as

$$\frac{L^*}{K_s} = 13.6\ (\sin\alpha)^{0.0796}(F^*)^{0713} \quad \text{..... (2.75)}$$

$$\frac{d^*}{K_s} = \frac{0.223}{(\sin\alpha)^{0.04}}\ (F^*)^{0\,643} \quad \text{..... (2.76)}$$

On stepped spillways, the position of the start of air entrainment is a function of the discharge, spillway roughness step geometry, and spillway geometry. Sorensen (1985) recorded the position of the start of air entrainment and the flow depth at the nearest measurement station. His results are compared with equations (2.75) and (2.76), where the roughness, K_s, was estimated as the depth of a step normal to the free

surface (i.e., K_s = h cos α). The results showed that equation (2.75) overestimates the location of the point of inception by approximately 40%. This result indicates that the growth of the boundary layer is enhanced by the geometry of the steps.

On stepped spillways, a large quantity of air is entrained along the channel, and the a mount of air entrained is usually defined in terms of the average air concentration. The analysis of self-aerated flow measurments on smooth spillways (Straub and Anderson 1958, Aivazyan 1986) showed that the average air concentration for uniform flow conditions, C_e, is independent of the upstream geometry and flow conditions (i.e, discharge, flow depth and roughness) and is a function of the slope only (Wood 1985; Chanson 1993a). For slopes flatter than 50°, the average air concentration may be estimated as:

$$C_e = 0.9 \sin \alpha \quad \text{..... (2.77)}$$

Using data of Hartung and Scheuerlein (1970) obtained with great natural roughness and steep slopes, Knauss (1979) indicated that the quantity of air entrained was estimated as:

$$C_e = 1.44 (\sin \alpha) - 0.08 \quad \text{..... (2.78)}$$

On stepped spillways, the uniform air concentration is expected to be similar to the results obtained on a smooth spillway, where the mean air concentration is a function of the slope only.

For uniform aerated flows the momentum equation yields:

$$f_e = \frac{8g(\sin\alpha)d_e^2}{q_w^2}\left(\frac{D_H}{4}\right) \quad \text{..... (2.79)}$$

where;

f_e is the friction factor for the uniform air-water mixture;
d_e is the water flow depth in uniform equilibrium flow;

If f is the friction factor of non-aerated flow, dimensional analysis suggests that the ratio f_e/f is a function of the average air concentration, the Reynolds number, and the relative roughness:

$$\frac{f_e}{f} = f_3(C_e ; Re; \frac{K_s}{D_H}) \quad \text{..... (2.80)}$$

The data of Straub and Anderson (1958) and Aivazyan (1986) indicated that the effect of the Reynolds number and the relative roughness on the ratio f_e/f is small, and equation (2.80) is estimated as

$$\frac{f_e}{f} = 0.5 \left\{1 + \tanh \left[0.70 \frac{0.490 - C_e}{C_e(1 - C_e)}\right]\right\} \quad \text{..... (2.81)}$$

A general trend is that, for a given non-aerated friction factor, the fiction factor for aerated flow, f_e, decreases when the average air concentration increases.

Hartung and Scheuerlein (1970) studied open channel flows on rock fill dams. The extremely rough bottom induced a highly turbulent flow with air entrainment. In the presence of air entrainment, their results are presented as:

$$\frac{f_e}{f} = \frac{1}{[1 - 32\sqrt{f} 10 g_{10}(1 - C_e)]^2} \quad \text{..... (2.82)}$$

where C_e is estimated from equation (2.78) and f is the non-aerated friction factor estimated by equation (2.32). Their results also show a reduction in the ratio f_e/f with an increase in air concentration. Also, in fully rough

turbulent flows, equation (2.82) suggests that the ratio f_e/f decreases with increasing roughness.

In uniform self-aerated flows on stepped spillways, the flow parameters can be deduced from the chute geometry (i.e., slope, roughness, width) and from the discharge. For any slope α, the average air concentration for uniform flow, C_e, can be obtained. If the value of the friction factor for non aerated flows, f, is available, the friction factor for an aerated flow, f_e, can be deduced as a function of the mean air concentration, C_e. d_e, may be deduced from, equation (2.79). For a wide channel (i.e., $D_H \sim 4de$), equation (2.79) yields:

$$d_e = \left(\frac{q_w^2 \, f_e}{8g \sin\alpha} \right)^{1/3} \quad \text{..... (2.83)}$$

knowledge of the equilibrium air concentration, C_e, friction factor, f_e, and flow depth, d_e, provides the characteristic depth, $y_{90} = d_e/(1-C_e)$. The depth y_{90} takes into account the bulk of the flow and may be used as a design parameter.

Chanson (1994b) carried out a series of oxygen transfer calculations in self aerated flows on stepped chutes, assuming an ungated spillway, zero salinity, constant channel slopes ranging from 15 to 60°, channel lengths between 20 and 250m, dimensionless discharges d_c/h from 0.8 to 21, a friction factor $f = 1.0$ and temperature between 7 and 30°C.

The analysis of the oxygen and nitrogen transfer computations indicates that the free-surface aeration efficiency is independent of the initial gas content. Furthermore, the aeration efficiency (for oxygen and nitrogen) can be correlated by:

$$E = \left(1 - \frac{q_w}{(q_w)_c}\right)^{\lambda} \quad \text{.....(2.84)}$$

Where $(q_w)_c$ is the discharge for which the growing boundary layer reaches the free surface at the spillway end and no self-aeration occurs, and the exponent λ is a function of the dissolved gas, the temperature and the spillway slope. For the range of the computation, the exponent λ ranges between 3 and 9, but no simple correlation (up to our knowledge) has been obtained between λ and the flow characteristics. The characteristic discharge $(q_w)_c$ can be deduced from (Chanson, 1994b):

$$(q_w)_c = 0.1277\ (L_{spillway})^{1.403}\ (\sin\alpha)^{0.388}\ (h_*\text{Cos}\ \alpha)^{0.0975} \quad \text{.....(2.85)}$$

where $L_{spillway}$ is the spillway length.

Chanson (1994b) stated that, free surface-aeration calculations indicate that the aeration decreases with an increase in discharge. Furthermore, the aeration efficiency resulting from free surface-aeration increases with increasing channel slopes from 15° to 45°, and is almost the same between 45° and 60°. For a given discharge an increase in channel slope causes an increase in the amount of air entrained, and hence an increase of the interface area.

The mean velocity also increases with the channel slope, and hence the residence time decreases with increasing slopes. For flat slopes, the quantity of air entrained is not large enough to obtain optimum aeration. For steep channels, the mean flow velocity might become too large and the residence time too short.

For a stepped chute with skimming flow, the air-water gas transfer caused by self-aeration increases with decreasing water discharges for a

constant channel slope, as the decrease of discharge reduces the length of unaerated flow. Hence the gas transfer caused by self aeration takes place over a longer distance. However the designer needs to keep in mind that the discharge must be large enough to satisfy the conditions of the skimming flow regime.

Also, for stepped chute with skimming flow the aeration efficiency is at maximum for channel slopes ranging between 45° and 60°, for a given discharge (Chanson, 1994b).

Chapter Three

Laboratory Apparatus and Test

Chapter Three

Laboratory Apparatus and Test

3.1 Introduction

The main goal of this research is to investigate the aeration efficiency of a cascade at different step geometry, heights and flow conditions. As stated before, the cascade is modeled and scaled with dimensions to suit the flume and the equipments available in the Hydraulics Laboratory in the Civil Engineering Department of University of Jordan.

In this chapter; the procedure of designing and executing the cascade models, the experimental setup and the methods used to measure the dissolved oxygen on each step, will be described in details.

3.2 Design of Cascade Models:

The key of proper modeling of hydraulic phenomena is the establishing of similitude between model and prototype. Three types of similitude are generally required; geometric, kinematics and dynamic similarity. Therefore, the model should be geometrically similar to the prototype, and the length ratio :

$$L_r = L_m / L_p \quad \text{.....(3-1)}$$

where;

L_m = the model length.

L_p = the prototype length.

Therefore, this ratio must have the identical value for each of the physical dimension involved in the cascade model and prototype. Once L_r is chosen the model may be constructed.

Secondly, the model and prototype should be kinematically similar, which means that the model flow characteristics must be similar to that of the prototype. This means that the velocities and accelerations are all scaled correctly.

Finally, dynamic similitude requires that all the significant forces; like pressure force (F_p), inertia force (F_i), gravity force (F_g) and viscous force (F_v) be properly scaled. In a way similar to the length ratio, the force ratios have to be identical;

$$F_{pr} = F_{ir} = F_{gr} = F_{vr}$$

or,

$$\frac{F_{pm}}{F_{pp}} = \frac{F_{im}}{F_{ip}} = \frac{F_{gm}}{F_{gp}} = \frac{F_{vm}}{F_{vp}} \quad \text{..... (3.2)}$$

The three forces may be written as;

Pressure force $F_p \sim \Delta p L^2$ ..... (3.3a)

Gravity force $F_g \sim \wp L^3$ ..... (3.3b)

Viscous force $F_v \sim \mu vL$ ..... (3.3c)

Where

Δp = pressure difference.

L = length dimension.

$\wp$ = fluid unit weight.

μ = fluid viscosity.

V = flow velocity.

The above relations (3.2) yield to three independent equations using equations (3.3).

$$\left(\frac{\Delta p}{\rho v^2}\right)_m = \left(\frac{\Delta p}{\rho v^2}\right)_p \quad \text{..... (3.4)}$$

$$\left(\frac{v^2}{L g / \rho}\right)_m^{1/2} = \left(\frac{v^2}{L g / \rho}\right)_p^{1/2} \quad \text{..... (3.5)}$$

$Fr_m = Fr_p$

Where;

Fr_m, Fr_p = model and prototype Froude number respectively.

$$\left(\frac{\rho v L}{\mu}\right)_m = \left(\frac{\rho v L}{\mu}\right)_p \quad \text{..... (3.6)}$$

$Re_m = Re_p$

Where

Re_m, Re_p = model and prototype Reynoldes number respectively.

For dynamic Similitude to be achieved, the above three equations should be satisfied. Applying dimensional analysis on the above three equations, show that only the Froude and Reynolds numbers must be held constant to accomplish dynamic similarity. For many hydraulic model studies, either the gravity or the viscous force will be predominant. In such conditions only one dimensionless parameter (i.e. Fr or Re) must be held constant rather than both.

For this research case, the gravity force is the predominant. force, therefore, Froude number should be held constant to achieve dynamic similitude.

First step in designing the cascade models is to choose appropriate dimensional ratio (L_r) to scale the cascade of:

1- Horizontal type of step height h_p equal 15 cm, 30 cm 45 cm and 60cm. And with height to length (L) ratio (h/L) = (1/2) and (1/4), as shown in Figure (3.1, a and b).

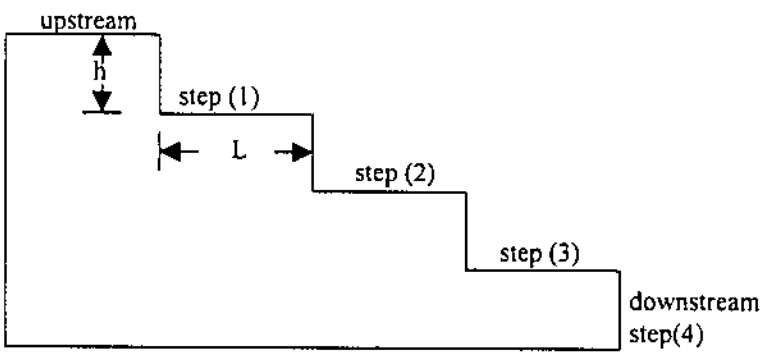

a) (h/L) = 1/2

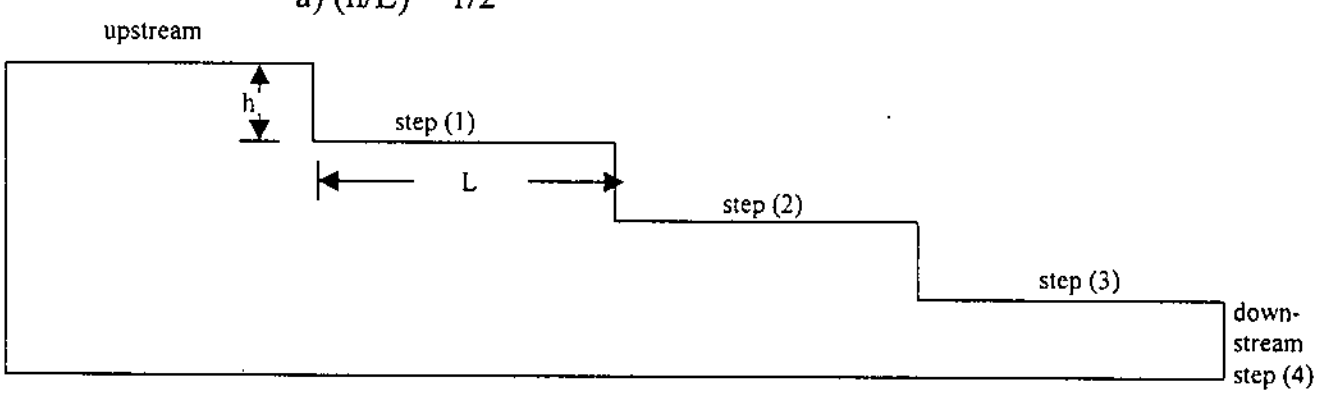

b) (h/L) = 1/4

Figure (3.1) Section of horizontal type cascade model.

2- Pooled type of step height h_P equal 15 cm, 30 cm, 45 cm, and 60 cm, and height to length ratio equal 1/2, and one model of step height 15cm with (h/L) ratio equal 1/4 for comparison. The pool depth equal (L / tanθ); where θ was selected as 60° to achieve total model height that fits the channel depth, as shown in Figure (3.2).

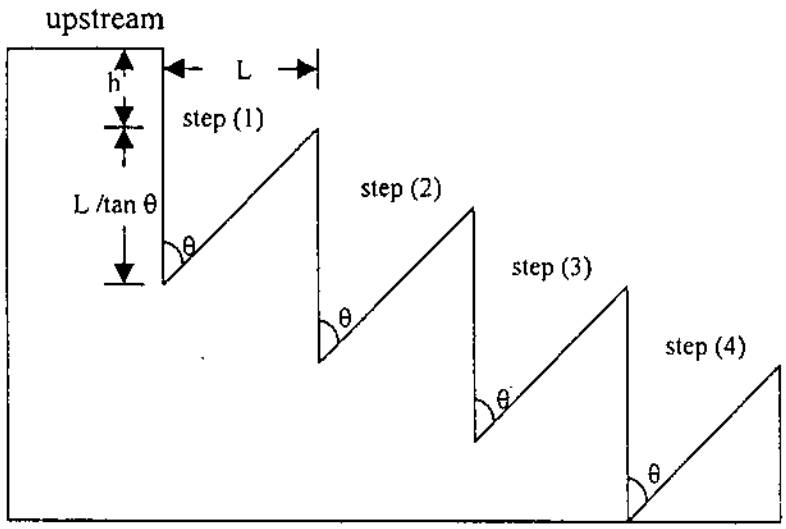

Figure (3.2) Section of pooled type cascade model.

3- Inclined type of step heights h_p equal 15 cm, 30 cm, 45 cm, and 60 cm, and height to length ratio equal 1/2, also one model of step height 15cm with (h/L) ratio equal 1/4 for comparison. The inclined step height equal sin $(\varphi - \pi/2)$; where φ was selected as 110° to achieve total model height that fits the channel depth, as shown in Figure (3.3).

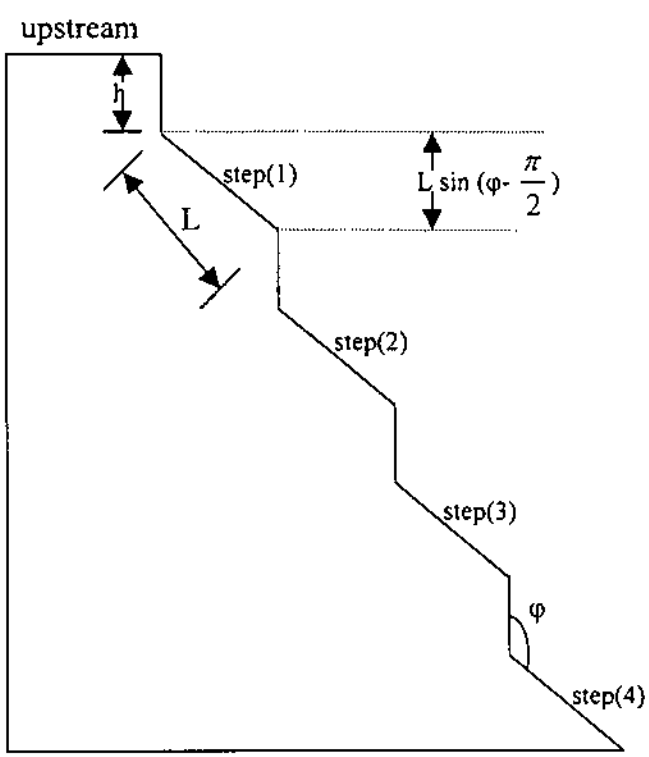

Figure (3.3) Section of inclined type cascade model.

All the types have the same number of steps, which is fixed by four steps. In choosing the scale ratio many constrains has to be considered carefully, such as :

1- Flume dimensions; model total height should not exceed the flume maximum depth
2- Flume capacity; model upstream total head must be less than maximum flume capacity
3- Pump and DO meter limitations; small models with very low flowrate to achieve nappe flow over its steps goes beyond pump minimum discharge and lower than DO meter sensitivity.

Unfortunately, taking consideration of previous constrains leads to different scale ratio; Tables (3.1), (3.2) and (3.3) show prototype-model dimensions according to the scale ratios of horizontal, pooled and inclined type cascades respectively.

Table (3.1): Prototype and model dimensions for horizontal type cascade

Prototype dimensions			Scale ratio $L_r = L_m/L_p$	Model dimensions		
h(cm)	L(cm) For (h/L)			h(cm)	L(cm) For (h/L)	
	1/2	1/4			1/2	1/4
15	30	60	1/5	3	6	12
30	60	120	1/5	6	12	24
40	90	180	1/5	9	18	36
60	120	240	1/8	7.5	15	30

Table (3.2): Prototype and model dimensions for pooled type cascade

Prototype dimensions		Scale ratio	Model dimensions	
h (cm)	L (cm)	$L_r = L_m/L_p$	h (cm)	L (cm)
15	30	1/5	3	6
30	60	1/5	6	12
45	90	1/8	5.6	11.2
60	120	1/8	7.5	15

Table (3.3): Prototype and model dimensions for inclined type cascade

Prototype dimension		Scale ratio	Model dimensions	
h (cm)	L (cm)	$L_r = L_m/L_p$	h (cm)	L (cm)
15	30	1/5	3	6
30	60	1/5	6	12
45	90	1/12	3.75	7.5
60	120	1/12	5	10

The next step in model designing is to define the upper flow discharge for each model in order to achieve the nappe flow. For horizontal steps, Chanson (1994b) showed that a nappe flow regime will occur at discharge smaller than critical value which is defined as:

$$\left(\frac{d_c}{h}\right)_{char} = 0.0916\left(\frac{h}{L}\right)^{-1.276} \quad \text{..... (3.7)}$$

Where

d_c = the critical flow depth.

The nappe flow occurs for $\frac{d_c}{h} \le \left(\frac{d_c}{h}\right)_{char}$ and the model discharge (Q_m) is calculated as shown in the following sample of calculation:

Sample of Calculation:

For horizontal step model with h_p = 15cm and (h/L) ratio equal to 1/2, the model critical discharge is computed as follows:

$$\left(\frac{d_c}{h}\right)_{char} = 0.0916\,(1/2)^{-1.276} = 0.222$$

Where the critical flow depth in prototype scale $(d_c)_p$ at step height in prototype scale (h_p = 15cm) is:

$(d_c)_p = 0.222 * 0.15m = 0.0333m$

Therefore; the prototype critical flowrate per unit channel width $(q_c)_p$ can be calculated by:

$$(q_c)_p = \sqrt{(d_c)_p^3 * g} = \sqrt{(0.0333)^2\, 9.81}$$
$$(q_c)_p = 0.019 m^2/s$$

To find the model critical flowrate per unit width (q_m) :

$$(q_c)_r = (q_c)_m / (q_c)_p = L_r^{1.5}$$

For $L_r = 1/5$ $\quad (q_c)_m = 1.7 * 10^{-3} m^2/s$

Finally, the model flowrate is:

$$Q_m = (q_c)_m * B = 1.7x10^{-3} m^2/s * 0.3m = 5.107x10^{-4} m^3/s = 0.51145 \text{ l/s}$$

as

B = the laboratory flume width = 0.3m.

Tables (3.4) and (3.5) show the result of calculation for horizontal cascade model of (h/L) =1/2 and 1/4 respectively.

Table (3.4): Critical flowrate for horizontal cascade of (h/L) ratio =1/2

h_p (cm)	h_m (cm)	$(q_c)_p$ (m^2/s)	$(q_c)_m$ (m^2/s)	Q_m (L/s)
15	3	1.90×10^{-2}	1.70×10^{-3}	0.511
30	6	5.38×10^{-2}	4.8×10^{-3}	1.44
45	9	9.90×10^{-2}	13.6×10^{-3}	2.65
60	7.5	15.20×10^{-2}	6.73×10^{-3}	2.02

Table (3.5): Critical flowrate for horizontal cascade of (h/L) ratio =1/4

h_p (cm)	h_m(cm)	$(q_c)_p$ (m^2/s)	$(q_c)_m$ (m^2/s)	Q_m (L/s)
15	3	7.2×10^{-2}	6.4×10^{-3}	1.92
30	6	20.3×10^{-2}	18.0×10^{-3}	5.40
45	9	37.3×10^{-2}	33.1×10^{-3}	9.93
60	7.5	57.3×10^{-2}	25.0×10^{-3}	7.50

For the pooled and inclined type cascade there is no available relation (to the best of our knowledge) to distinct between the nappe and skimming flow. Therefore, the experiments are started with the lowest flowrate which is possible to measure DO, then the flowrate increases and passing the transition region to perform one skimming flow in addition.

Table (3.6) shows the schematic of laboratory work for the three different cascade types together with water head ranges above the V-notch, as measured for nappe flowrate at the channel.

Table (3.6): Schematic of the laboratory work with model nappe flowrate region.

	Nappe flow Height H'(mm)												
h cm	30-35	36-40	41-45	46-50	51-55	56-60	61-65	66-70	71-75	76-80	81-85	86-90	91-95
Horizontal (h/L) = 1/2													
3		*	*										
6			*	*	*		*						
9						*	*	*	*				
7.5			*	*		*							
Horizontal (h/L) = 1/4													
3		*	*		*	*							
6			*	*	*		*						
9						*	*		*				*
7.5			*	*		*							
Pooled (h/L) = 1/2													
3		*		*	*	*							
6			*		*	*	*		*				
5.6			*		*		*	*	*				
7.5	*		*	*	*		*		*			*	
Pooled (h/L) = 1/4													
3		*		*	*	*							
Inclined (h/L) = 1/2													
3	*	*	*	*									
6							*		*	*	*		
3.7			*	*	*	*							
5			*	*	*	*	*						
Inclined (h/L) = 1/4													
3	*	*	*	*									

H':The height of water above the v-notch weir in model scale corresponding to the nappe flowrate.
h: The step height in model scale.
L : Length of the step.
* : Number of conducted experiments.
Total number of conducted experiments; 74.

Figures (3.4), (3.5), and (3.6) show photographs of horizontal cascade model, pooled type cascade and inclined type cascade inside the channel with nappe and skimming flow region above each, respectively. Figure (3.7) shows horizontal cascade with a transition region over it.

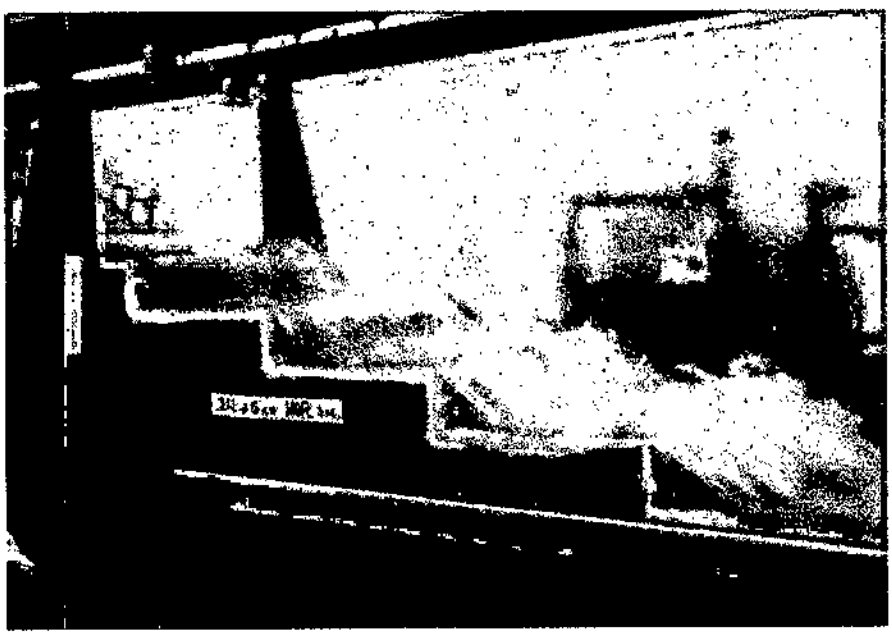

(a) Nape Flow

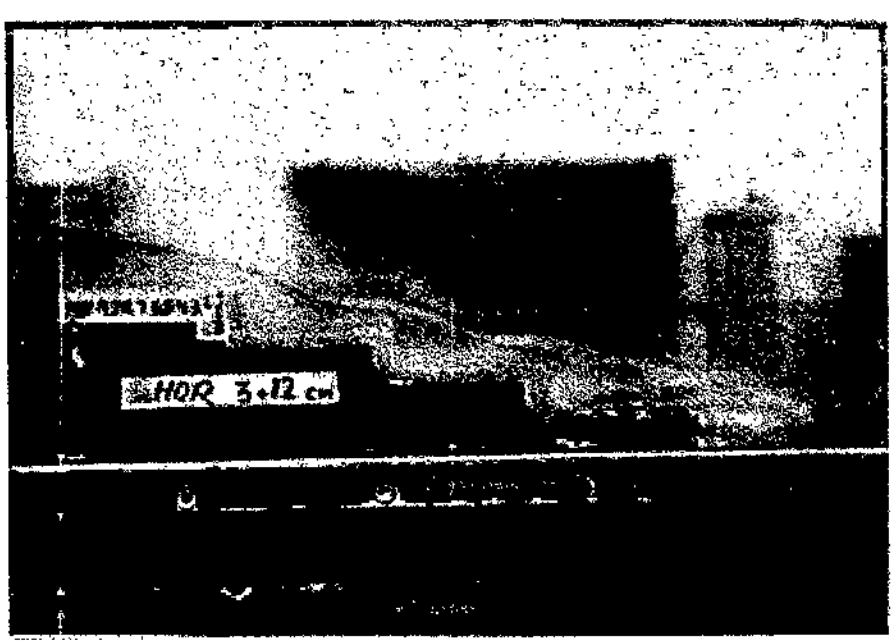

(b) Skimming Flow

Figure (3.4) Photograph of the horizontal cascade model (a) Nape flow region; (b) Skimming flow region.

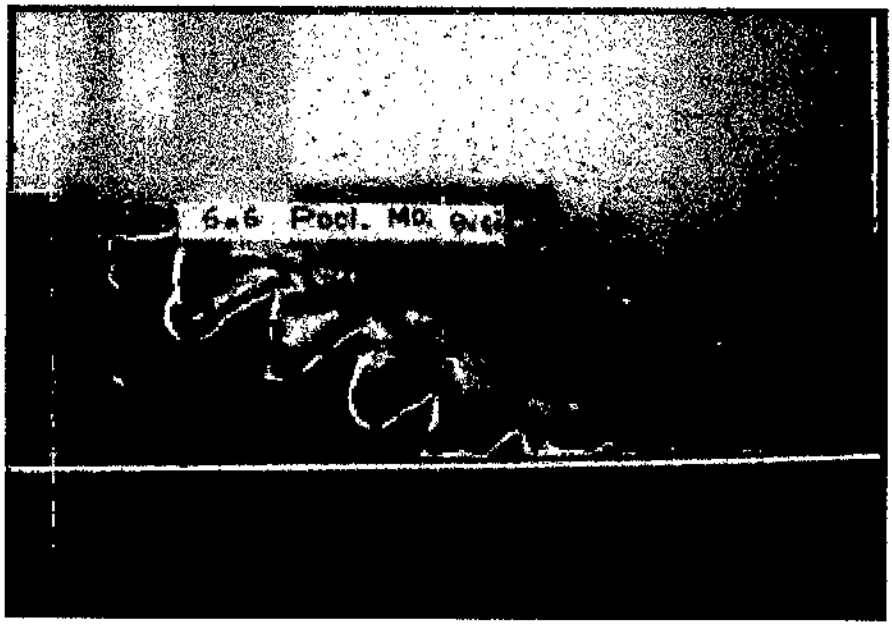

(a) Nape Flow

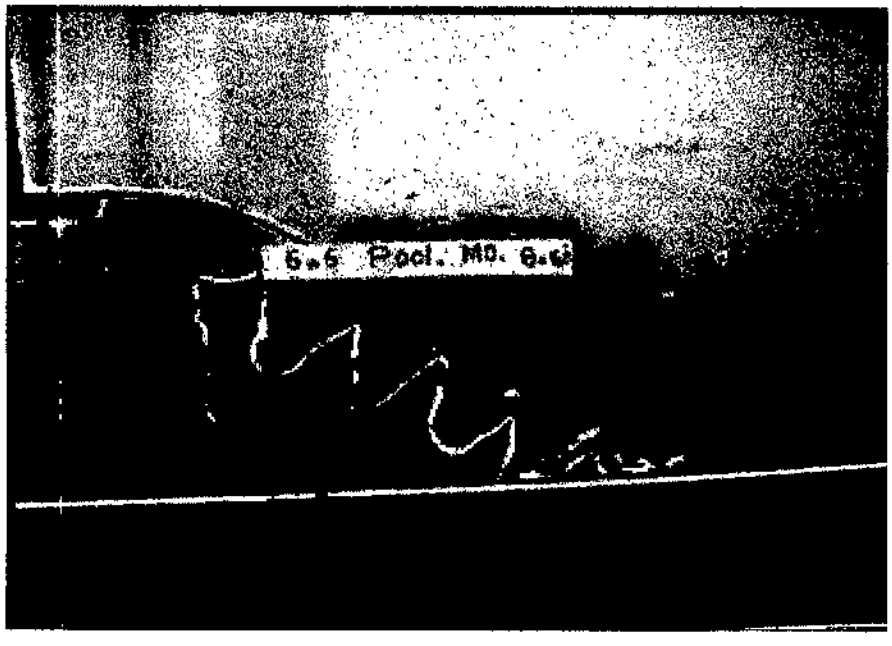

(b) Skimming Flow

Figure (3.5) Photograph of the pooled cascade model (a) Nape flow region; (b) Skimming flow region.

(a) Nape Flow

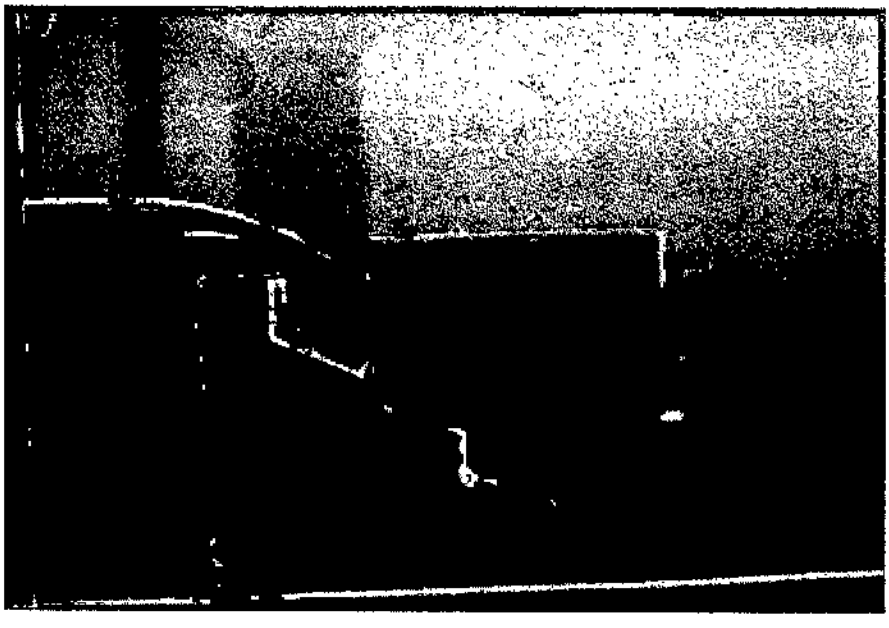

(a) Skimming Flow

Figure (3.6) Photograph of the inclined cascade model (a) Nappe flow region; (b) Skimming flow region.

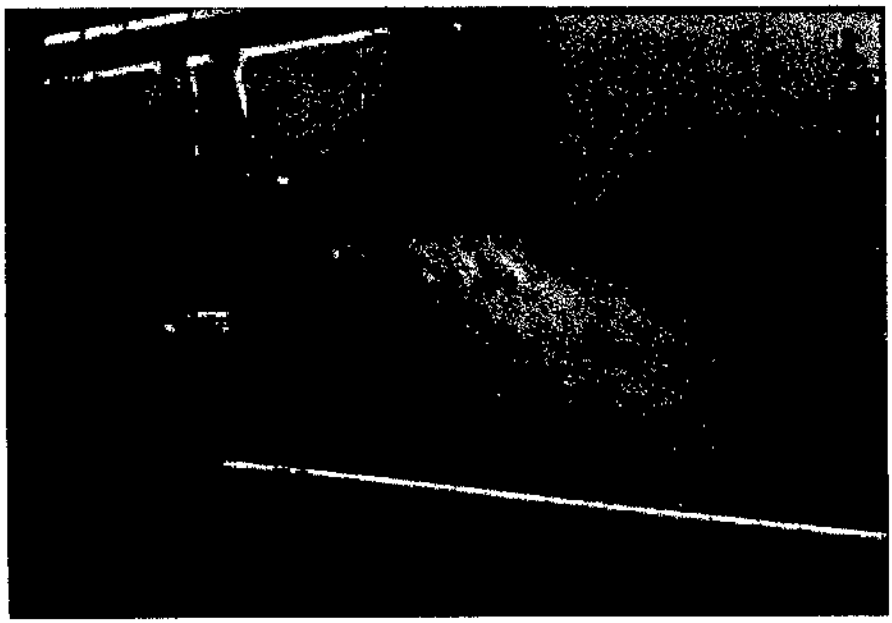

Figure (3.7) Photograph of the horizontal cascade with transition region.

3.3 The Experimental Setup:

All the experiments were carried out in the Hydraulics Laboratory of the Department of Civil Engineering, University of Jordan, using a flume of 11000mm length, 300mm width and 450mm depth, the sides are manufactured from toughened glass, in order to minimize the sidewalls effect. The flume is fed through an inlet tank incorporating a stilling arrangement which is designed to produce near uniform flow conditions. After passing through the working section (the experiment setup section), the water travels by of an adjustable overshot weir to a discharge tank to direct the water to the sump or reservoir tank through a V-notch weir to measure the flow rate, since the original currentmeter fitted to the flume was unfortunately out of order.

The calibration of the V-notch was conducted and the discharge coefficient (Cd) was estimated through the following:

$$Q_{th} = \frac{8}{15}\sqrt{2g}\tan(\beta/2)\,H'^{5/2} \quad \text{.....(3.8)}$$

Where;

Q_{th} = theoretical discharge;

H' = depth of water above the V-notch;

β = V-notch angle = 90, as indicated in Figure (3.8).

$$Q_{act} = \frac{\text{volume}}{\text{time}} \quad \text{.....(3.9)}$$

Where:

Q_{act} = actual flowrate in (m^3/s)

and,

$$Cd = Q_{act}/Q_{th} \quad \text{.....(3.10)}$$

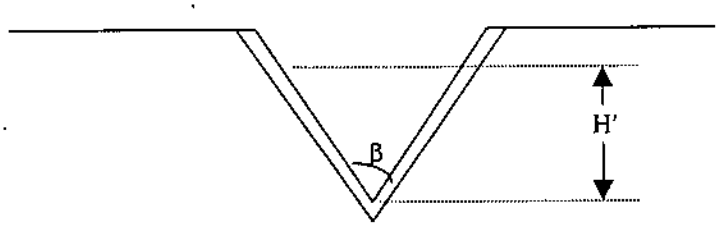

Figure (3.8) Section of the V-notch weir.

Six runs illustrated in Table (3.7) (the average of many runs) were carried out to estimate Cd.

Table (3.7): Calibration of V-notch to estimate discharge coefficient Cd.

Iteration no	H' (mm)	Time (s)	Volume (l)	Q_{th} (m^3/s)	Q_{act} (m^3/s)
1	55.30	53.50	60	1.70×10^{-3}	1.12×10^{-3}
2	56.20	52.50	60	1.77×10^{-3}	1.14×10^{-3}
3	63.52	38.50	60	2.40×10^{-3}	1.56×10^{-3}
4	69.80	30.20	60	3.04×10^{-3}	1.86×10^{-3}
5	73.40	26.00	60	3.45×10^{-3}	2.23×10^{-3}
6	74.90	25.30	60	3.63×10^{-3}	2.37×10^{-3}

Plotting Q_{th} against Q_{act} in linear relationship and computing the slope, which is equal to Cd, which is equal to 0.6503 as shown in Figure (3.9).

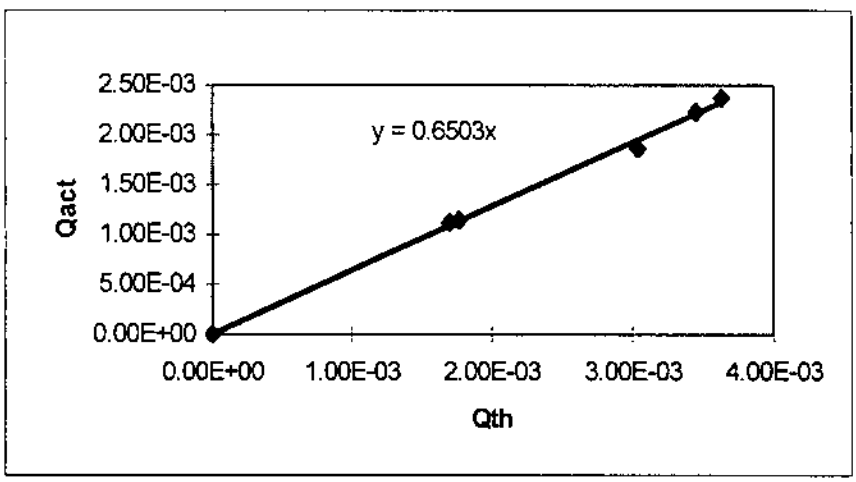

Figure (3.9) Theoretical flowrate vs. actual flowrate for the V-notch weir

The flumehood is a closed circuit system, and as a result of continuos circulation, the water will be aerated to saturation after few runs. Therefore, it was necessary to deoxygenate the water to a level enough to conduct a number of tests before reaching the saturation level once more. This was done by dose control of sodium sulphite solution in presence of cobalt catalyst. Precaution was taken to ensure sufficient reaction time so that residues of sulphite were not carried forward to the experimental flow section.

All models were fixed in the channel using a special pin on the channel bed and sealing the gaps with acrylic paste which is insoluble in water, non-reactive and easy to be removed, but it takes at least 48 hours to dry.

3.4 Determination of Dissolved Oxygen

Two methods for dissolved oxygen (DO) analysis have been used; the Winkler or idometric method and the electrometric method using membrane electrode. The Winkler method is titrimetric procedure based on the oxidizing property of DO, while the membrane electrode procedure is based on the rate of diffusion of molecular oxygen across a membrane.

Measuring DO over the model steps was very critical. Top priority was to measure DO using membrane electrode procedure on the positions; upstream, step 1, step 2, step 3 and downstream for the horizontal cascade. And upstream, step1, step 2, step 3 and step 4, for the pooled and inclined type cascades so as all the types would account for four drops of flow. Starting with the DO meter available in the Sanitary Lab in the Civil Engineering Department, but unfortunately this DO meter was not suitable due to low accuracy in flowing water. Therefore, another DO meter was tested from the chemical Engineering Department, but again unfortunately this DO meter needed appreciable depth of water over the step to be accurate in measurement, while this appreciable depth of water is not available in the horizontal and inclined cascades for nappe flow.

For horizontal and inclined step type models, where no appreciable depth is available over the steps, the DO was measured using the Winkler method, which is a titrimetric procedure based on the addition of divalent manganese solution, followed by strong alkali, to the sample in a glass stopered bottle. DO rapidly oxidizes an equivalent amount of dissolved divalent manganous hydroxide precipitate to hydroxide of higher valency states. In the presence of iodide ions in an acidic solution, the oxidized manganese reverts to the divalent rate, with the liberation of iodine equivalent to the original DO content. The iodine is then titrated with a standard solution of theiosulfate.

It is worth mentioning that samples of water were taken from the positions mentioned earlier, samples were collected using narrowmouth glass stopered BOD bottles of 300ml capacity with tapered and pointed ground glass stoppers, to avoid entraining or dissolving atmospheric oxygen. The samples then immediately titrated to eliminate errors as much as possible.

For the pooled type cascade, there was enough depth of water at each step to use the membrane electrode method. The oxygen sensitive membrane electrode is composed of two solid metal. Electrodes in content with supporting electrolyte separated from the test solution by a selective membrane. The diffusion current is nearly proportional to the concentration of molecular oxygen.

The DO meter of the chemical engineering department was used in the pooled type cascade after it was calibrated properly against Winkler method.

Chapter Four
Results Analysis

Chapter Four
Results Analysis

4.1 General

Aeration efficiency over stepped structure is a parameter affected by many variables; e.g. type of cascade, step height, height to length step ratio (h/L), flowrate and type of flow over the cascade. These variables are greatly dependent on each other, and it's not easy to test the effect of each variable independently with reasonable number of experiments.

In the present research all the above variables had been tested with different flow rates, through:

- Three types of cascade;

1- Horizontal.

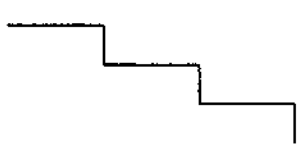

2- Pooled.

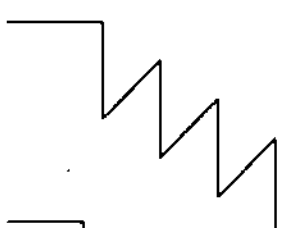

3- Inclined.

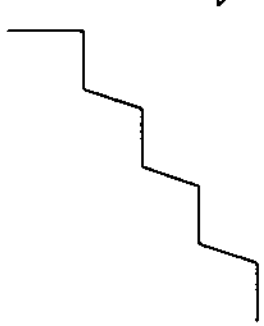

- Four prototype step heights (h_p)

  - 15cm.
  - 30cm.
  - 45cm.
  - 60cm.

- Two height to length ratios ($h/_L$)
  - 1/2.
  - 1/4.
- Two types of flow
  - Nappe flow

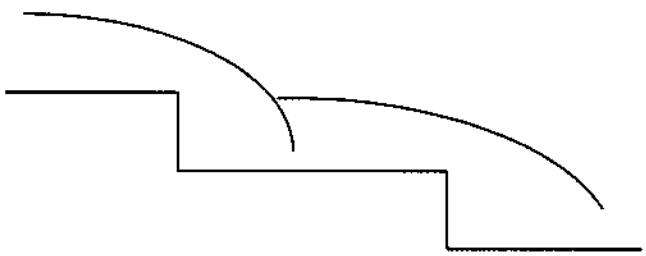

  - Skimming flow

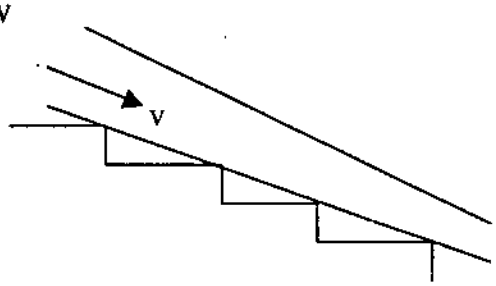

In general, horizontal type cascade of (h/L) = 1/2 revealed highest results regarding aeration efficiency, followed with minor difference by the pooled type and finally by the inclined type model, with the least efficiency. Aeration efficiency increased with increasing flowrate. In nappe flow region the ratio (h/L) =1/2 seemed more efficient than the (h/L)=1/4, while the opposite is true for skimming flow region, for horizontal type cascade.

Thus, the experimental results for nappe flow are presented in three groups; the first group shows the DO concentration upstream and downstream the model and at each step along with aeration efficiency, for each operating flow over the model. The second group shows the change of the aeration efficiency with the change of flowrate for each model. The last group shows the change of the aeration efficiency with the change of

height, and for horizontal cascade with height to length ratio. Separate section deals with aeration efficiency at skimming flow for the three models.

4.2 Dissolved Oxygen Concentration Over Steps.

The tests for horizontal cascade with (h/L) = 1/2 show increasing of dissolved oxygen concentration (DO) from step to step in rate ranging from 0.13 to 0.16, 0.29 to 0.42, 0.43 to 0.55 and 0.17 to 0.26 for step heights 15cm, 30cm, 45cm and 60cm respectively and with (h/L) = 1/2 respectively. Lower rates are noted for horizontal cascade of (h/L) = 1/4 when the increasing DO rate ranges from 0.11 to 0.25, 0.17 to 0.26, 0.18 to 0.36 and 0.05 to 0.20 for step height 15cm, 30cm, 45cm, and 60cm respectively. The increasing rate of height to length ratio 1/4 has less DO than that of (h/L) = 1/2. The results are presented in Figures (4.1) to (4.8). The maximum efficiency step number was changed in different trend at each model. For horizontal cascade of (h/L) = 1/2, step 1 achieved max aeration efficiency for 7% of the operating flow rates, step 2 for 43% of the operating flowrate, step 3 for 14% of the operating flowrates and the downstream step achieved max aeration efficiency for 36% of the operating flowrates.

For horizontal cascade of (h/L) = 1/4 maximum aeration efficiency was achieved on step 1 for 38% of the operating flowrates, on step 2 for 6% of the operating flowrates, on step 3 for 25% of operating flowrates and finally downstream step achieved maximum efficiency for 31% of the operating flowrates.

For the pooled type cascade, DO concentration increases in a parabolic trend. First step accomplished maximum aeration efficiency at all tests and with values extensively higher than the incoming steps. The results of the pooled cascade exhibited in Figures (4.9) to (4.13).

While the inclined type cascade behaved differently and gave limited increase in the DO concentration, but the aeration efficiency didn't give a trend of maximum value at first step. Maximum aeration efficiency was achieved on step 1, step 2, step 3 and step 4 for 20% , 22% , 22% and 36% of the different operating flowrates, respectively. The results are presented in Figures (4.14) to (4.18).

Table(4.1): Dissolved oxygen concentration for horizontal type cascade of hp=15cm and (h/L)=1/2

Qm=0.43 l/s	Qp=24.1 l/s		Qm=0.49 l/s	Qp=27.4 l/s	
T=25C	Cs=7.35 mg/l		T=24.4C	Cs=7.44 mg/l	
step number	DO(mg/L)	Efficiency%	step number	DO(mg/L)	Efficiency%
us	4.9		us	5.8	
1	5	4.08	1	6	12.20
2	5.3	12.77	2	6.2	13.89
3	5.4	4.88	3	6.3	8.06
ds	5.5	5.13	ds	6.3	0.00
		Total eff. 24.51%			Total eff. 30.48%

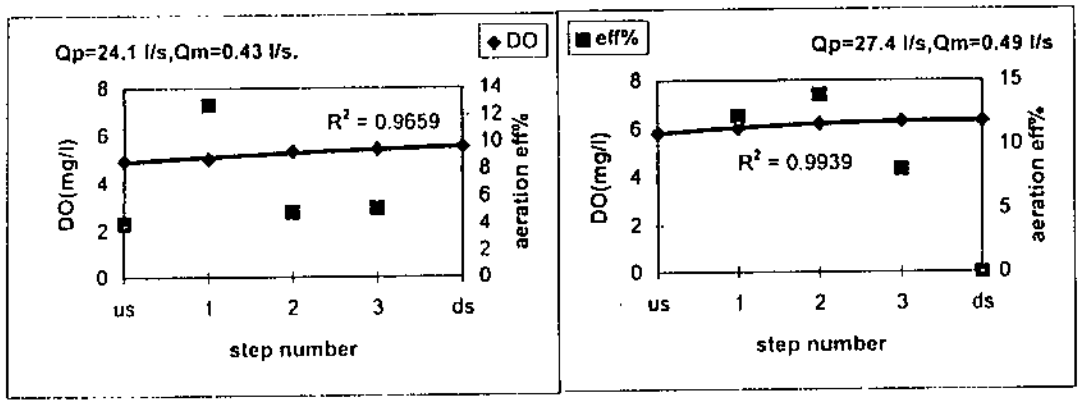

Figure(4.1) Dissolved oxygen concentration vs step number for horizontal cascade of hp=15cm,(h/L)=1/2

* R^2 For second degree polnomial of DO vs step number.

Table(4.2):Dissolved oxygen concentration for horizontal type cascade of hp=15cm and (h/L)=1/4

Qm=0.43 l/s Qp=24.1 l/s			Qm=0.59 l/s Qp=32.8 l/s			Qm=0.94 l/s Qp=52.7 l/s			Qm=1.24 l/s Qp=69.3 l/s		
T=25.6C Cs=7.27 mg/l			T=25.6C Cs=7.27 mg/l			T=25.0C Cs=7.35 mg/l			T=24.7C Cs=7.39 mg/l		
step number	DO(mg/L)	Efficiency%	step number	DO(mg/L)	Efficiency%	step number	DO(mg/L)	Efficiency%	step number	DO(mg/L)	Efficiency%
us	5		us	5.7		us	4.3		us	5.9	
1	5.3	13.22	1	6	19.11	1	4.5	6.56	1	6.1	13.42
2	5.4	5.08	2	6.2	15.75	2	4.8	10.53	2	6.4	23.26
3	5.5	5.35	3	6.1	***	3	5.2	15.69	3	6.3	***
ds	5.5	0.00	ds	6.2	8.55	ds	5.2	0.00	ds	6.6	27.52
		Total eff.22.06%			Total eff 31.92%			Total eff 29.12%			Total eff 46.97%

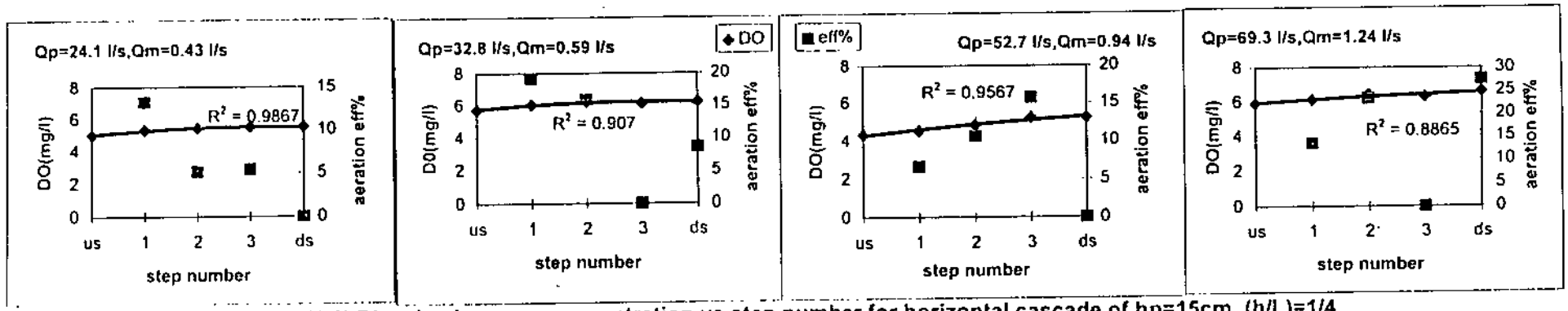

Figure(4.2) Dissolved oxygen concentration vs step number for horizontal cascade of hp=15cm, (h/L)=1/4

* R^2 For second degree polnomial of DO vs step number.

Table(4.3): Dissolved oxygen concentration for Horizontal cascade of hp=30cm, (h/L)=1/2

Qm=0.62 l/s	Qp=34.73 l/s		Qm=0.77 l/s	Qp=43.17 l/s		Qm=1.08 l/s	Qp=60.68 l/s		Qm=1.41 l/s	Qp=78.60 l/s	
T=24.4C	Cs=7.44 mg/l		T=24.4C	Cs=7.44 mg/l		T=24.4C	Cs=7.44 mg/l		T=24.4C	Cs=7.44 mg/l	
step number	DO(mg/L)	Efficiency%	step number	DO(mg/L)	Efficiency%	step number	DO(mg/L)	Efficiency%	step number	DO(mg/L)	Efficiency%
us	4.1		us	4.3		us	4.4		us	4.4	
1	4.3	5.81	1	4.7	12.74	1	4.5	3.29	1	5.6	39.47
2	4.8	15.43	2	5.2	18.25	2	5.4	30.61	2	5.8	10.87
3	5	7.30	3	5.4	8.93	3	5.7	14.71	3	6	12.20
ds	5.2	7.87	ds	5.6	9.80	ds	5.9	11.49	ds	6.1	6.94
		Ttotal eff 32.93%			Total eff 41.40%			Total eff 49.34%			Total eff 55.92%

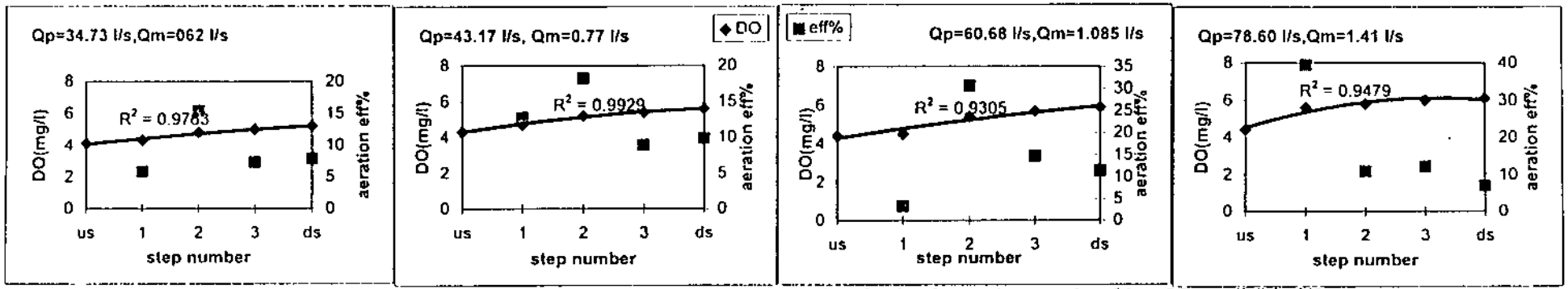

Figure(4.3) Dissolved oxygen concentration vs. step number for horizontal cascade of hp=30cm, (h/L)=1/2

* R^2 For second degree polnomial of DO vs step number.

Table(4.4): Dissolved oxygen concentration for horizontal cascade of hp=30cm, (h/L)=1/4

Qm=0.66 l/s	Qp=36.74 l/s		Qm=0.85 l/s	Qp=47.81 l/s		Qm=1.085 l/s	Qp=60.68 l/s		Qm=1.46 l/s	Qp=81.86 l/s	
T=22.5C	Cs=7.585 mg/l		T=22.5C	Cs=7.585 mg/l		T=22.5C	Cs=7.585 mg/l		T=22.5C	Cs=7.585 mg/l	
step number	DO(mg/L)	Efficiency%	step number	DO(mg/L)	Efficiency%	step number	DO(mg/L)	Efficiency%	step number	DO(mg/L)	Efficiency%
us	4.9		us	5.2		us	5		us	5.3	
1	5.2	11.81	1	5.6	13.39	1	5.5	20.49	1	5.7	18.69
2	5.4	8.93	2	5.6	5.15	2	5.7	10.31	2	5.8	5.75
3	5.5	4.90	3	5.8	10.87	3	5.9	11.49	3	6.2	24.39
ds	5.6	5.15	ds	5.9	6.10	ds	6.1	12.99	ds	6.3	8.06
	Total eff 26.07%			Total eff. 29.35%			Total eff 42.55%			Total eff 43.76%	

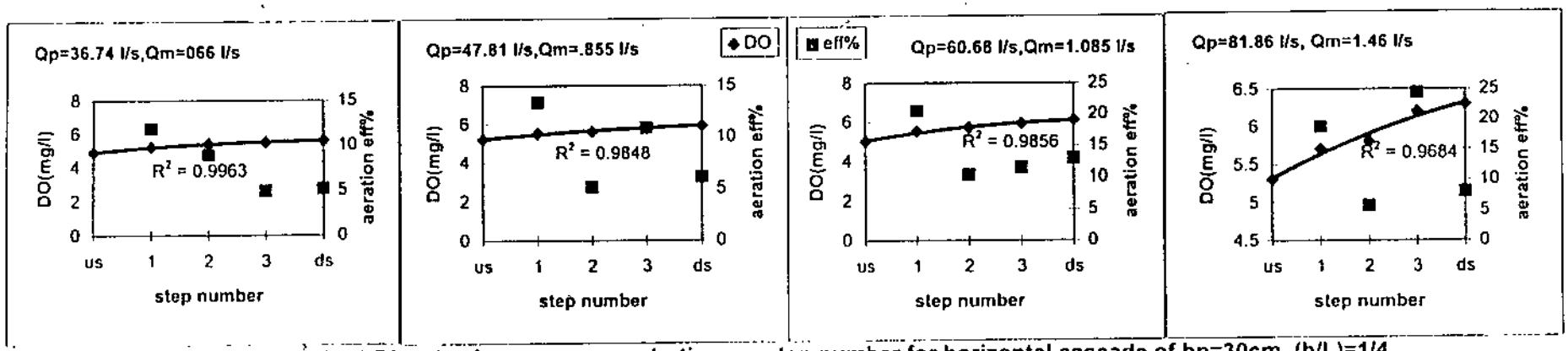

Figure(4.4) Dissolved oxygen concentration vs. step number for horizontal cascade of hp=30cm, (h/L)=1/4

* R^2 For second degree polnomial of DO vs step number.

Table(4.5): Dissolved oxygen concentration for horizontal cascade of hp=45cm, (h/L)=1/2

Qm=1.41 l/s	Qp=78.6 l/s		Qm=1.58 l/s	Qp=88.6 l/s		Qm=1.98 l/s	Qp=111 l/s		Qm=2.28 l/s	Qp=127 l/s	
T=24.8C	Cs=7.37 mg/l		T=25.3C	Cs=7.30 mg/l		T=25.3C	Cs=7.30 mg/l		T=25.7C	Cs=7.28 mg/l	
step number	DO(mg/L)	Efficiency%	step number	DO(mg/L)	Efficiency%	step number	DO(mg/L)	Efficiency%	step number	DO(mg/L)	Efficiency%
us	3.6		us	4.2		us	4		us	3.8	
1	3.9	7.96	1	4.8	19.35	1	4.7	21.21	1	4.7	25.86
2	4.5	17.29	2	4.6	***	2	5	11.54	2	5.5	31.01
3	5	17.42	3	5.3	25.93	3	5.5	21.74	3	4.8	***
ds	5.8	33.76	ds	6.1	40.00	ds	6.1	33.33	ds	5.9	44.35
		Total eff 58.35%			Total eff. 61.29%			Total eff. 63.58%			Total eff 60.03%

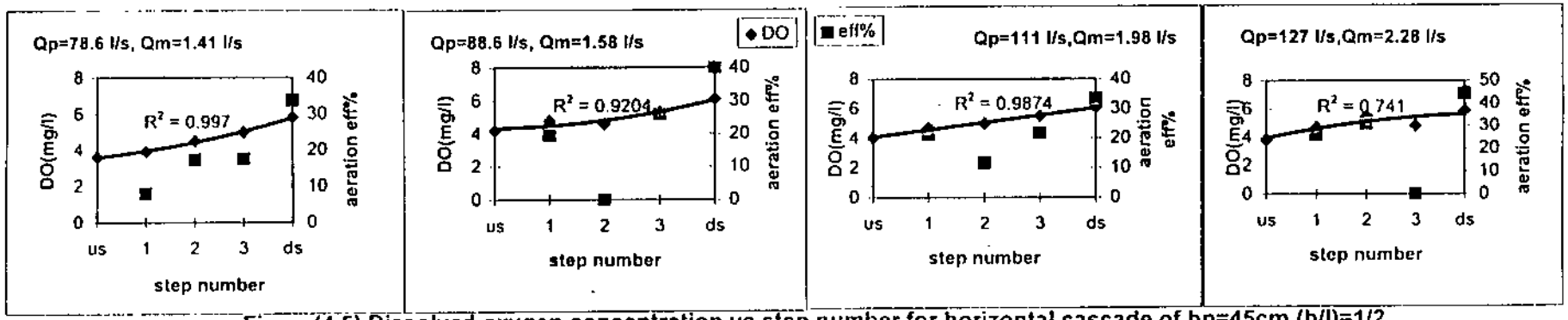

Figure(4.5) Dissolved oxygen concentration vs step number for horizontal cascade of hp=45cm,(h/l)=1/2

* R^2 For second degree polnomial of DO vs step number.

Table(4.6): Dissolved oxygen concentration for horizontal cascade of hp=45cm, (h/L)=1/4.

Qm=1.41 l/s Qp=78.6 l/s T=35C Cs=6.16 mg/l			Qm=1.65 l/s Qp=92.1 l/s T=35C Cs=6.16 mg/l			Qm=2.36 l/s Qp=132.0 l/s T=35C Cs=6.16 mg/l			Qm=3.93 l/s Qp=219 l/s T=35C Cs=6.16 mg/l		
step number	DO(mg/L)	Efficiency%	step number	DO(mg/L)	Efficiency%	step number	DO(mg/L)	Efficiency%	step number	DO(mg/L)	Efficiency%
us	4.4		us	3.2		us	3		us	3.8	
1	4.8	22.73	1	3.7	16.89	1	3.5	15.82	1	3.3	***
2	4.7	***	2	4.14	17.89	2	3.6	3.76	2	3.5	6.99
3	5	20.55	3	4.2	2.97	3	4	15.63	3	4.5	37.59
ds	5.2	17.24	ds	4.5	15.31	ds	4.4	18.52	ds	5	30.12
		Total eff.45.45%			Total eff.43.95%			Total eff.44.30%			Total eff.50.84%

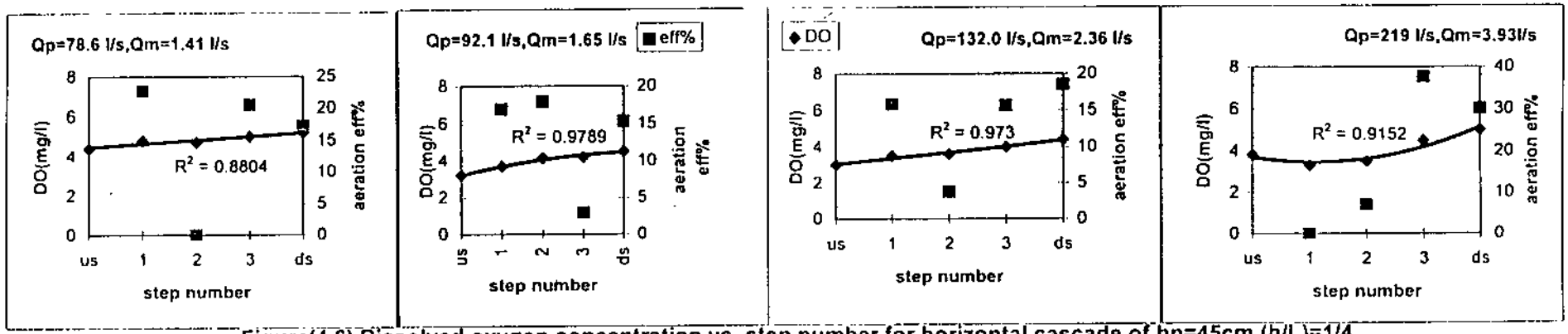

Figure(4.6) Dissolved oxygen concentration vs. step number for horizontal cascade of hp=45cm,(h/L)=1/4.

* R^2 For second degree polnomial of DO vs step number.

Table(4.7): Dissolved oxygen concentration for horizontal cascade of hp=60cm, (h/L)=1/2.

Qm=0.52 l/s Qp=94.3 l/s T=26C Cs=7.21 mg/l			Qm=0.62 l/s Qp=113 l/s T=26C Cs=7.21 mg/l			Qm=0.73 l/s Qp=133 l/s T=26C Cs=7.21 mg/l			Qm=1.19 l/s Qp=215 l/s T=26C Cs=7.21 mg/l		
step number	DO(mg/L)	Efficiency%	step number	DO(mg/L)	Efficiency%	step number	DO(mg/L)	Efficiency%	step number	DO(mg/L)	Efficiency%
us	2.9		us	2.5		us	3.1		us	3.5	
1	3	2.32	1	2.9	8.49	1	3.8	17.03	1	3.9	10.78
2	3.3	7.13	2	3	2.32	2	3.6	***	2	3.7	***
3	3.5	5.12	3	3.5	11.88	3	4	11.08	3	4	8.55
ds	3.5	0.00	ds	3.5	0.00	ds	4	0.00	ds	4.4	12.46
		Total eff.13.90%			Total eff. 21.22%			Total eff 21.89%			Total eff. 24.26%

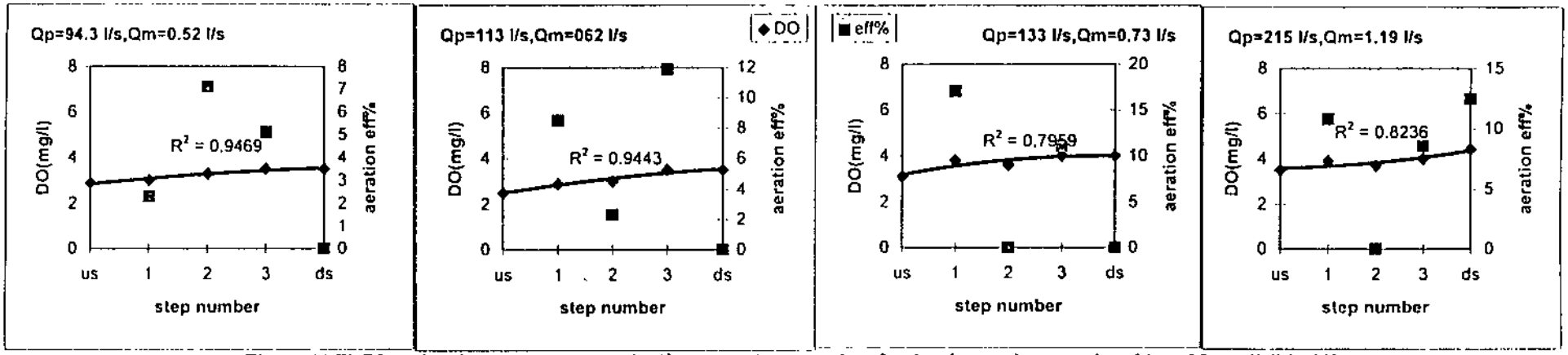

Figure(4.7) Dissolved oxygen concentration vs. step number for horizontal cascade of hp=60cm,(h/L)=1/2.

*** R^2 For second degree polnomial of DO vs step number.**

Table(4.8): Dissolved oxygen concentration for horizontal cascade of hp=60cm, (h/L)=1/4.

Qm=0.52 l/s Qp=94.3 l/s T=26C Cs=7.21 mg/l			Qm=0.62 l/s Qp=113 l/s T=26C Cs=7.21 mg/l			Qm=0.855 l/s Qp=155 l/s T=26C Cs=7.21 mg/l			Qm=1.24 l/s Qp=224 l/s T=26C Cs=7.21 mg/l		
step number	DO(mg/L)	Efficiency%	step number	DO(mg/L)	Efficiency%	step number	DO(mg/L)	Efficiency%	step number	DO(mg/L)	Efficiency%
us	3.5		us	3.9		us	4		us	3	
1	3.4	***	1	4	3.02	1	4.2	6.23	1	3.4	9.50
2	3.6	5.25	2	3.8	***	2	4	***	2	3.6	5.25
3	3.5	***	3	4	5.87	3	4.3	9.35	3	3.4	***
ds	3.7	5.39	ds	4.3	9.35	ds	4.4	3.44	ds	4	15.75
		Total eff. 5.40%			Total eff 12.08%			Total eff. 12.46%			Total eff. 23.74%

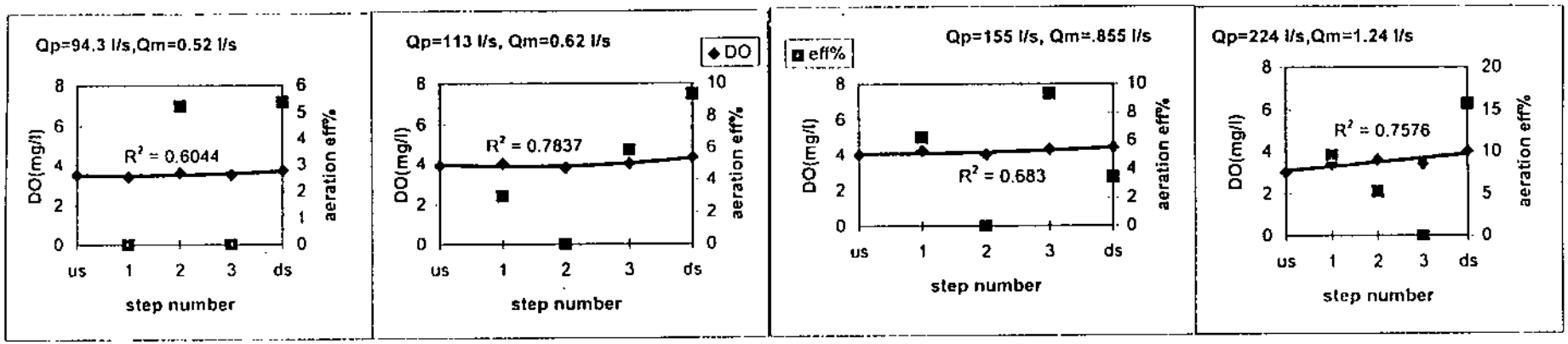

Figure(4.8) Dissolved oxygen concentration vs step number for horizontal cascade of hp=60 cm,(h/L)=1/4

* R^2 For second degree polnomial of DO vs step number.

Table(4.9): Dissolved oxygen concentration for pooled cascade of hp=15cm, (h/L)=1/2.

Qm=0.49 l/s Qp=27.4 l/s T=20.8C Cs=7.98 mg/l			Qm=0.69l/s Qp=39.0 l/s T=21.2C Cs=7.92 mg/l			Qm=0.94l/s Qp=52.7 l/s T=21.2C Cs=7.92 mg/l			Qm=1.35l/s Qp=75.4 l/s T=21.2C Cs=7.92 mg/l		
step number	DO(mg/L)	Efficiency%	step number	DO(mg/L)	Efficiency%	step number	DO(mg/L)	Efficiency%	step number	DO(mg/L)	Efficiency%
us	3		us	4.1		us	4.1		us	5.8	
1	3.6	12.05	1	4.6	13.09	1	4.7	15.71	1	6.2	18.87
2	3.7	2.28	2	4.7	3.01	2	4.8	3.11	2	6.2	0.00
3	3.8	2.34	3	4.8	3.11	3	4.9	3.21	3	6.3	5.81
4	3.9	2.39	4	4.9	3.21	4	5.1	6.62	4	6.4	6.17
		Total eff 18.08%			Total eff.20.96%			Total eff.26.20%			Total eff 28.35%

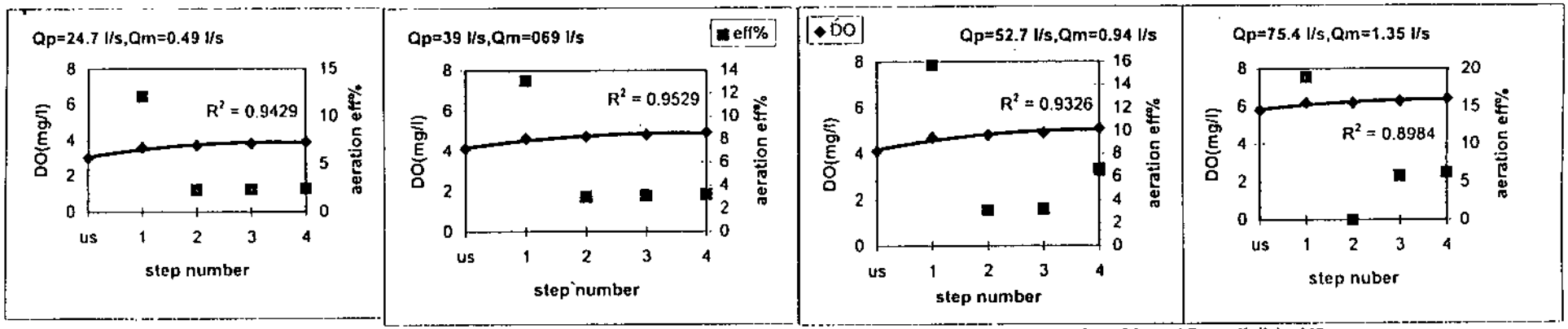

Figure(4.9) Dissolved oxygen concentration vs step number for pooled type cascade of hp=15cm,(h/L)=1/2.

* R^2 For second degree polnomial of DO vs step number.

Table(4.10): Dissolved oxygen concentration for pooled cascade of hp=15cm, (h/L)=1/4.

Qm=0.49 l/s Qp=27.4 l/s T=26.0C Cs=7.21 mg/l			Qm=0.65l/s Qp=36.34l/s T=26.0C Cs=7.21 mg/l			Qm=1.04l/s Qp=13.43 l/s T=26.0C Cs=7.21 mg/l			Qm=1.35l/s Qp=75.47 l/s T=26.0C Cs=154 mg/l		
step number	DO(mg/L)	Efficiency%	step number	DO(mg/L)	Efficiency%	step number	DO(mg/L)	Efficiency%	step number	DO(mg/L)	Efficiency%
us	3.8		us	3.1		us	2		us	2.5	
1	4	5.87	1	3.3	4.86	1	2.4	7.67	1	2.8	6.37
2	4	0.00	2	3.3	0.00	2	2.5	2.07	2	2.7	***
3	3.9	***	3	3.4	2.55	3	2.6	2.12	3	2.9	4.43
4	4	3.02	4	3.5	2.62	4	2.7	2.12	4	3	2.32
	Total eff 5.85%			Total eff.9.73%			Total eff.13.43%			Total eff 10.62%	

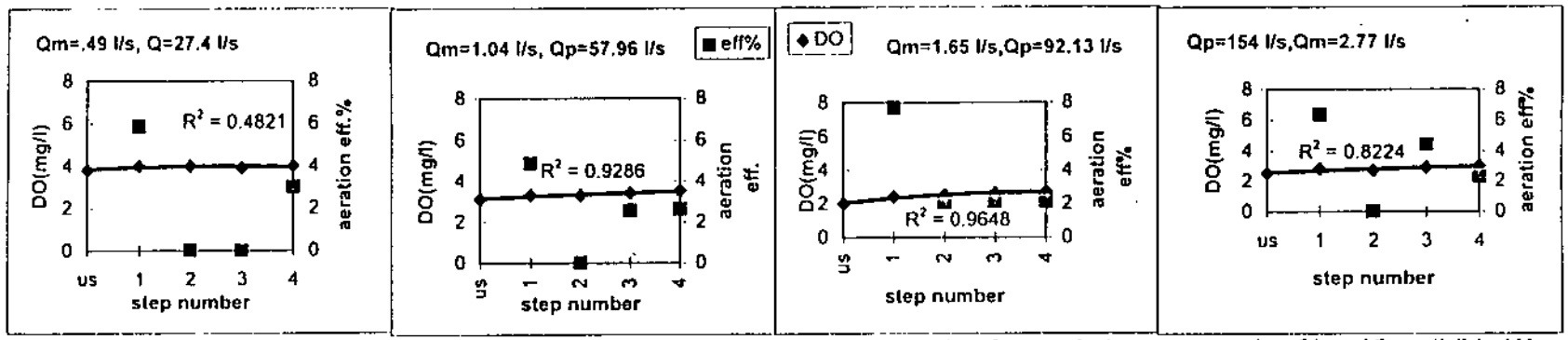

Figure(4.10) Dissolved oxygen concentration vs step number for pooled type cascade of hp=15cm,(h/L)=1/4.

*** R^2 For second degree polnomial of DO vs step number.**

Table(4.11): Dissolved oxygen concentration for pooled cascade of hp=30cm, (h/L)=1/2.

Qm=0.66 l/s Qp=36.7 l/s T=21.4C Cs=7.88 mg/l			Qm=1.08 l/s Qp=60.7 l/s T=21.2C Cs=7.92 mg/l			Qm=1.35 l/s Qp=75.40 l/s T=21.4C Cs=7.88 mg/l		
step number	DO(mg/L)	Efficiency%	step number	DO(mg/L)	Efficiency%	step number	DO(mg/L)	Efficiency%
us	5.1		us	5.2		us	5.4	
1	5.6	17.99	1	5.7	18.38	1	5.9	20.16
2	5.7	4.39	2	5.8	4.50	2	5.9	0.00
3	5.6	***	3	5.8	0.00	3	6	5.05
4	5.7	4.39	4	5.9	4.72	4	6.1	5.32
		Total eff. 21.58			Total eff. 25.78			Total eff. 28.23%

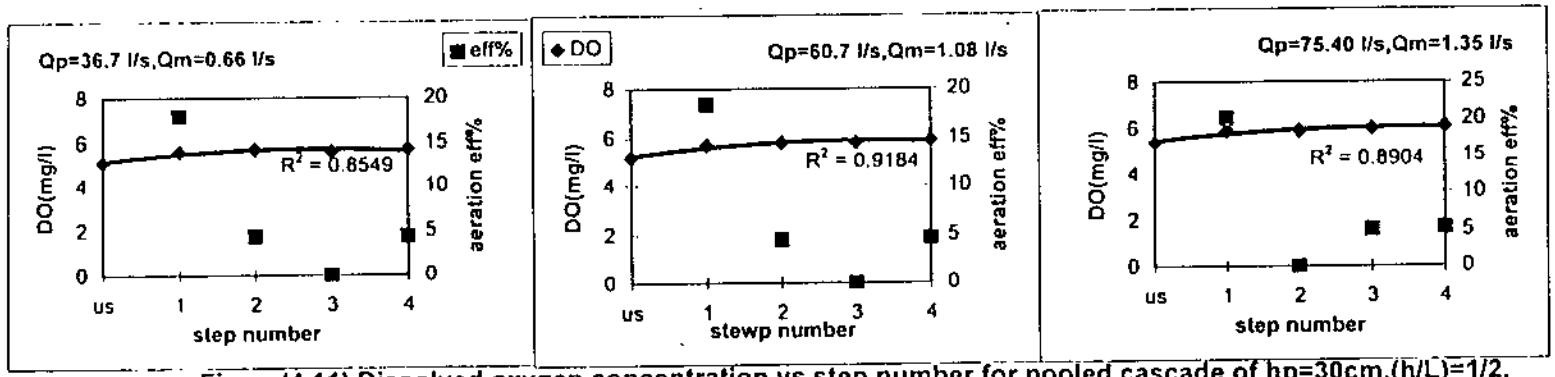

Figure(4.11) Dissolved oxygen concentration vs step number for pooled cascade of hp=30cm,(h/L)=1/2.
* R^2 For seco * R^2 For second * R^2 For second degree polnomial of DO vs step number.

Table(4.11):contd.

Qm=1.65 l/s Qp=92.1 l/s T=20.6C Cs=8.00 mg/l			Qm=2.05 l/s Qp=115 l/s T=20.5C Cs=8.99 mg/l		
step number	DO(mg/L)	Efficiency%	step number	DO(mg/L)	Efficiency%
us	4.8		us	5.6	
1	5.3	15.63	1	6	11.80
2	5.4	3.70	2	6.2	6.69
3	5.5	3.85	3	6.1	***
4	5.6	4.00	4	6.2	3.46
		Total eff.24.95%			Total eff. 24.75%

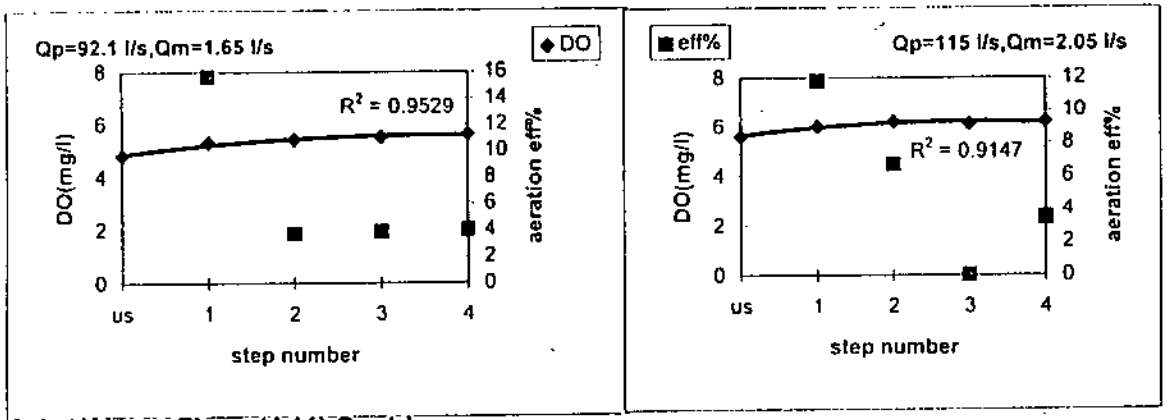

Figure(4.11) Contd.

*** R^2 For second degree polnomial of DO vs step number.**

Table(4.12): Dissolved oxygen concentration for pooled cascade of hp=45cm, (h/L)=1/2.

Qm=0.59 l/s Qp=106 l/s T=19.3C Cs=8.22 mg/l			Qm=0.94 l/s Qp=171 l/s T=19.3C Cs=8.22 mg/l			Qm=1.46 l/s Qp=265 l/s T=19.1C Cs=8.25 mg/l			Qm=1.98 l/s Qp=359 l/s T=19.2C Cs=8.23 mg/l		
step number	DO(mg/L)	Efficiency%	step number	DO(mg/L)	Efficiency%	step number	DO(mg/L)	Efficiency%	step number	DO(mg/L)	Efficiency%
us	6.3		us	6.2		us	3.6		us	5.8	
1	7.2	46.88	1	7.2	49.50	1	4.8	25.81	1	6.3	20.58
2	7.3	9.80	2	7.3	9.80	2	4.8	0.00	2	6.3	0.00
3	7.3	0.00	3	7.3	0.00	3	4.9	2.90	3	6.4	5.18
4	7.3	0.00	4	7.4	10.87	4	5.1	5.97	4	6.5	5.46
		Total eff. 52.03%			Total eff. 59.35%			Total eff. 32.26%			Total eff.28.80%

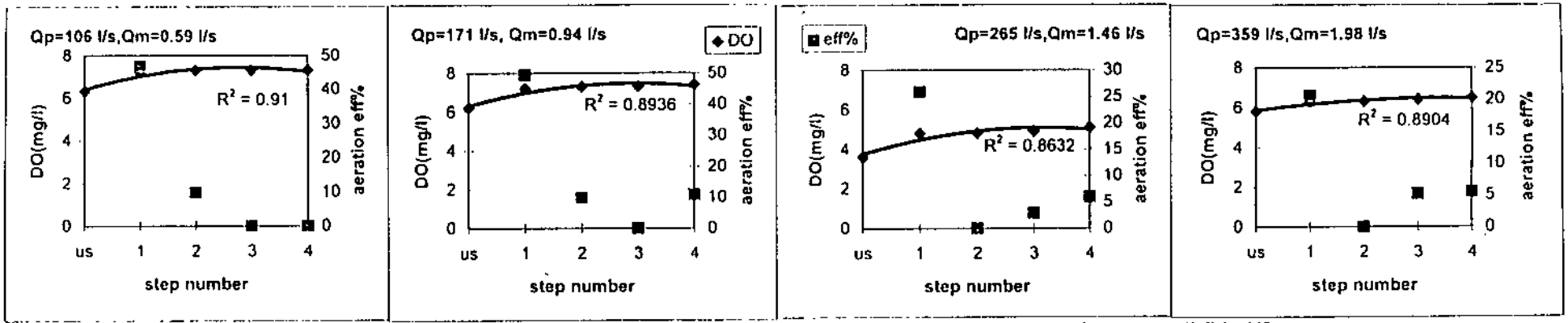

Figure(4.12) Dissolved oxygen concentration vs step number for pooled cascade of hp=45cm,(h/L)=1/2.

*** R^2 For second degree polnomial of DO vs step number.**

Table(4.13): Dissolved oxygen concentration for pooled cascade of hp=60cm, (h/L)=1/2.

Qm=0.35 l/s Qp=63.5 l/s T=19.4C Cs=8.20 mg/l			Qm=0.66 l/s Qp=119 l/s T=19.5C Cs=8.19 mg/l			Qm=0.77 l/s Qp=140 l/s T=19.5C Cs=8.19 mg/l			Qm=1.08 l/s Qp=196 l/s T=20.5C Cs=8.02 mg/l		
step number	DO(mg/L)	Efficiency%	step number	DO(mg/L)	Efficiency%	step number	DO(mg/L)	Efficiency%	step number	DO(mg/L)	Efficiency%
U/S	4.4		us	6.4		us	6.3		us	6.3	
1	5.3	23.68	1	7.2	44.69	1	7.2	47.62	1	7.1	46.51
2	5.3	0.00	2	7.2	0.00	2	7.2	0.00	2	7.3	21.74
3	5.5	6.90	3	7.3	10.10	3	7.3	10.10	3	7.4	13.89
4	5.5	0.00	4	7.3	0.00	4	7.3	0.00	4	7.4	0.00
		Total eff. 28.93%			Total eff. 50.4%			Total eff. 53.0%			Total eff. 63.81%

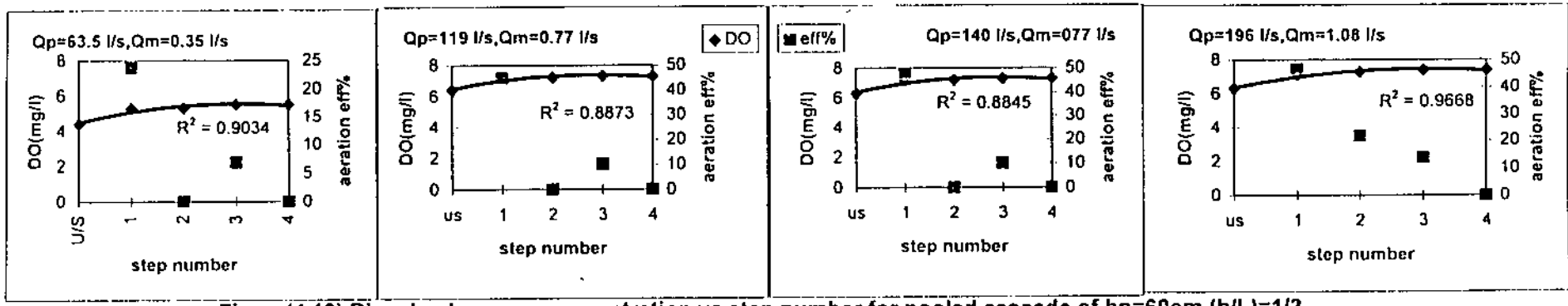

Figure(4.13) Dissolved oxygen concentration vs step number for pooled cascade of hp=60cm,(h/L)=1/2.

* R^2 For second degree polnomial of DO vs step number.

Table(4.13): contd.

Qm=1.58 l/s Qp=287 l/s T=20.5C Cs=8.02 mg/l			Qm=2.28 l/s Qp=413 l/s T=20.5C Cs=8.02 mg/l			Qm=3.52 l/s Qp=636 l/s T=20.5C Cs=8.02 mg/l		
step number	DO(mg/L)	Efficiency%	step number	DO(mg/L)	Efficiency%	step number	DO(mg/L)	Efficiency%
us	6.4		us	6.5		us	6.9	
1	7.4	61.73	1	7.3	52.63	1	7.4	44.64
2	7.4	0.00	2	7.4	13.89	2	7.4	0.00
3	7.6	32.26	3	7.5	16.13	3	7.5	16.13
4	7.6	0.00	4	7.6	19.23	4	7.5	0.00
		Total eff. 73.90%			Total eff. 72.20%			Total eff. 53.40%

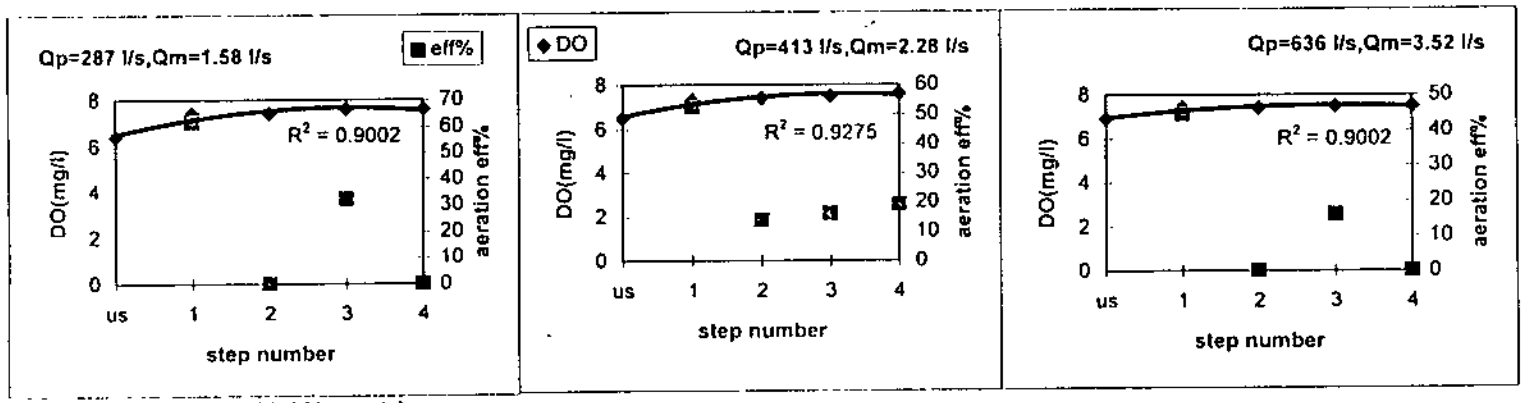

Figure(4.13) contd.

*** R^2 For second degree polnomial of DO vs step number.**

Table(4.14): Dissolved oxygen concentration for inclined cascade of hp=15cm, (h/L)=1/2.

Qm=0.24 l/s Qp=13.3 l/s T=17.1C Cs=8.60mg/l			Qm=0.35 l/s Qp=19.6 l/s T=17.4C Cs=8.55mg/l			Qm=0.55 l/s Qp=30.9 l/s T=17.3C Cs=8.56mg/l			Qm=0.73 l/s Qp=41.0 l/s T=17.2C Cs=8.58mg/l		
step number	DO(mg/L)	Efficiency%	step number	DO(mg/L)	Efficiency%	step number	DO(mg/L)	Efficiency%	step number	DO(mg/L)	Efficiency%
us	5.7		us	6.8		us	6.9		us	4.5	
1	5.8	3.45	1	6.9	5.71	1	7	6.02	1	4.6	2.45
2	5.9	3.57	2	6.9	0.00	2	7	0.00	2	4.7	2.51
3	5.9	0.00	3	7	6.06	3	7.1	6.41	3	4.8	2.58
4	6	3.70	4	7	0.00	4	7.1	0.00	4	4.9	2.65
		Total eff. 10.35%			Total eff. 11.43%			Total eff. 12.05%			Total eff. 9.80%

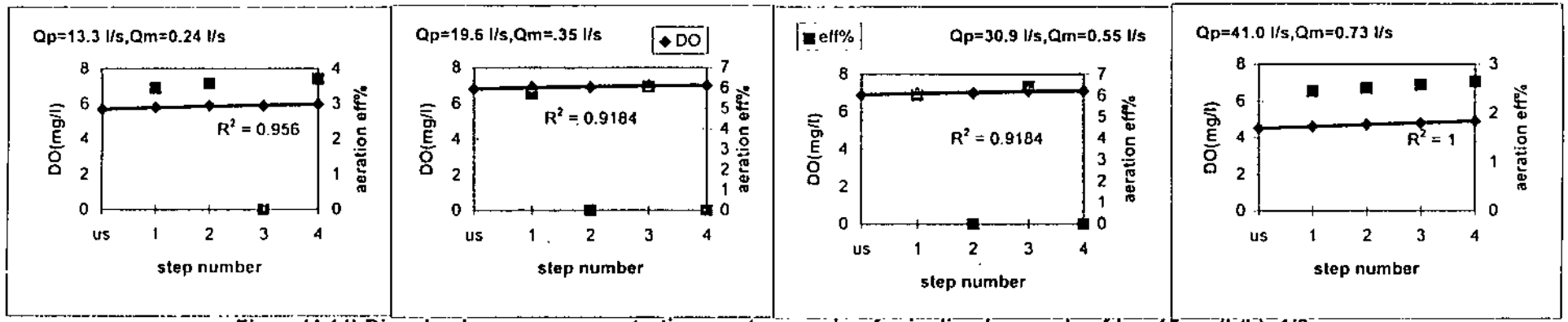

Figure(4.14) Dissolved oxygen concentration vs step number for inclined cascade of hp=15cm,(h/L)=1/2.

*** R^2 For second degree polnomial of DO vs step number.**

Table(4.15): Dissolved oxygen concentration for inclined cascade of hp=15cm, (h/L)=1/4.

Qm=0.49 l/s Qp=27.4 l/s T=26C Cs=7.21mg/l			Qm=0.99 l/s Qp=55.30 l/s T=26C Cs=7.21mg/l			Qm=1.35 l/s Qp=75.42 l/s T=26C Cs=7.21mg/l			Qm=2.36 l/s Qp=131.75 l/s T=17.2C Cs=8.58mg/l		
step number	DO(mg/L)	Efficiency%	step number	DO(mg/L)	Efficiency%	step number	DO(mg/L)	Efficiency%	step number	DO(mg/L)	Efficiency%
us	1.5		us	2.2		us	1.1		us	2	
1	1.7	3.50	1	2.3	1.99	1	1.3	3.27	1	2.4	7.68
2	1.8	1.81	2	2.5	4.07	2	1.8	8.46	2	2.5	2.08
3	2	3.69	3	2.8	6.37	3	2	3.70	3	2.6	2.12
4	2.2	3.83	4	2.9	2.26	4	2.1	1.92	4	2.7	2.17
		Total eff. 12.26%			Total eff. 13.97%			Total eff. 16.36%			Total eff: 13.43%

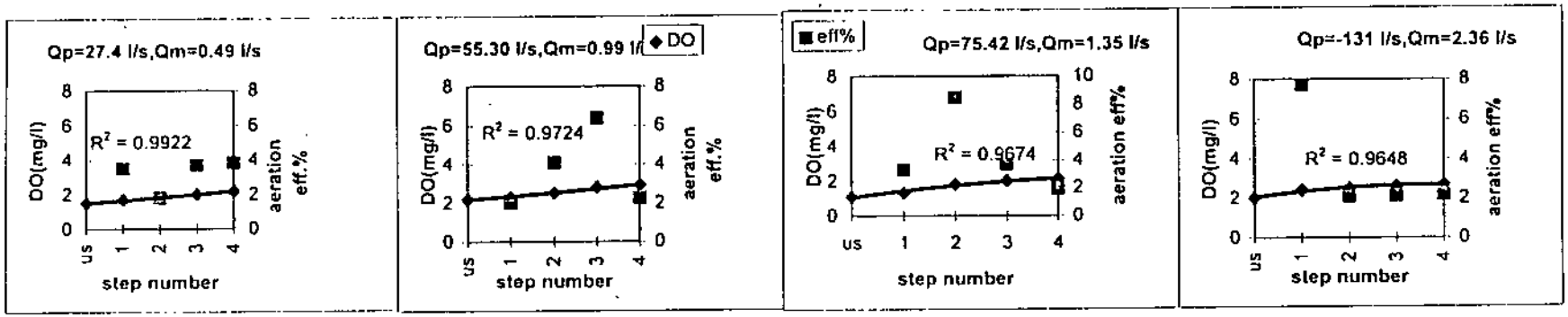

Figure(4.15) Dissolved oxygen concentration vs step number for inclined cascade of hp=15cm,(h/L)=1/4.

* R^2 For second degree polnomial of DO vs step number.

Table(4.16): Dissolved oxygen concentration for inclined cascade of hp=30cm, (h/L)=1/2.

Qm=1.58 l/s Qp=88.6 l/s T=16.9C Cs=8.64mg/l			Qm=2.13 l/s Qp=120.0 l/s T=17.1C Cs=8.60mg/l			Qm=2.68 l/s Qp=150 l/s T=17.3C Cs=8.56 mg/l			Qm=3.22 l/s Qp=180 l/s T=17.2C Cs=8.58 mg/l		
step number	DO(mg/L)	Efficiency%	step number	DO(mg/L)	Efficiency%	step number	DO(mg/L)	Efficiency%	step number	DO(mg/L)	Efficiency%
us	6.7		us	7		us	7.2		us	7.1	
1	6.8	5.15	1	7.2	12.50	1	7.3	7.35	1	7.2	6.76
2	6.9	5.43	2	7.2	0.00	2	7.4	7.94	2	7.3	7.25
3	6.9	0.00	3	7.3	7.14	3	7.4	0.00	3	7.3	0.00
4	7	5.75	4	7.4	7.69	4	7.4	0.00	4	7.3	0.00
		Total eff.15.50%			Total eff. 25.0%			Total eff. 14.66%			Total eff. 13.50%

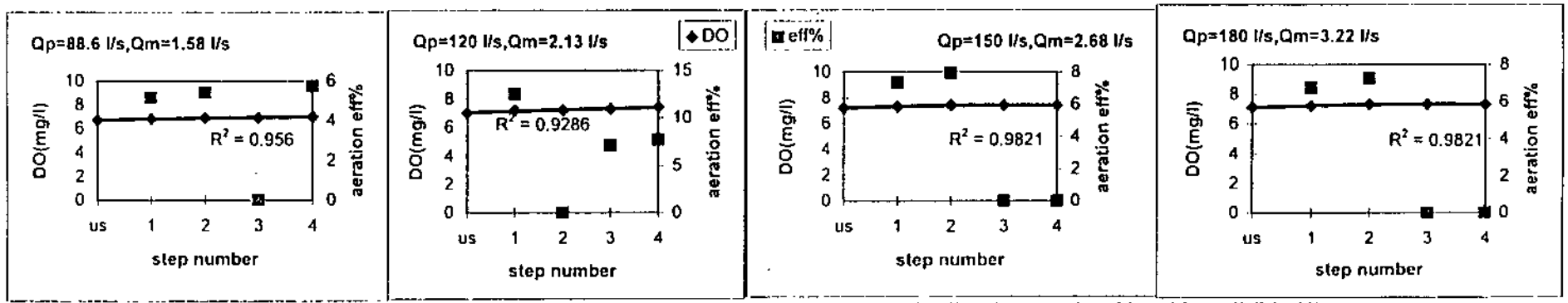

Figure(4.16) Dissolved oxygen concentration vs step number for inclined cascade of hp=30cm,(h/L)=1/2.

*** R^2 For second degree polnomial of DO vs step number.**

Table(4.17): Dissolved oxygen concentratio for inclined cascade of hp=45cm, (h/L)=1/2.

Qm=0.55 l/s Qp=276 l/s T=16.1C Cs=8.79mg/l			Qm=0.77 l/s Qp=385 l/s T=16.2C Cs=8.77mg/l			Qm=0.99 l/s Qp=494 l/s T=16.6C Cs=8.69mg/l			Qm=1.29 l/s Qp=645 l/s T=16.8C Cs=8.65mg/l		
step number	DO(mg/L)	Efficiency%	step number	DO(mg/L)	Efficiency%	step number	DO(mg/L)	Efficiency%	step number	DO(mg/L)	Efficiency%
us	8.1		us	7.3		us	8.3		us	8.2	
1	8.1	0.00	1	7.4	6.80	1	8.4	25.65	1	8.2	0.00
2	8.2	14.49	2	7.5	7.30	2	8.4	0.00	2	8.3	22.03
3	8.2	0.00	3	7.6	7.87	3	8.4	0.00	3	8.3	0.00
4	8.2	0.00	4	7.6	0.00	4	8.4	0.00	4	8.3	0.00
		Total eff. 14.5%			Total eff. 20.41%			Total eff. 25.65%			Total eff 22.03%

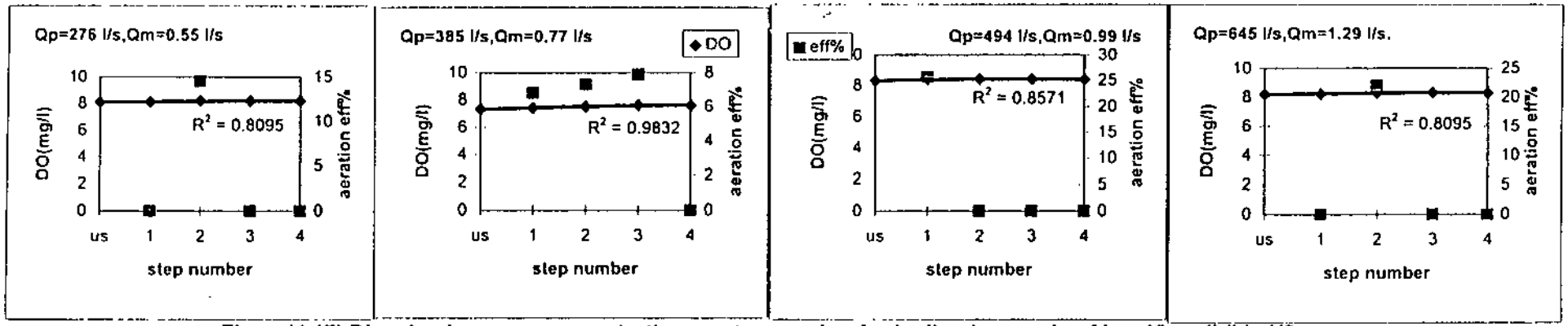

Figure(4.17) Dissolved oxygen concentration vs step number for inclined cascade of hp=45cm,(h/L)=1/2.

*** R^2 For second degree polnomial of DO vs step number.**

Table(4.18): Dissolved oxygen concentration at for inclined cascade of hp=60cm, (h/L)=1/2.

Qm=0.55 l/s Qp=276 l/s T=14.8C Cs=9.04mg/l			Qm=0.85 l/s Qp=427 l/s T=15.2C Cs=8.96mg/l			Qm=1.04 l/s Qp=517 l/s T=15.3C Cs=8.94mg/l		
step number	DO(mg/L)	Efficiency%	step number	DO(mg/L)	Efficiency%	step number	DO(mg/L)	Efficiency%
us	8.1		us	5.9		us	7.9	
1	8.2	10.70	1	5.9	0.00	1	8	9.62
2	8.1	***	2	6	3.27	2	8	0.00
3	8.2	10.70	3	6.2	6.76	3	8.1	10.64
4	8.2	0.00	4	6.4	7.25	4	8.2	11.90
		Total eff. 10.705			Total eff. 16.35%			Total eff. 28.85%

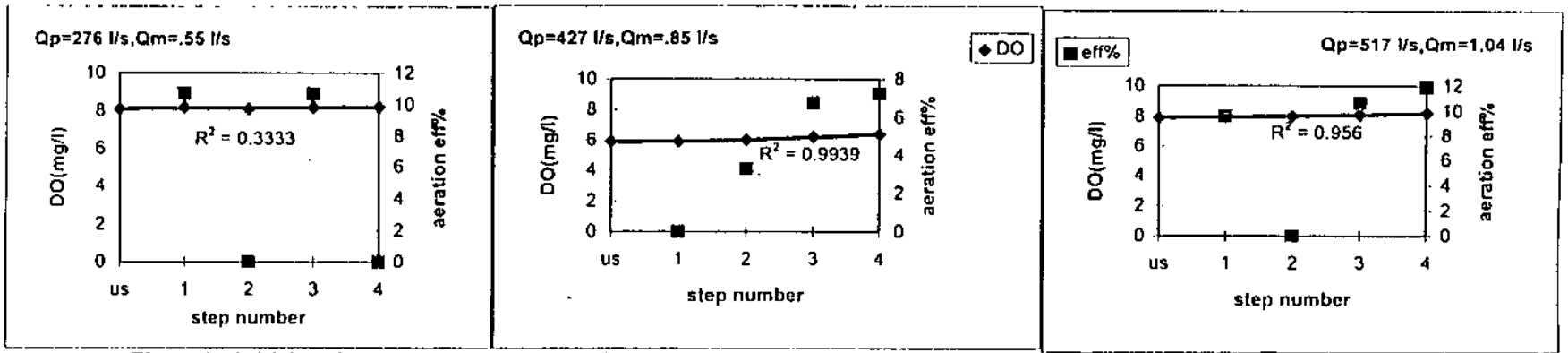

Figure(4.18) Dissolved oxygen concentration vs step number for inclined cascade of hp=60cm,(h/L)=1/2.

* R^2 for second degree polynomial.

Table(4.18): contd.

Qm=1.24 l/s	Qp=618 l/s		Qm=1.65 l/s	Qp=822 l/s	
T=15.6C	Cs=8.88mg/l		T=15.5C	Cs=8.90mg/l	
step number	DO(mg/L)	Efficiency%	step number	DO(mg/L)	Efficiency%
us	7.6		us	8.1	
1	7.6	0.00	1	8.2	12.48
2	7.7	7.81	2	8.2	0.00
3	7.8	8.47	3	8.3	14.27
4	7.9	9.26	4	8.3	0.00
		Total eff. 23.20%			Total eff. 24.97%

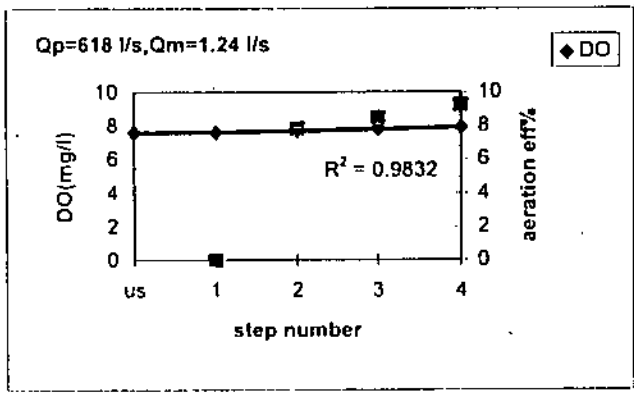

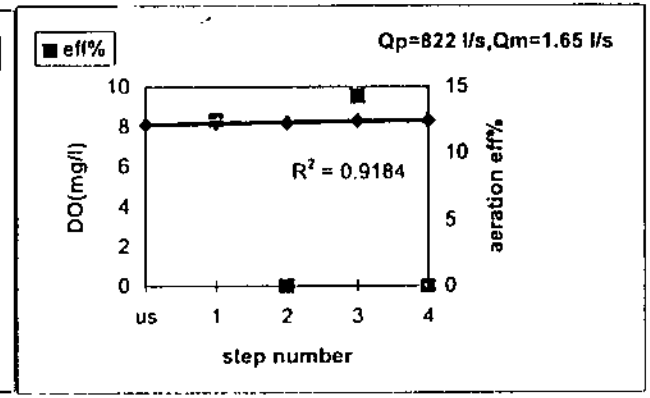

Figure(4.18): contd.

* **R^2 For second degree polnomial of DO vs step number.**

4.3 Nappe Flow Aeration Efficiency.

4.3.1 Effect of Flowrate on Aeration Efficiency.

As stated before, nappe flow condition is controlled by the model size. Models with small step heights and height to length ratio (h/L) = 1/2 need low flowrate to achieve nappe flow where the $(d_c/h)_{char}$ is low. Therefore, number of operating flowrates are limited due to apparatus limitiations. However, the change of total aeration efficiency according to different flowrates is presented in this section; where this change in total aeration is defined by equation (2.5):

$$\text{Total transfer efficiency}^{*} = \frac{C_{ds} - C_{us}}{C_s - C_{us}}$$

The results of horizontal cascade show that total aeration efficiency increases with flowrate. Avery and Novak (1978) stated that for falling jet, aeration efficiency increases with decreasing flowrate, which is against our results. Nakasone (1987) stated that aeration efficiency increases with discharge up to a certain point and then decreases with further increase of discharge. Unfortunately the horizontal cascade results didn't have the chance to show this trend due to the limited range of operating flowrate. Change of total aeration efficiency at different flowrates for the horizontal cascade models is presented in Figure (4.19). While total aeration efficiency at different flowrates for pooled cascade followed the above trend of increasing efficiency with increasing flowrate up to some point differs according to model and then decrease with a further increase in flowrate. This result can be justified due to the increasing tailwater depth with increasing flowrate, which provide larger depth for bubbles to

* For pooled and inclined models step 4, is considered as the downstream concentration, so as all the types would account for four drops.

penetrate, and therefor larger contact time. Further increase in flowrate lead to drop in oxygen transfer, due to the reduction in the height of fall. These results are developed in Figure (4.20).

For inclined type cascade aeration efficiency increased also with increasing flowrate till some point where it started to decrease with increasing flowrate. The results for inclined type cascade are presented in Figure (4.21).

Comparing total aeration efficiency between height to length ratios equal to 1/2 and 1/4 for horizontal and pooled cascade, showed that at the same flowrate region efficiency for former is higher than the later. This phenomena can be justified due to longer step length at ratio (h/L) = 1/4, which provided longer space for de-aeration to occur. the opposite is true for the inclined cascade as the (h/L) ratio equal 1/4 induced higher aeration efficiencies than the 1/2 ratio. Concavity of the figures was downward for 80% of the cases and upward for 20% unfortunately four point is not enough to give clear idea about the concavity.

Table (4.19) : Total aeration efficiency at different flow rates for horizontal cascade type.

h_p = 15 cm				h_p = 30 cm				h_p = 45 cm				h_p = 60 cm			
(h/L) = 1/2		(h/L) = 1/4		(h/L) = 1/2		(h/L) = 1/4		(h/L) = 1/2		(h/L) = 1/4		(h/L) = 1/2		(h/L) = 1/4	
Q_m (l/s)	Total Eff.%	Q_m (l/s)	Total Eff.%	Q_m (l/s)	Total Eff.%	Q_m (l/s)	Total Eff.%	Q_m (l/s)	Total Eff.%	Q_m (l/s)	Total Eff.%	Q_m (l/s)	Total Eff.%	Q_m (l/s)	Total Eff.%
0.43	24.51	0.43	22.06	0.62	32.93	0.66	26.07	1.41	58.35	1.41	45.45	0.52	13.91	0.52	10.22
0.49	30.48	0.59	31.92	0.77	41.40	0.85	29.35	1.58	61.29	1.65	43.95	0.62	21.22	0.62	12.08
		0.94	29.12	1.08	49.34	1.09	42.55	1.98	63.58	2.36	44.30	0.73	21.89	0.86	12.46
		1.24	46.97	1.41	55.92	1.46	43.76	2.28	60.03	3.93	50.84	1.19	24.26	1.24	23.74

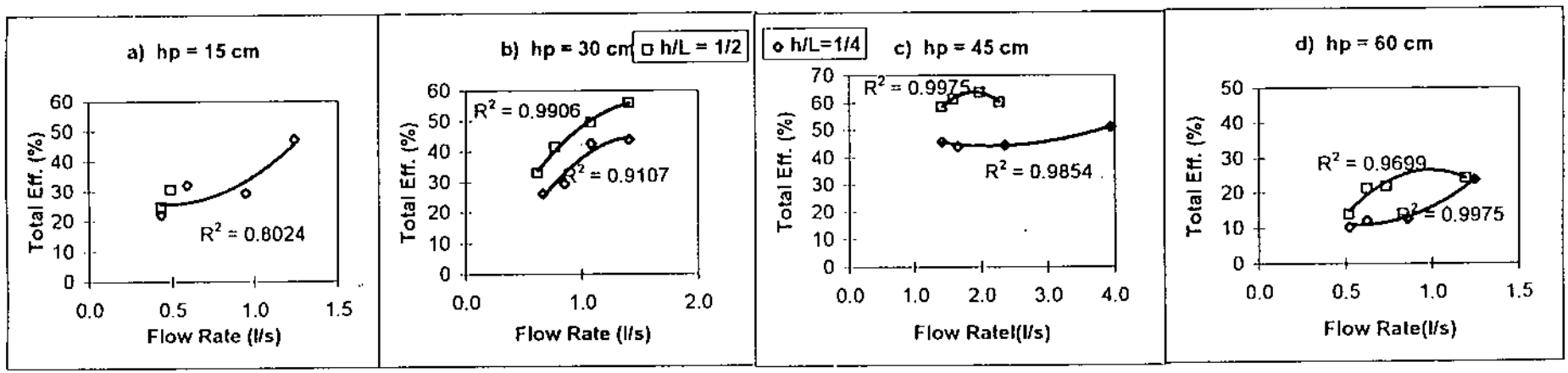

Figure (4.19) : Total aeration efficiency at different flow rates for horizontal cascade type.

Table (4.20) : Total aeration efficiency at different flow rates for pooled cascade type.

h_p = 15 cm				h_p = 30 cm		h_p = 45 cm		h_p = 60 cm	
(h/L)=1/2		(h/L)=1/4		(h/L) = 1/2		(h/L) = 1/2		(h/L) = 1/2	
Q_m (l/s)	Total Eff.%	Q_m (l/s)	Total Eff.%	Q_m (l/s)	Total Eff.%	Q_m (l/s)	Total Eff.%	Q_m (l/s)	Total Eff.%
0.49	18.08	0.49	5.85	0.66	21.60	0.59	52.00	0.35	28.93
0.69	20.96	0.65	9.73	1.08	25.78	0.94	59.35	0.66	50.40
0.94	26.21	1.04	13.43	1.35	28.23	1.46	32.26	0.77	53.02
1.35	28.35	1.35	10.62	1.65	24.95	1.98	28.80	1.08	63.81
				2.05	24.75			1.58	73.89
								2.28	72.18
								3.52	53.40

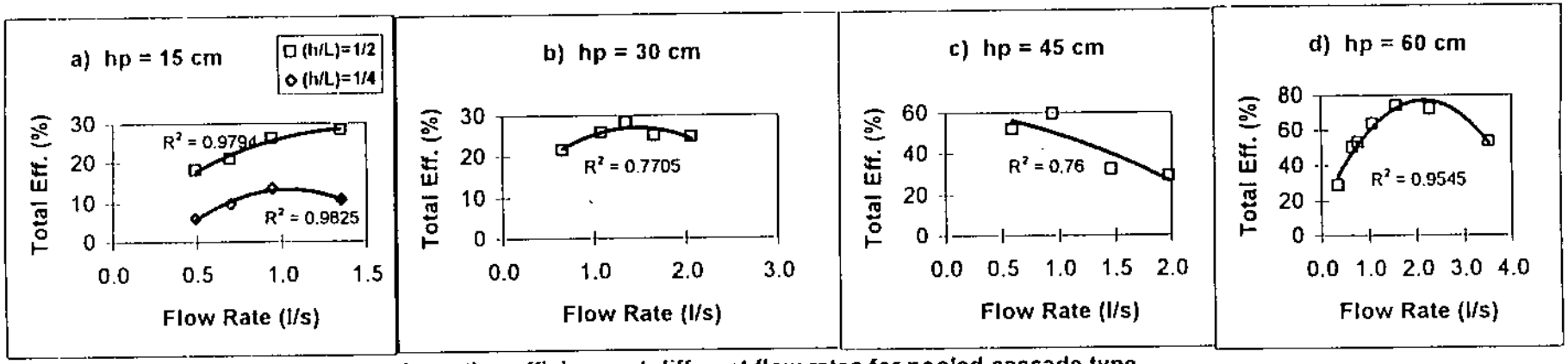

Figure (4.20) Total aeration efficiency at different flow rates for pooled cascade type.

Table (4.21) : Total aeration efficiency at different flow rates for inclined cascade type.

h_P=15 cm				h_p = 30 cm		h_p = 45 cm		h_p = 60 cm	
(h/L) = 1/2		(h/L)=1/4		(h/L) = 1/2		(h/L) = 1/2		(h/L) = 1/2	
Q_m (l/s)	Total Eff.%	Q_m (l/s)	Total Eff.%	Q_m (l/s)	Total Eff.%	Q_m (l/s)	Total Eff.%	Q_m (l/s)	Total Eff.%
0.24	10.35	0.35	12.26	1.58	15.50	0.55	14.50	0.55	10.70
0.35	11.43	0.49	13.97	2.13	25.02	0.77	20.41	0.86	16.35
0.55	12.05	0.65	16.36	2.68	14.66	0.99	25.65	1.04	28.85
0.73	9.80	0.85	13.43	3.22	13.55	1.29	22.03	1.24	23.50
								1.65	24.97

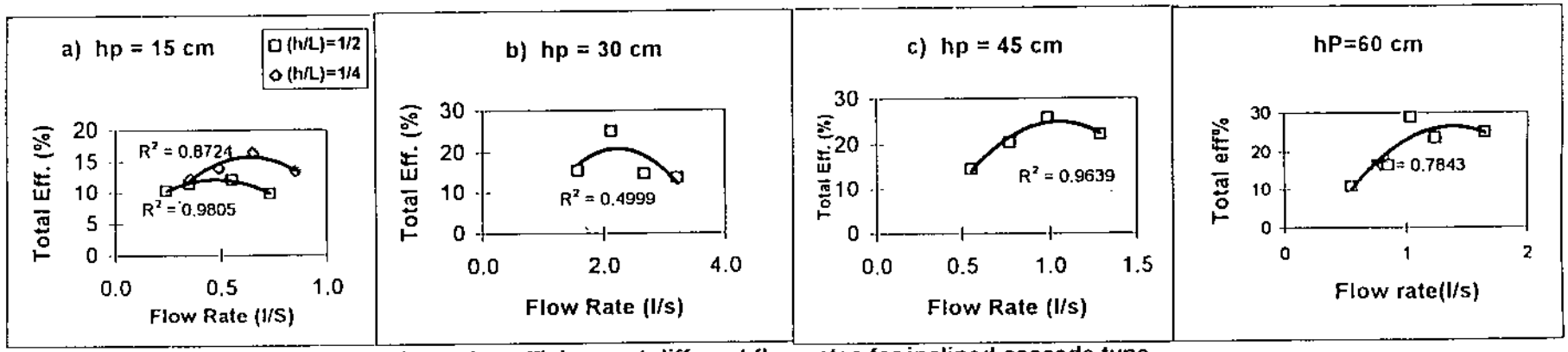

Figure (4.21) Total aeration efficiency at different flow rates for inclined cascade type.

4.3.2 Effect of Step Height on Aeration Efficiency.

For horizontal cascade with (h/L) = 1/2 aeration efficiency increases with increasing step height starting with 15cm step height to 45cm height, then decrease again at step height 60cm. For horizontal cascade with (h/L) = 1/4 aeration efficiency increases with increasing step height up to 45cm, and also decrease at step height 60cm. The results of horizontal cascade with (h/L) = 1/2 and 1/4 are presented in Figures (4.22) and (4.23) respectively.

For pooled type cascade efficiency increases with increasing step height from h_p = 15cm to h_p = 60cm. The results of pooled type are presented in Figure (4.24).

In the inclined type, efficiency increased from step height 15cm to step height 30cm, but step heights 30cm, 45 cm and 60cm revealed almost same efficiency. The results are shown in Figure (4.25).

As it's obvious from Figures (4.22) to (4.25) there is some overlapping in the aeration efficiency between the different step height, and this is probably due to the effect of discharge, as small step height might induce high aeration efficiency if it's operated under optimum discharge regarding aeration, as compared with higher step operated under discharge value away from the optimum.

Discussing effect of type on aeration efficiency, we conclude that horizontal cascade with (h/L) = 1/2 induced highest levels of aeration efficiency, followed by pooled cascade. For step height 15cm, horizontal cascade with (h/L) = 1/2 gave aeration efficiency ranges from 25% to 30%, while the pooled type gave for the same step height efficiencies ranges from 18% to 30%, for step height 30cm horizontal cascade of (h/L) 1/2

gave aeration efficiency ranges from 33% to 56% while pooled type gave efficiency ranges between 20% and 28%. For step height 45cm efficiency ranges were between 58% to 64% and 28% to 60% for horizontal and pooled cascade respectively. For step height 60cm pooled type induced higher aeration efficiency (30% to 74%) than the horizontal cascade (14% to 25%).

Inclined type cascade induced lower levels of aeration efficiency, ranges between 10% to 12%, 13%-25%, 14% to 25% and 10% to 28% for step height 15cm, 30cm, 45cm and 60cm respectively.

Table(4.22): Change of aeration efficiency with change of step Height for horizontal type cascade of (h/l)=1/2.

step height(cm)	efficiency%(nappe flowrate operating at in (l/s))				eff%(skimming flowrate operating at in (l/s))
15	24.51(0.43)	30.48(0.49)	*	*	14.9(7.95)
30	32.93(0.62)	41.40(0.77)	49.34(1.08)	55.92(2.28)	18.86(10.24)
45	58.35(1.41)	61.29(1.58)	63.58(1.98)	60.03(2.28)	**
60	13.9(0.52)	21.22(0.62)	21.89(0.73)	24.26(1.19)	19.61(13.33)

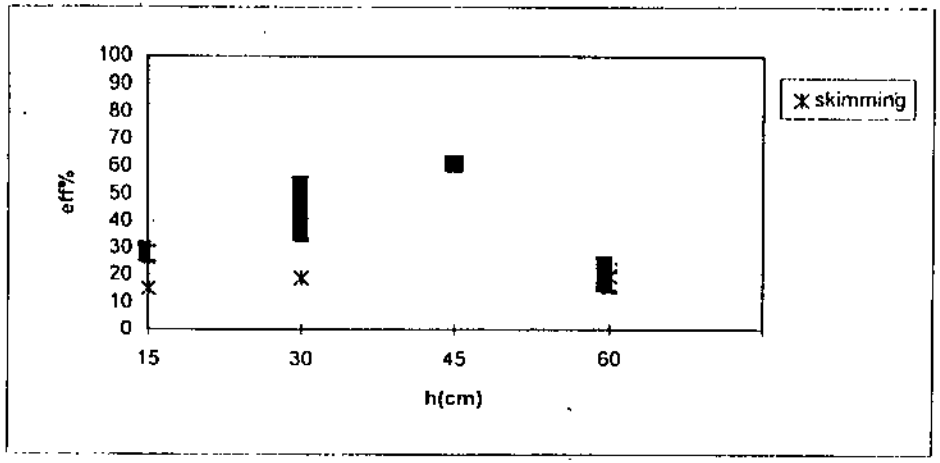

Figure(4.22) Efficiency vs. step height for horizontal type cascade of (h/L)=1/2.

* Above the two operating flowrates, flow region is transefered to transition region.

** Skimming flow couldn't be achieved, as the upstream total head exceedes the maximum flume capacity.

Table(4.23): Change of aeration efficiency with change of step height for horizontal type cascade of (h/L)=1/4.

step height(cm)	efficiency%(flowrate operating at in (l/s))				eff%(skimming flowrate operating at in (l/s))
15	22.6(0.43)	31.92(0.59)	29.12(0.94)	46.97(1.24)	21.98(7.63)
30	26.07(0.60)	29.35(0.855)	42.55(1.08)	43.76(1.46)	23.62(10.24)
45	45.45(1.41)	43.95(1.65)	44.3(2.36)	50.84(3.93)	**
60	5.40(0.52)	12.08(0.62)	12.46(0.85)	23.74(1.24)	24.69(13.33)

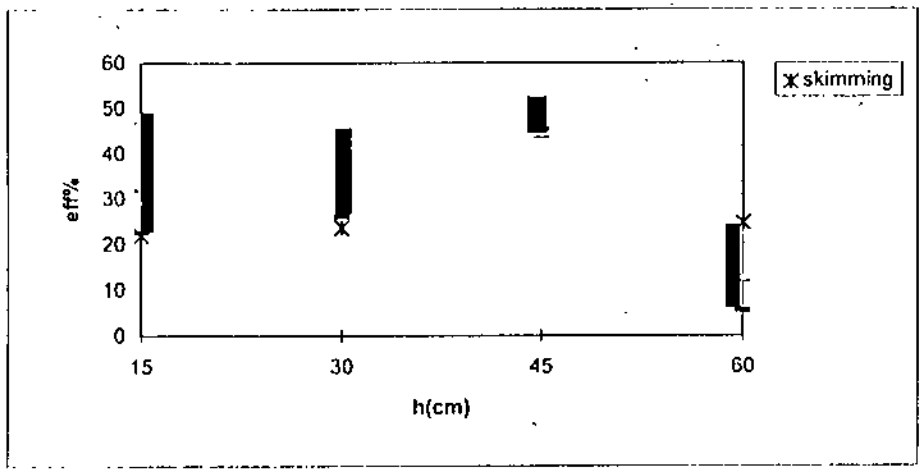

Figure (4.23) Efficiency vs. step height for horizontal type cascade of (h/L)=1/4.

** Skimming flow couldn't be achieved, as the upstream total head exceedes the maximum flume capacity.

Table(4.24): Change of aeration efficiency with change of step height for pooled type cascade of (h/L)=1/2.

step height(cm)	efficiency%(flowrate operating at in (l/s))							eff%(skimming flowrate operating at in (l/s))
15	18.08(0.49)	20.96(0.69)	26.2(0.94)	28.35(1.35)				14.5(7.95)
30	21.58(0.66)	25.78(1.08)	28.23(1.35)	24.95(1.65)	24.75(2.05)			18.52(10.24)
45	52.03(0.59)	59.35(0.94)	32.26(1.46)	28.8(1.98)				18(7.95)
60	28.93(0.35)	50.4(0.66)	53(0.77)	63.81(1.08)	73.9(1.58)	72.2(2.28)	53.4(3.52)	**

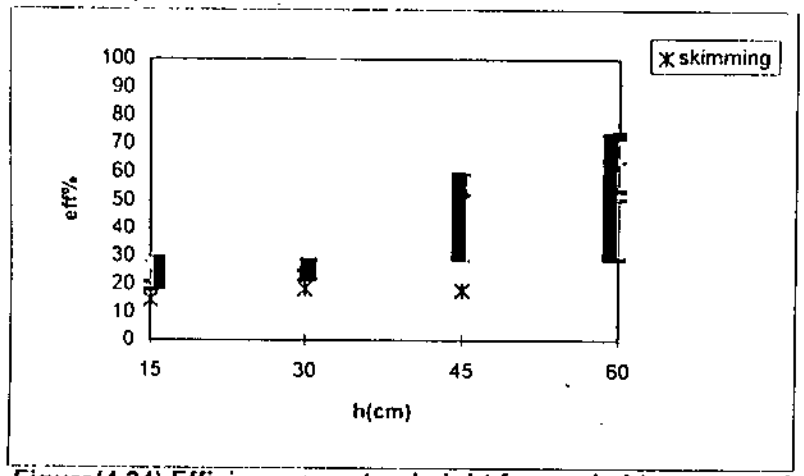

Figure(4.24) Efficiency vs. step height for pooled type cascade of (h/L)=1/2.

** Skimming flow couldn't be achieved, as the upstream total head exceedes the maximum flume capacity.

Table(4.25): Change of aeration efficiency with change of step height for inclined type cascade with (h/L)=1/2.

step height(cm)	efficiency%(flowrate operating at in (l/s))					eff%(skimming flowrate operating at in (l/s))
15	10.35(0.24)	11.43(0.35)	12.05(0.55)	9.8(0.73)		10.25(7.95)
30	15.5(1.58)	25(2.13)	14.66(2.68)	13.5(3.22)		16.04(10.24)
45	14.5(0.55)	20.41(0.77)	25.65(0.99)	22.03(1.29)		16.74(6.14)
60	10.71(0.55)	16.35(0.85)	28.85(1.04)	23.2(1.24)	24.97(1.65)	9.43(7.95)

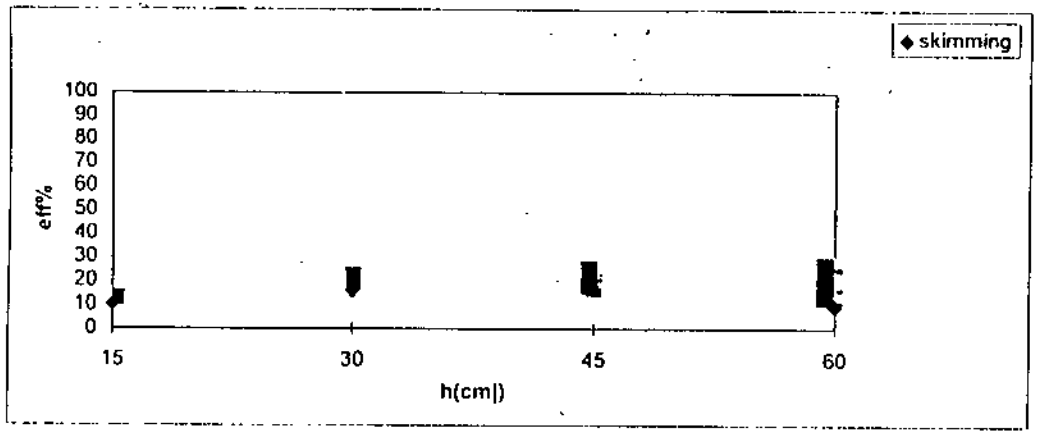

Figure(4.25) Efficiency vs. step height for inclined type cascade of (h/L)=1/2.

4.4 Skimming Flow Aeration Efficiency.

In this research one skimming flow had been operated for each model, but unfortunately due to apparatus limitations skimming flow couldn't be achieved on large models (h_p= 45cm & 60cm).

Results on horizontal cascade showed that height to length ratio (1/4) induced higher aeration efficiency than the (1/2) ratio in skimming flow region. This can be justified due the larger length of the stepped spillway in the case of (h/L) 1/4 than the 1/2 ratio, which provided the flow with longer fully aerated area. Pooled and inclined models with (h/L) 1/4 gave the same result of higher aeration efficiency than the 1/2 ratio at skimming flow regime.

The results showed also that skimming flow aeration increase with increasing drop height for horizontal type cascade. For pooled type cascade, efficiency increase with increasing step height from 15cm to 30 cm, and it's almost the same for step heights 30cm and 45cm. For inclined type cascade aeration efficiency increase with increasing step heights from 15cm to 45cm and it's less for step height 60cm.

Horizontal cascade with (h/L) = 1/4 gave highest level of aeration efficiency in skimming flow region. Followed by horizontal cascade with (h/L) = 1/2 and pooled type, which gave almost similar efficiency levels. Inclined type cascade induced the lowest aeration levels.

For horizontal and pooled cascades, of (h/L) = 1/2 skimming flow revealed less aeration efficiency than nappe flow, but this result is not applicable to the horizontal cascade of (h/L) = 1/4 or the inclined type cascade. Skimming flow aeration efficiencies are shown in Figures (4.22), (4.23), (4.24) and (4.25) for horizontal type of (h/L) = 1/2, horizontal with (h/L) = 1/4, pooled with (h/L) = 1/2 and inclined with (h/L) = 1/2, respectively.

Table(4.26): Aeration Efficiency at Skimming flow region.

Type	hp(cm)	Q_m(l/s)	Q_p(l/s)	T(c)	C_s(mg/l)	C_{us}(mg/l)	C_{ds}(mg/l)	Total efficiency%
Horizontal (h/L)=1/2	15	7.95	444.65	23	7.64	6.3	6.5	14.9
	30	10.24	572.43	24	7.49	5.9	6.2	18.86
	45	*	*	*	*	*	*	*
	60	13.33	2413.48	26	7.22	6.2	6.4	19.61
Horizontal (h/L)=1/4	15	7.63	426.65	24.6	7.41	6.5	6.7	21.98
	30	10.24	572.43	24.7	7.37	6.1	6.4	23.62
	45	*	*	*	*	*	*	*
	60	13.33	2413.48	25	7.35	3.3	4.3	24.69
Pooled (h/L=1/2)	15	7.95	444.65	21.5	7.87	5.8	6.1	14.5
	30	10.24	572.73	20.8	7.98	6.9	7.1	18.52
	45	7.95	1439	19.3	8.22	6	6.4	18
	60	*	*	*	*	*	*	*
Pooled (h/L)=1/4	15	7.95	444.65	26	7.21	3	3.7	16.6
Inclined	15	7.95	444.65	17.4	8.55	6.6	6.8	10.25
	30	10.24	572.73	17.3	8.57	6.4	6.7	16.04
	45	6.14	3062	17.3	8.59	6.2	6.6	16.74
	60	7.95	3967	16.9	8.65	4.4	4.8	9.43
Inclined (h/L)=1/4	15	7.95	444.65	26	7.21	2.1	2.8	13.7

* Not available due to apparatus limitations.

4.5 Deficit Ratio Relations

As stated before in details in Ch.2, many researchers have proposed relations for aeration efficiency over spillways or jet fall drop, but few took into account the multiple steps situations. Gameson (1958) proposed a relation for deficit ratio over spillway as function of drop height and temperature and introduced a parameter concerning stepped spillway.

$$r = 1 + 0.361\ MN\ (1+0.046T)\ H_T \quad \ldots\ldots\ldots\ldots\ldots\ldots\ldots\ldots\ldots\ldots\ldots\ldots\ (4.1)$$

where;

r = deficit ratio = $\frac{C_s - C_{us}}{C_s - C_{ds}}$;

H_T = total drop height (m), and equal to (h_p* number of steps)

M = water quality parameter equal to 0.85 for sewage effluents, 1.0 for moderately polluted, 1.25 for slightly polluted.

N = weir geometry parameter, 0.2 (slope), 1.0 (weir), 1.1 (step weir).

T, in (°C).

As it's obvious Gameson et al. (1959) relation takes into account the height which water falls, beside the temperature but doesn't take into account the flowrate or the type of flow over the structure or the height to length ratio of the steps.

Gameson et al. (1958) has been applied on the horizontal type cascade with (h/L) = 1/2 and 1/4, with the following form.

Gameson $\rightarrow r = 1 + 0.361\ (1.25)\ (1.1)\ (1 + 0.046T)\ H_T$

Where H_T was taken as total drop height and it's equal to the height of single step multiplied by the number of steps. The results are shown in tables (4.27) and (4.28). Experimental deficit ratio and Gameson deficit ratio has been plotted against total drop height in Figures (4.26) and (4.27). The figures show that experimental deficit ratio coincide well with Gameson deficit ratios for small drop heights, but the lag between them increase with high drop heights. Also experimental results for horizontal cascade of (h/L) = 1/2 correlate with Gameson relation better than the (h/L) = 1/4.

It's naturally that experimental results don't have full correlation's with Gameson relation, because the relation doesn't take into account many important variables affecting cascade aeration.

As mentioned before Avery and Novak (1978) also proposed a correlation for aeration efficiency of free overall, and they stated that if the cascade consisted of a series of n equal steps, the deficit ratio for this type of cascade will be r^n in which r, deficit ratio for one step. Avery and Novak relation; equation (2.53):

$$r_{15} - 1 = 0.627 \times 10^{-4} \left(\frac{g}{2}\right)^{0.445} (\nu)^{-0.53} h^{1.335} q^{-0.36}$$

has been applied to the pooled type cascade as it's the nearest configuration to their experiments. Deficit ratio has been corrected from T = 15°C to the operating temperature using the following equation (2.44)

$$\frac{Ln\, r_T}{Ln\, r_{15}} = 1.0241^{(T-15)}$$

Detailed calculation are shown in Table (4.29). Experimental deficit ratio and Avery and Novak deficit ratio has been plotted against step

height, as shown in Figure (4.28), Figure (4.29) shows the correlation of the two deficit ratios. The two figures imply reasonable correlation between the two deficit ratios, better than that achieved by Gameson relation, because of the introduction of discharge.

Computing total transfer efficiency of a cascade through the ratio r^n implies that all steps contribute with same amount in total efficiency, which disagree with this research results as step 1 achieved max efficiency and with value extensively higher than the following steps. If deficit ratio of step 1 is used in the ratio r^n total efficiency would be overestimated, and if any of the following steps is used total efficiency would be underestimated, so typical r_{exp} has been computed through the ratio $(r_{exp})^{1/4}$ and $E_{typical}$ through equation (2.43); $E = 1 - \frac{1}{r}$. This $E_{typical}$ has been compared to each step efficiency of pooled cascade and it was almost the average of the 4 steps efficiencies, but it's less than the total aeration efficiency.

Table(4.27):Comparison of experimental deficit ratio with values computed from Gameson relation for horizontal type cascade of (h/L)=1/2.

H_T	(h/L)	Q_p	T	C_s	C_{us}	C_{ds}	r(gameson)	rexp
(m)		(m^3/s)	(c)	(mg/L)	(mg/L)	(mg/L)		
0.6	0.5	2.41E-02	25	7.35	4.9	5.5	1.64	1.32
0.6	0.5	2.74E-02	24.4	7.44	5.8	6.3	1.63	1.44
1.2	0.5	3.47E-02	24.4	7.44	4.1	5.2	2.26	1.49
1.2	0.5	4.32E-02	24.4	7.44	4.3	5.6	2.26	1.71
1.2	0.5	6.07E-02	24.4	7.44	4.4	5.9	2.26	1.97
1.2	0.5	7.86E-02	24.4	7.44	4.4	6.1	2.26	2.27
1.8	0.5	7.86E-02	24.8	7.37	3.6	5.8	2.91	2.40
1.8	0.5	8.86E-02	25.3	7.30	4.2	6.1	2.93	2.58
1.8	0.5	1.11E-02	25.3	7.30	4	6.1	2.93	2.75
1.8	0.5	1.27E-01	25.7	7.28	3.8	5.9	2.95	2.52
2.4	0.5	9.43E-02	26	7.21	2.9	3.5	3.62	1.16
2.4	0.5	1.13E-01	26	7.21	2.5	3.5	3.62	1.27
2.4	0.5	1.33E-01	26	7.21	3.1	4	3.62	1.28
2.4	0.5	2.15E-01	26	7.21	3.5	4.4	3.62	1.32

Table(4.28):Comparison of experimental deficit ratio with values computed from Gameson relation for horizontal type cascade of (h/L)=1/4.

H_T	(h/L)	Q_p	T	C_s	C_{us}	C_{ds}	r(gameson)	rexp
(m)		(m^3/s)	(c)	(mg/L)	(mg/L)	(mg/L)		
0.6	0.25	2.41E-02	25.6	7.27	5	5.5	1.65	1.28
0.6	0.25	3.28E-02	25.6	7.27	5.7	6.2	1.65	1.47
0.6	0.25	5.27E-02	25	7.35	4.3	5.2	1.64	1.42
0.6	0.25	6.93E-02	24.7	7.39	5.9	6.6	1.64	1.89
1.2	0.25	3.67E-02	22.5	7.58	4.9	5.6	2.21	1.35
1.2	0.25	4.78E-02	22.5	7.58	5.2	5.9	2.21	1.42
1.2	0.25	6.07E-02	22.5	7.58	5	6.1	2.21	1.74
1.2	0.25	8.19E-02	22.5	7.58	5.3	6.3	2.21	1.78
1.8	0.25	7.86E-02	35	6.16	4.4	5.2	3.33	1.83
1.8	0.25	9.21E-02	35	6.16	3.2	4.5	3.33	1.78
1.8	0.25	1.32E-01	35	6.16	3	4.4	3.33	1.80
1.8	0.25	2.19E-01	35	6.16	3.8	5	3.33	2.03
2.4	0.25	9.43E-02	26	7.21	3.5	3.7	3.62	1.06
2.4	0.25	1.13E-01	26	7.21	3.9	4.3	3.62	1.14
2.4	0.25	1.55E-01	26	7.21	3.9	4.4	3.62	1.18
2.4	0.25	2.24E-01	26	7.21	3	4	3.62	1.31

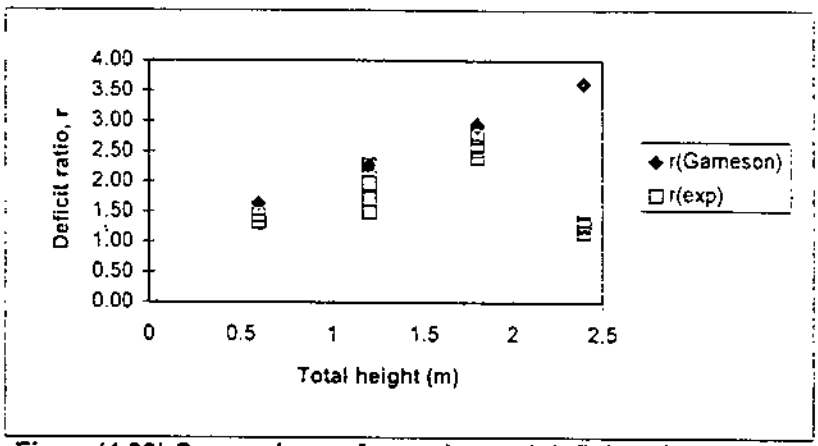

Figure(4.26) Comparison of experimental deficit ratio with Gameson relation for horizontal type cascade of (h/L)=1/2.

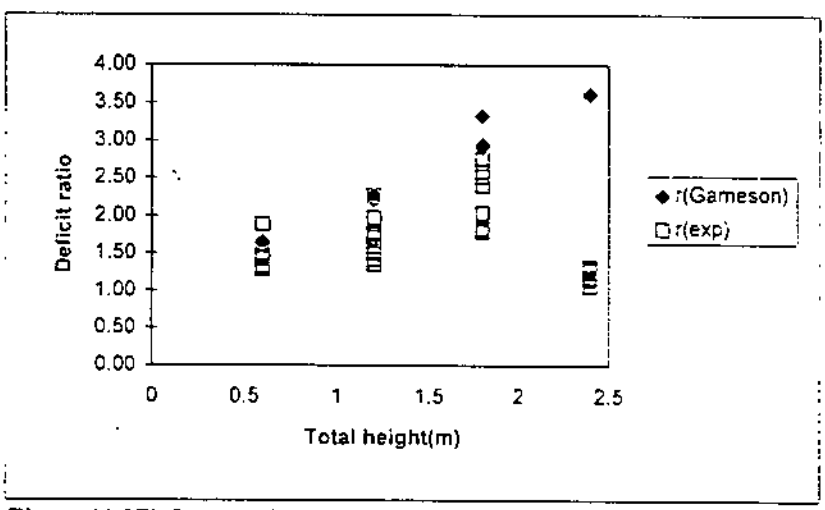

Figure(4.27) Comparison of experimental deficit ratio with Gameson relation for horizontal type cascade of (h/L)=1/4.

Table(4.29):Comparison of experimental deficit ratio with valued computed from Avery & Novak relation for pooled type cascade of (h/L)=1/2.

h_p(m)	Q_p(l/s)	q(m^2/s)	T(c)	C_s(mg/l)	C_{us}(mg/l)	C_{ds}(mg/l)	r(exp)	r_{15}	r_T	r_T^4	$r(exp)_{typical}$	$E_{typical}$
0.15	27.40	0.09	20.80	7.98	3.00	3.90	1.22	1.03	1.04	1.16	1.05	4.86
0.15	39.00	0.13	21.20	7.92	4.10	4.90	1.26	1.03	1.03	1.15	1.06	5.71
0.15	52.70	0.18	21.20	7.92	4.10	5.10	1.35	1.03	1.03	1.13	1.08	7.31
0.15	75.40	0.25	21.20	7.92	5.80	6.40	1.39	1.02	1.03	1.11	1.09	7.98
0.30	36.70	0.12	21.40	7.88	5.10	5.70	1.28	1.08	1.09	1.41	1.06	5.90
0.30	60.70	0.20	21.20	7.92	5.20	5.90	1.35	1.06	1.07	1.33	1.08	7.17
0.30	75.40	0.25	21.40	7.88	5.40	6.10	1.39	1.06	1.07	1.31	1.09	7.96
0.30	92.10	0.31	20.60	8.00	4.80	5.60	1.33	1.05	1.06	1.28	1.07	6.94
0.30	115.00	0.38	20.50	8.99	5.60	6.20	1.22	1.05	1.06	1.25	1.05	4.75
0.45	106.00	0.35	19.30	8.22	6.30	7.30	2.09	1.09	1.10	1.46	1.20	16.80
0.45	171.00	0.57	19.30	8.22	6.20	7.40	2.46	1.08	1.08	1.38	1.25	20.18
0.45	265.00	0.88	19.10	8.25	3.60	5.10	1.48	1.06	1.07	1.32	1.10	9.28
0.45	359.00	1.20	19.20	8.23	5.80	6.50	1.40	1.06	1.06	1.28	1.09	8.14
0.60	63.50	0.21	19.40	8.20	4.40	5.50	1.41	1.16	1.18	1.92	1.09	8.19
0.60	119.00	0.40	19.50	8.19	6.40	7.30	2.01	1.13	1.14	1.70	1.19	16.03
0.60	140.00	0.47	19.50	8.19	6.30	7.30	2.12	1.12	1.13	1.65	1.21	17.16
0.60	196.00	0.65	20.50	8.02	6.30	7.40	2.77	1.11	1.12	1.58	1.29	22.52
0.60	287.00	0.96	20.50	8.02	6.40	7.60	3.86	1.09	1.11	1.49	1.40	28.64
0.60	413.00	1.38	20.50	8.02	6.50	7.60	3.62	1.08	1.09	1.42	1.38	27.50
0.60	636.00	2.12	20.50	8.02	6.90	7.50	2.15	1.07	1.08	1.36	1.21	17.45

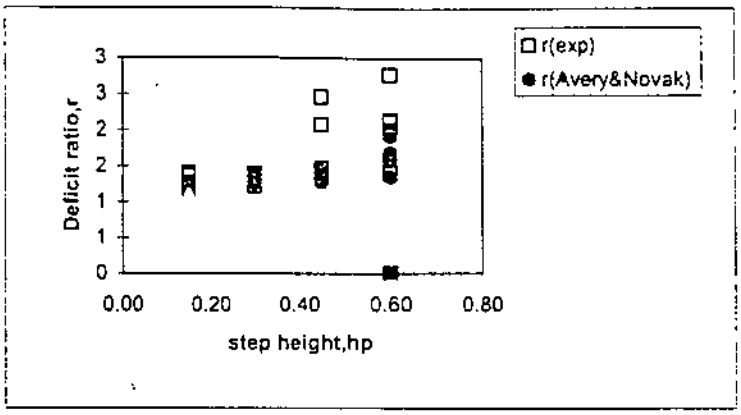

Figure(4.28) Comparison of experimental deficit ratio with Avery and Novak relation for pooled type cascade.

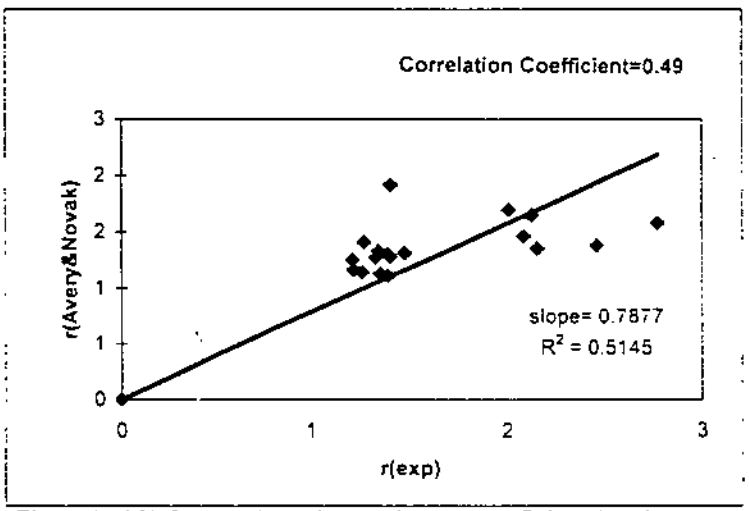

Figure(4.29) Correlation of experimental deficit ratio with Avery and Novak relation.

Chapter Five
Conclusions and Recommendations

Chapter Five

Conclusions and Recommendations.

Stepped spillway contribute to the enhancement of air-water transfer, and the dissipation of flow energy. On stepped spillway two types of flow regime can occur; nappe flow and skimming flow. In Chapter Four, the experimental results were analyzed in form of tables and figures, while in this chapter the main conclusions will be presented.

(1) Horizontal type cascade of (h/L) = 1/2 produced highest levels of aeration efficiency at nappe flow, followed by minor difference with pooled type cascades and finally by the inclined type.

(2) For nappe flow, horizontal and pooled cascades with height to length ratio equal 1/2 gave higher aeration efficiency than the height to length ratio equal 1/4, while for the inclined type, the ratio 1/4 was better than the 1/2 ratio regarding aeration efficiency.

(3) In nappe flow region, the horizontal cascade aeration efficiency increased with increasing step height from 15cm to 45cm, but the step height 60cm introduced a reduction in aeration efficiency. For pooled type cascade aeration efficiency increased with increasing step height, while for the inclined type aeration efficiency increase from step height 15cm to 30cm, but step heights 30cm, 45cm and 60cm revealed almost same efficiency.

(4) Aeration efficiency in nappe flow region increases with increasing flowrate up to some point differs according to type and dimensions, of the model, where it start to decrease again, (as explained in section 4.3.1).

(5) In skimming flow region, horizontal cascade showed that height to length ratio (1/4) induced higher efficiency than the (1/2) ratio.

(6) In skimming flow region, horizontal cascade with (h/L) 1/4 gave highest efficiency, followed by the horizontal cascade of (h/L) 1/2, by the pooled, and finally by the inclined type.

Recommendation:

It is well clear that stepped structures improve the quality of water by increasing the dissolved oxygen content, so it's recommended to use stepped structures as a postaeration stage for wastewater in wastewater plants and to be introduced along rivers and stream to elevate the dissolved oxygen content.

As mentioned earlier, many variables are involved in the aeration process on stepped structures, and up to our knowledge there is lack of researches on multiple steps structures. Therefore continuation of research on stepped cascade is needed to introduce a more data to develop it's performance. Suggested researches are listed in below:

(1) Study aeration efficiency along different step numbers, and more height to length ratios.

(2) Study aeration efficiency for skimming flow region, with different flow rates.

(3) Study pooled and inclined types with different upgrading and downgrading percentages.

(4) Study the effect of step surface friction factor on aeration efficiency.

References

Aivazyan, O. M., 1986, "Stabilized aeration on chutes", Gidrotekhni cheskoe stroitel'stvo, No. 12, PP. 33-40.

Albrecht, D., 1969, "Schatzung der sauerstoffzunfuhr durch where and kaskaden", Die wasserwirtschalft, Vol. 11.

APAHA, AWWA and WPCF., 1989, Standard methods for the examination of water and wastewater, American Public Health Association Publication, 7th ed.

Apted, R.W. and Novak, P., 1973 "Oxygen uptake at weirs", Proc. 15th IAHR Congr. Istanbul, Vol. 1, PP. 177-186.

Avery, S.T., and Novak, P., 1975, "Oxygen uptake in hydraulic jump and at overfalls." Proc. 16th IAHR Congr., Sao Paulo, PP. 329-337.

Avery, S.T., and Novak, P., 1978, "Oxygen transfer at hydraulic structures", Journal of Hydraulics Division, ASCE, Vol. 104, No. Hyll., PP. 1521-1541.

Barret, M.J., Gameson, A. L. H., and Ogden, C. G., 1960, "Aeration studies at four weir systems", Water and Wastes Engineering, Vol. 64, No. 9, PP. 407-413.

Chanson, H., 1992 a, "Drag reduction in self aerated flows analogy with dilute polymer solution and sediment flows", Department of Civil Engineering, University of Queensland, Australia, Oct, Research Report CE 141.

Chanson, H., 1992 b, "Air entrainment in chutes and spillways", Department of Civil Engineering, University of Queensland, Australia, Research Report No. CE 133.

Chanson, H., 1993a, "Stepped spillway flows and air entrainment", Canadian Journal of Civil Engineering, Vol. 20, PP. 422-435.

Chanson, H., 1993b, "Self-aerated flows on chutes and spillways", Journal of Hydraulic Engineering, Vol. 119, No. 2, PP. 221-243.

Chanson, H., 1993c, "Environmental impact of large water releases in chutes: oxygen and nitrogen content due to self-aeration", Proceeding 25th IAHR, No. 5, PP. 273-280.

Chanson, H., 1994a, "Hydraulics of nappe flow regime above stepped chute and spillways", Australian Civil Engineering Transactions, Vol. CE 36, No. 1, January, PP. 69-76.

Chanson, H., 1994b, "State of the art of the hydraulic design of stepped chute spillways", Hydropower and Dams, July, PP. 33-41.

Chanson, H., 1995 a, "Predicting oxygen content downstream of weirs, spillways and waterways", Proc Instn. Civ. Engrs Wat. Marit. and Energy, No. 112, PP. 20-30.

Chanson, H., 1995 b, "History of stepped channels and spillways: a rediscovery of the wheel", Journal of Civil Engineering, Vol. 22, PP. 247-259.

Christodoulou, C., 1993, "Energy dissipation on stepped spillways", Journal of Hydraulic Engineering , Vol. 119, No. 5, May, PP. 644-650.

Danil, E.I., and Gulliver, J., 1988, "Temperature dependence of liquid film coefficient for gas transfer", J. Envirom. Engng., Vol. 114, No. 5, PP. 1224-1229.

Danil, E.I., and Gulliver, J. and Thene, J.R., 1991, "Water quality assessment for hydropower", J. Envirom. Engng., ASCE, Vol. 117, No. 2, PP. 179-193.

Diez-Cascon, J., Blanco, J., Revilla, J. and Garcia, R., 1991 "Studies on the hydraulic behavior of stepped spillway", Water power and Dam Constructions, September, PP. 22-26.

Elmore, H.L., and West, W.F., 1961, "Effect of water temperature on stream re-aeration", Journal of Sanitary Engineering, ASCE, Vol. 87, No. SA6, PP. 59-71.

Ervine, D. A., and Falvey, H.T., 1987, "Behavior of turbulent water jets in the atmosphere and in plunge pools", Proceedings of the Institution of Civil Engineering, Part 2, 83, PP. 295-319.

Essery, I.T.S., and Horner, M. W., 1978, "The hydraulic design of stepped spillway", 2nd ed CIRIA Report No. 33, Construction Industry Research and Information Association, London, United kingdom.

Forster, C. F., 1985, Biotechnology and Wastewater Treatment, Cambridge Studies and Biotechnology; 2nd ed..

Gameson, A. L. H., 1957, "Weirs and the aeration of rivers", J. Inst. Water Eng. Sc., Vol. 11, PP. 477-490.

Gameson, A. L. H., Vandyke, K.G., and Ogden, C.G., (1958). "The effect of temperature on aeration at weirs", Water and Water Engng, Nov., PP. 489-492.

Geankoplis, J., 1983, Transport Processes and Unit Operations, Allyn and Bacon., Inc., 2nd ed.

Grindrod, J., 1962, "British research on aeration at wear", Water and Sewage Works, October.

Gulliver, J. S., Thene, J. K. and Rindels, A.J., 1990, "Indexing gas transfer in self aerated flows", J. Envirom. Engng, ASCE, Vol. 116, No. 3, PP. 503-523.

Gulliver, J.S., and Rindles, A.J., 1993, "Measurement of air-water oxygen transfer at hydraulic structures", Journal of Hydraulic Engineering, ASCE, Vol. 119, No. 3, March, PP. 327-349.

Gulliver, J.S., Hibbs, D.E., and Mac-Donald, J.P., 1997, "Measurement of effective saturation concentration for gas transfer", Journal of hydraulic Engineering, ASCE, Vol. 123, No. 2, February, PP. 86-97.

Hager, H., Bremen, R., and Kawagoshi, N., 1990, "Chemical hydraulic jump: length of the roller", Journal of Hydraulic Research., IAHR, Vol. 28, No. 5, PP. 591-608.

Hager, H., 1991, "Uniform aerated chute flow", Journal of Hydraulic Engineering, ASCE, Vol. 117, No. 4, April, PP. 528-533.

Hartung, F., and Scheuerlein, H., 1970, "Design of overflow rockfill dams", Proceeding, 10th International Congress on Large Dams, Montreal, Que., Q. 36, R. 35, PP. 587-598.

Henderson, F. M., 1966, "Open channel flow", Macmillan Company, New York.

Higbie, R., 1935, "Rate of absorption of a gas into a still liquid", Trans. Am. Inst. Chem. Engng., 31, PP. 365-389.

Holler, A.G., 1971, "The mechanism describing oxygen transfer from atmosphere to discharge through hydraulic structures", Proceedings, XIV Congress, International Association for Hydraulics Research, Paper A45, PP. 373-382.

Javis, P. J., 1970, "A study in the mechanics of aeration at weirs", Thesis presented to the University of Newcastle upon Tyne, England, In Partial Fulfillment of the Requirements for the Degree of Doctor of Philosophy.

Kawase, Y. and Moo-young, M., 1992, "Correlation for liquid-phase mass transfer coefficients in bubble column reactors with Newtonian and non-Newtonian fluids", Can. J. Chem. Engng., Vol. 70, February, PP. 48-54.

Keller, R. J., and Rastogi, A. K., 1977, "Design chart for predicting critical point on spillways", Journal of the Hydraulic Divison, ASCE, Vol. 103, No. Hy 12, PP. 1417-1429.

Knauss, J., 1979, "Computation of maximum discharge of overflow rockfill dams", Proceedings, 13th International Congress on Large Dams, New Delhi, India, Q., 50 R. 9, PP. 143-159.

Knight, D. W., and Mac-Donald, J. A., 1979, "Hydraulic resistance of artificial strip roughness", Journal of the Hydraulic Divison, ASCE, Vol. 105, NO. Hy6, PP. 675-690.

Labocha, M., Corsi, L., and Zytne, G., 1996, "Parameters influencing oxygen uptake at clarifies weirs", Water Environmental Research, Vol. 68, No. 6, PP. 988-994.

Markofsky, M., and kobus, H., 1978, "Unified presentation of weir aeration data", Journal of Hydraulic Division, ASCE, Vol. 104, No. H Y4, April, PP. 562-568.

Moore, W.L., 1943, "Energy loss at the base of a free overfall", Transactions, ASCE, Vol. 108, PP. 1343-1360.

Morris, H. M., 1955, "A new concept of flow in rough conduits". ASCE Transactions. 120, PP. 373-410.

Munz, C., and Roberts, P.V., 1989, "Gas and liquid phase mass transfer resistance of organic compounds during mechanical surface aeration", Water Res., Vol. 23, No. 5, PP. 589-601.

Nakasone, H., 1987, "Study of aeration at weirs and cascade", Journal of Environmental Engineering, Vol. 113, No. 1, February, PP. 64-81.

Peyras, L., Royet, P., and DeGoutte, G., 1992," Flow and energy dissipation over stepped gabion weirs", Journal of Hydraulic Engineering, ASCE, Vol. 118, NO. 5, PP. 707-717.

Popel, H. J., 1974, "Aeration and gas transfer", Delft University of Technology, PP. 61-64.

Princince, A. B., 1991, "Transfer of oxygen and emission of volatile organic compounds at clarifier weirs", J. Water Pollut. Control, Feb. 63, 114.

Rajaratnam, N., 1990, "Skimming flow in stepped spillways", Journal of Hydraulic Engineering, ASCE, Vol. 116, No. 4, PP. 857-591.

Rand, W., 1955, "Flow geometry at straight drop spillway", Proceedings, ASCE, Vol. 81, No. 791, Sept., PP. 587-591.

Sorensen, R. M., 1985, "Stepped spillway hydraulic model investigation", Journal of Hydraulic Engineering, ASCE, Vol. 111, No. 2, PP. 1461-1472.

Stephenson, D., 1991, "Energy dissipation down stepped spillway", International Water Power and Dam Construction, September, PP. 27-30.

Straub, L. G., and Anderson, A.G., 1958, "Experiments on self-aerated flow in open channels", Journal of the Hydraulic Division, ASCE, Vol. 113, No. 2, PP. 225-237.

Streeter, V. L., and Wyile, E. B., 1981, Fluid Mechanics. 1st SI metric edition, McGraw-Hill, Singapore.

Wagner, M., and popel, J., 1996, "Surface active agents and their influence on oxygen transfer", Water Society Technology, Vol. 34, No. 3-4, PP. 249-256.

White, M.P., 1943, "Energy loss at the base of free overfall" Discussion. Transactions, ASCE, Vol. 108, PP. 1361-1364.

Wilhelms, S. C., 1981, "Gas transfer in hydraulics jump", US Army Engineer Waterways Experiment Station, CE, Vicksburg, Mississippi, Technical Report E81-10.

Wood, I. R., 1985, "Air water flows", IAHR Congress 21st, Melbourne, PP. 18-29.

Van Der Kroon, G. T. M., and Schram A.H., 1969, "Weir aeration", H_2O No. 22, PP. 528-537.

الملخص

استخدام المنشآت المدرجة في الحصول على التهوية اللاحقة

إعـــداد

غادة نصري كساب

أشراف

د. عدنان حمودي الصالحي

تهدف الدراسة الحالية للحصول على أفضل فعالية ممكنة للمنشـــآت المدرجـــة فيمـــا يخص التهوية، عن طريق تغيير الصفات الهيدروليكية للمدرجات مثل نوع المدرج، ارتفـــاع الدرجة، النسبة بين ارتفاع الدرجة وطولها وأخيراً تدفق المياه فوق المدرج.

الجانب العملي في هذه الدراسة تم في مختبر هندسة المائيات في قسم الهندسة المدنيـــة في الجامعة الأردنية. قدمت الدراسة ثلاث أنواع من المدرجات، هي المدرجـــــات الأفقيـــة، المدرجات الحوضية وأخيراً المدرجات المائلة. فحصت أربع ارتفاعات للدرجة هي ١٥ســـم، ٣٠سم، ٤٥سم و٦٠سم وباستخدام نسبتين لطول الدرجة وارتفاعها هما ٢/١ و ٤/١ وعـــن طريق نوعين من التدفق، التدفق النفثي والتدفق القشدي.

المدرجات الأفقية كانت ذات فعالية فضلى تتراوح بين ٣٠% إلى ٦٤% بالنسبة إلـــى ارتفاعات الدرجات المختلفة، تليها المـــدرجات الحوضية بفعالية تتراوح بيـــن ١٨% إلـــى ٦٠%، وأخيراً المدرجات المائلة بفعالية تتراوح بين ١٠% إلى ٢٨% ، وهي الأقل. ارتفـــاع الدرجة ٤٥سم كان هو الأفضل بالنسبة للمدرجات الأفقية ، بينما ارتفاع الدرجة ٦٠سم كـــان هـــو الأفضل بالنسبة للمدرجات الحوضية والمائلة. في حالة التدفق النفثي كانت فعالية نســـبة الطول إلى الارتفاع ٢/١ أفضل من النسبة ٤/١، بينما العكس كان في حالة التدفق القشدي.